Ref. Ares(2022)4044794 - 31/05/2022

NEGEM

Quantifying and Deploying Responsible Negative Emissions in Climate Resilient Pathways

Global NETP biogeochemical potential and impact analysis constrained by interacting planetary boundaries

Horizon 2020, Grant Agreement no. 869192

Number of the Deliverable	Due date	Actual submission date
D3.2	**31.05.2022**	**31.05.2022**

Work Package (WP): 3 – Impact Assessment
Task: T3.1 – Impacts on Earth system state and functioning

Lead beneficiary for this deliverable: PIK
Editors/Authors: Johanna Braun (PIK); Constanze Werner (PIK); Wolfgang Lucht (PIK), Dieter Gerten (PIK)

Dissemination level: Public

Call identifier: H2020-LC-CLA-02-2019 - Negative emissions and land-use based mitigation assessment

Document history

V	Date	Beneficiary	Author/Reviewer
1.0	2021-05-17	PIK	Johanna Braun; Constanze Werner; Wolfgang Lucht; Dieter Gerten/ Solene Chiquier (ICL), Rolf David Vogt (NIVA)
1.1	2021-05-31	PIK	Johanna Braun; Constanze Werner; Wolfgang Lucht; Dieter Gerten

This project has received funding from the European Union's Horizon 2020 research and innovation programme under grant agreement No 869192

NEGEM

Partners

VTT – VTT Technical Research Centre of Finland Ltd, Finland
PIK - Potsdam Institute for Climate Impact Research, Germany
ICL - Imperial College of Science Technology and Medicine, United Kingdom
UCAM - University of Cambridge, United Kingdom
ETH - Eidgenössische Technische Hochschule Zürich, Switzerland
BELLONA - Bellona Europa, Belgium
ETA - ETA Energia, Trasporti, Agricoltura, Italy
NIVA - Norwegian Institute for Water Research, Norway
RUG - University of Groningen, Netherlands
INSA - Institut National des Sciences Appliquées de Toulouse, France
CMW - Carbon Market Watch, Belgium
UOXF - University of Oxford, United Kingdom
SE - Stockholm Exergi, Sweden
St1 - St1 Oy, Finland
DRAX - Drax Power Limited, United Kingdom
SAPPI - Sappi Netherlands Services, The Netherlands

Statement of Originality
This deliverable contains original unpublished work except where clearly indicated otherwise. Acknowledgement of previously published material and of the work of others has been made through appropriate citation, quotation or both.

Disclaimer of warranties
The sole responsibility for the content of this report lies with the authors. It does not necessarily reflect the opinion of the European Union. Neither the European Commission nor INEA are responsible for any use that may be made of the information contained therein.

Executive Summary

The recent IPCC report on climate change mitigation once again reinforced that, along with rapid and stringent decarbonisation, carbon dioxide removal (CDR) will be unavoidably required to reach net zero greenhouse gas emissions and thus to comply with the Paris Agreement. Most of the 1.5° or 2°C compatible scenarios from cost-optimizing integrated assessment models (IAMs) featured within the report assume deployment of negative emission technologies and practices (NETPs) at large scale, typically relying to a large degree on Bioenergy with Carbon Capture and Storage (BECCS) with median CDR rates of ~9 $GtCO_2\,yr^{-1}$ for BECCS by the end of the century. However, aside from scepticism regarding the economic, political and technological preconditions needed for a rapid scale-up of BECCS, these high assumed deployment rates might cause severe environmental side-effects. Considering the importance to holistically safeguard critical Earth system functions, this report focuses on quantifying global BECCS potentials as constrained by its impacts on the biosphere, thus adopting a supply-driven perspective to negative emission (NE) potentials. Responding to the need to assess a portfolio of diverse land based NETPS within an integrated framework, the analysis further assesses the potential to complement the limited NE capacity of environmentally constrained BECCS by reforestation and Pyrogenic Carbon Capture and Storage (PyCCS), two promising NETPs with potential synergies regarding further sustainable development targets. Specifically addressing the environmental dimension, the analysis thus contributes to the overall aim of NEGEM to assess *realistic* and *responsible* NE potentials.

For the assessment of global spatially explicit NE potentials for BECCS, reforestation and PyCCS, we simulate second-generation biomass plantations and their impact on terrestrial planetary boundaries (PBs; biosphere integrity, land-system change, freshwater use and nitrogen flows), as well as carbon sequestration in forests, with the state-of-the-art dynamic global vegetation model LPJmL. Building on the model developments of LPJmL5-NEGEM (see D.1), the representation of biomass plantations, incl. fertilization dependant nitrogen flows, as well as the spatially explicit modelling of PBs, i.e. critical thresholds of anthropogenic interference with key Earth System processes, have been further enhanced. To convert simulated biomass yields to net NEs, we rely on several CDR efficiency (CEff) scenarios based on a comprehensive representation of emissions along the BECCS/PyCCS supply chain as modelled with the MONET framework (see D7.1 and D7.2).

With ~ 2 billion additional people added to the world's current population by 2050, increasing consumption of this population and rising interest in biomass-based products such as construction materials and bioplastics, reserving current arable land for BECCS does not seem realistic. However, opportunities to expand land use for biomass plantations without further PB transgressions are very limited, against the backdrop of already severe anthropogenic pressures on the terrestrial biosphere, with only 30% of the global ice-free land surface free of direct human use. To assess the PB-compatible NE potential from plantation-based BECCS, we optimize geographic distribution of dedicated bioenergy crops under the condition that plantations may only be added outside of current agricultural areas up to the point that regional environmental boundaries are reached. In this, we refer to geographically explicit boundaries for freshwater, nitrogen, land-system change and biosphere integrity to capture the strong regional patterning of terrestrial PBs. The optimization results in simulated NE potentials of 1.2 $GtCO_2$-eq yr^{-1} (1.0 - 1.4 $GtCO_2$-eq yr^{-1} assuming a lower/more optimistic CEff). While the exact magnitude of maximum NE supply is still uncertain and strongly depends on scientific and normative assumptions for PB constraints as well as the input data used for the evaluation, the *order of magnitude* is clearly constrained by widespread and severe PB transgressions through current agricultural production. The estimated maximum PB-compatible NE potential is further reduced to almost zero if the conversion of forests to biomass plantations is additionally precluded. This emphasizes that any additional conversion of natural vegetation is extremely difficult to reconcile with terrestrial PBs and other environmental targets. While BECCS from other feedstocks

such as residues from forestry and agriculture have not been considered here, a broader earth-system stability perspective thus calls for a very cautious consideration of BECCS from dedicated bioenergy crops. This result contrasts common assumptions in demand-driven and cost-optimizing IAMs, but estimated PB-limited NEs are compatible with mitigation scenarios that feature stringent and rapid decarbonisation, reductions in energy demand and/or achievement of broader sustainable development goals. This argues for the need of rapid socioeconomic transformations if risks associated with PB transgressions are to be minimized.

For reforestation, we simulate scenarios of 200, 300 and 400 Mha rededication of pasture areas, corresponding to ~7-16% of global pastures, based on literature estimates on reduction potentials through diet changes and/or efficiency increases in animal husbandry. Due to potential adverse effects on PBs, we deliberately exclude afforestation and define reforestation as the restoration of natural forest ecosystems given the potential co-benefits for PBs as well as the higher resilience of sequestered carbon. Prioritizing the proximity to intact forest areas to countervail fragmentation, on average up to 2.9 $GtCO_2$-eq of annual NEs may be achieved by reforesting 300 Mha predominantly in tropical and temperate zones (2.0-3.7 $GtCO_2$-eq yr^{-1} for 200-400 Mha; referring to an evaluation timeframe of 40 years). This is well in line with simulated NEs from agriculture, forestry and other land use for 2050 in "Paris-compatible" scenarios included in the recent IPCC report. If the food system was comprehensively transformed towards sustainability with associated decreases in land demand, NEs from reforestation could even be increased, unlocking further co-benefits, especially regarding increases in the resilience of natural forest ecosystems through reductions in land-system change pressures.

Finally, we estimate relatively low potentials for PyCCS (0-0.2 $GtCO_2$-eq yr^{-1}) in our assessment of land- and calorie-neutral biochar provision, i.e. exploiting biochar mediated yield-increases and associated reductions in cropland demand to rededicate agricultural area to biochar feedstock production – thus providing NEs without further pressures on PBs nor decreases in calorie production. This conservative estimate results however from comparatively low simulated yields in the new LPJmL version with nitrogen limitation, which needs further assessment and validation. Addressing this dependency, we additionally assess the NE potentials of plantations with optimal nitrogen supply showing NE potentials of 0.17–0.45 $GtCO_2$-eq yr^{-1}.

Adding up simulated NE potentials from BECCS, reforestation and PyCCS results in ~4 $GtCO_2$-eq yr^{-1} of CDR, referring to the medium scenario for each of the analysis parts. This compares to 88% of the total NEs projected for the year 2050 in IAM scenarios limiting global warming to 2°C or below and 32% of the respective NEs for 2100 (median for C1-C3 scenarios in the 6th Assessment report of the IPCC). However, these results should be cautiously interpreted as upper ceiling potentials, as climate change impacts on biomass plantations and forests have not been included, and all remaining opportunity spaces to expand land use for biomass plantations without further PB transgressions have been exploited. Yet, even this estimated upper ceiling potential is significantly lower than assumed CDR rates in most mitigation scenarios of climate economics as crucial environmental limits are considered here. Nonetheless, it may considerably contribute to compensate for hard-to-abate emissions needed to reach net zero greenhouse gas emissions. Although this limited potential might be expanded when including other feedstocks for BECCS and PyCCS, additional NETPs with synergies for PBs, i.e. agroforestry and improved forest management or advanced technologies with less land demand (e.g. direct air capture and storage systems), this assessment clearly underpins that any delayed decarbonisation and associated high NE demands would likely come at the cost of other crucial Earth system components. This global perspective on PBs should be carefully considered for developing CDR strategies in the EU, as it is likely that European CDR demands can only partially rely on sequestration on its own territory. Assumptions about realistic CDR potentials within and beyond EU territory should thus be founded on careful consideration of all PBs, not just the climate targets.

This report aims to contribute to a more holistic Earth system perspective on NETP potentials, by expanding the focus on climate change mitigation to also consider other crucial dimensions of Earth system stability. To further investigate limits and opportunities of NETPs as constrained by environmental impacts, a more thorough analysis

of NETP impacts on biosphere integrity (D3.3), the interdependence of NETP potentials with developments within the food sector (D3.7), and the effects of climate extremes on NETP potentials (D3.4) are studied in NEGEM. Complemented by material flows analyses, life cycle assessments and more regional EU-specific assessments (ETH, INSA, VTT, NIVA), these results on the environmental dimension are combined with technical, social, economic and governance barriers to contribute to the overall NEGEM agenda of deriving realistic and responsible NE pathways for the EU.

NEGEM

Table of contents

NEGEM

List of acronyms

AR6	-	6th Assessment report of the Intergovernmental Panel on Climate Change (IPCC)
BECCS	-	Bioenergy with Carbon Capture and Storage
BFT	-	Bioenergy Functional Type
BII	-	Biodiversity Intactness Index
C	-	Carbon
CCS	-	Carbon Capture and Storage
CDR	-	CO_2 Removal
CEff	-	CO_2 Removal Efficiency
CFT	-	Crop Functional Type
DM	-	Dry Matter
EFR	-	Environmental Flow Requirement
IAM	-	Integrated Assessment Model
LCN-PyCCS	-	Land- and Calorie-Neutral PyCCS
N	-	Nitrogen
NE	-	Negative Emission
NETPs	-	Negative Emission Technologies and Practices
PB	-	Planetary Boundary
PFT	-	Plant Functional Type
PyCCS	-	Pyrogenic Carbon Capture and Storage
VMF	-	Variable Monthly Flow method

NEGEM

List of figures

List of tables

1 Introduction

In the Paris Agreement, 195 nations signed a convention that aims for "holding the increase in the global average temperature to well below 2°C above pre-industrial levels and pursuing efforts to limit the temperature increase to 1.5°C above pre-industrial levels" (UNFCCC, 2015). A particular challenge to reaching this goal is that collective human mitigation action needs to start immediately, in order to eventually stabilize the Earth system in a habitable interglacial-like state (Rockström et al., 2017). The required actions do not only involve the complete phasing out of fossil carbon combustion until the mid of this century, but also CO_2 removal (CDR) from the atmosphere through negative emission technologies and practices (NETPs) (Rockström et al., 2017; Rogelj et al., 2015). In climate economics and the corresponding models of cost optimization (Integrated assessment models = IAMs), scenarios solving the equation for the emission budget of 1.5- and 2°-compatible climate targets usually assume achievement of substantial amounts of negative emissions (NE), particularly if there were low ambitions for rapid and stringent decarbonisation measures. To meet these NE demands, most IAM-based scenarios rely to a large degree on Bioenergy with Carbon Capture and Storage (BECCS) and project rates of up to above 9 $GtCO_2\,yr^{-1}$ around the year 2050 (median: 2.75 $GtCO_2\,yr^{-1}$), reaching maximum levels of more than 16 $GtCO_2\,yr^{-1}$ by 2100 (median: 8.96 $GtCO_2\,yr^{-1}$, 15th - 85th percentile: 2.63-16.15 $GtCO_2\,yr^{-1}$) (IPCC, 2022).

However, there is large scepticism that these simulated high deployment ranges of NETPs can realistically be reached given the economic, political and technological preconditions of the assumed rapid scale-up of NETPs (Anderson & Peters, 2016; Bednar et al., 2019; Lenzi et al., 2018; Nemet et al., 2018). Also, there have been strong concerns regarding the severe environmental and social side-effects: Large deployment of BECCS from dedicated bioenergy crops would lead to additional land degradation, competition for land with both food production and biodiversity protection, and could cause strong increases in human water and fertilization use, amongst others (Boysen et al., 2017; Humpenöder et al., 2014; Stenzel et al., 2019). By consequence, it is questionable how these high NE rates of demand driven IAMs are compatible with Earth system resilience. Even without large-scale NETP deployment, anthropogenic interference with natural processes and exploitation of natural resources is already exerting severe pressures on key functions of the Earth system (Gerten et al., 2020; Heck et al., 2018; Steffen et al., 2015). More than 70% of the world's ice-free land surface is directly impacted by human use (IPCC, 2019) with agriculture acting as one of the major drivers for global environmental change, including biodiversity loss, soil degradation, water scarcity and critical interference with the nitrogen cycle (Campbell et al., 2017; Foley et al., 2005; Steffen et al., 2015). Referring to a safe operating space for humanity, several planetary boundaries (PBs), representing dangerous levels of human interference with critical Earth system processes, have already been transgressed (Rockström et al., 2009; Steffen et al., 2015). Therefore, introducing a new factor of massive human appropriation of land and resources for NETPs (e.g. vast areas for biomass plantations for BECCS) must be considered carefully. While releasing pressure on the climate change PB, severe trade-offs could emerge through additional pressures on land, biodiversity, water and nitrogen flows.

1.1 Environmental limits to BECCS from dedicated energy crops

In contrast to demand-driven perspectives of cost-optimizing IAMs, subtask 3.1.1 in WP3 aims to assess environmentally constrained NETP potentials in a supply-driven approach, contributing to NEGEM's real-world, multi-disciplinary assessments to quantify the potential for NETP deployment in a socially, environmentally and economically conscious manner. Rather than defining an emission target and quantifying the NE required under certain (more or less ambitious) decarbonization measures, we consider environmental limits defined to secure Earth system functioning and quantify the achievable potential NE supply while maintaining terrestrial PBs (freshwater use, nitrogen flows, biosphere integrity, land-system change), extending the work of Heck et al. (2018).

Earlier studies have addressed only some aspects of environmental constraints to biomass production for bioenergy (with and without CCS), with varying levels of ambition (in general biodiversity protection and land-system change), but often neglected other dimensions such as water use and nitrogen pollution (Beringer et al., 2011; Erb et al., 2012; Frank et al., 2021; Haberl et al., 2010; Schueler et al., 2013; Searle & Malins, 2015; Wu et al., 2019). Addressing this deficit, Heck et al. (2018) were the first to account for all terrestrial PBs (freshwater use, nitrogen flows, biosphere integrity, land-system change) in one assessment.

The PB framework enables the integrated assessment of human interference with interconnected key functions of the Earth system and, thus, serves as a solid assessment tool for the evaluation of environmentally constrained NETP potentials. Given the fundamental importance to not only consider some aspects of environmental protection but to holistically safeguard critical biogeochemical processes for Earth system stability, this study sets out to derive global NE potentials from dedicated energy crops which do not lead to additional transgression of spatially distributed PBs. In line with Heck et al. (2018), we here assume that NETP deployment should – as a minimal requirement – not lead to additional transgressions of PBs if further risks through their transgressions are to be avoided. As an update to Heck et al. (2018), we include (i) a new available dataset on the current spatially-explicit status of a "Biodiversity Intactness Index" (Newbold et al., 2016) and (ii) a dynamic representation of the PB for nitrogen use implemented within a new version of the dynamic global vegetation model LPJmL. This allows for a more thorough consideration of the PB for biosphere integrity and nitrogen use. While feedstocks for BECCS may be complemented by uncertain and limited amounts of residues from forestry and agriculture (Hanssen et al., 2020) as well as by logs from managed forests amongst others, we focus on biomass from lignocellulosic energy crops as main source of BECCS feedstocks in most IAM scenarios (Rose et al., 2022) to assess the source that is most critical in regard to impacts on PBs.

1.2 Opportunities for reforestation and PyCCS within planetary boundaries

As the analysis by Heck et al. (2018) already pointed to very limited PB-compatible NE potentials from plantation-based BECCS outside of agricultural areas, we further expand the analysis to include two additional NETPs: reforestation of pasture and pyrogenic carbon capture and storage (PyCCS), the latter of which could be realized on current agricultural areas, neither compromising food security nor further transgressing PBs. The study thus responds to the need to consider multiple land-based NETPs within an integrated framework, considering that an expansion of the NETP portfolio can help to add up environmentally and socially constrained potentials of individual NETPs, thereby increasing the overall sustainable potential (Fuss et al., 2018).

1.2.1 Reforestation

Apart from BECCS, afforestation and reforestation (A/R) is the second most frequently modelled NETP within the IAM scenario literature included in the IPCC 6th Assessment report (AR6, IPCC, 2022). In contrast to BECCS from dedicated energy crops, A/R reduces the pressure on the PB for land-system change and may also have positive effects on biodiversity – if locally adapted and diverse species are planted (e.g. Aerts & Honnay, 2011; Smith, Adams, et al., 2019). A/R may however also have negative impacts on biosphere integrity if large-scale tree monocultures are replacing biodiverse-rich natural non-forested ecosystems such as grasslands and savannas (Gómez-González et al., 2020; Seddon et al., 2019, NEGEM Deliverable 3.6). Large-scale A/R could also significantly alter regional water cycles (e.g. Schwärzel et al., 2020), and strongly compete with food provision potentially threatening food security (Kreidenweis et al., 2016; Smith, Nkem, et al., 2019).

To safeguard the intactness of non-forested ecosystems, we assume that only areas which naturally sustain forest ecosystems but have been deforested in the past would be potentially available for reforestation. Due to the negative impacts of afforestation on biosphere integrity in non-forested ecosystems (see above, Gómez-González et al 2020), afforestation is not considered in this study. Further, we specifically assess restoration of natural forests with no or little anthropogenic disturbance, e.g. through harvesting. While the focus on forest

ecosystem regeneration neglects the potential contribution of plantation forests to local and increasingly bio-based economies, restoration of natural forests is also favourable from a NE perspective: Carbon sequestration in natural forests is likely higher over the long-term and more resilient to rapidly changing climate conditions (Erb et al., 2018; Lewis et al., 2019; Littleton et al., 2021).

Given the competition for land between climate change mitigation and the food sector, the future availability of land for reforestation strongly depends on reduced agricultural land use. In light of a growing and increasingly affluent world population, any rededication of cropland is difficult to reconcile with food security. However, pasture requirements have a potential to decrease through increasing efficiency in husbandry and possible diet changes (Hayek et al., 2021; Smith et al., 2013; Stehfest et al., 2009). Building on estimates of such future developments from the literature, we assume the conversion of scenario-specific shares of global pasture areas to forests, which could release pressures on the already transgressed PBs for land-system change and biosphere integrity while providing NEs.

1.2.2 Land- and calorie-neutral PyCCS

While any replacement of cropland is difficult to justify given the competition with food production for a growing world population, the land- and calorie-neutral PyCCS (LCN-PyCCS) approach may allow for PyCCS feedstock production within cropland bounds while maintaining calorie production (Werner et al., 2022, in revision). LCN-PyCCS is a system of land-neutral biomass production on (sub-)tropical croplands using enhanced soil properties and resultant yield increases after biochar application to maintain calorie production while realizing net CO_2 extraction from the atmosphere. This NETP is based on pyrolysis, the thermochemical decomposition of biomass at high temperatures (350–900°C) in an oxygen-deficient atmosphere. The three main carbonaceous pyrolysis products can subsequently be stored in different ways to produce NE: as solid biochar in soils, as bio-oil in depleted fossil oil repositories and as CO_2 after combustion of permanent pyrogas in geological storages in very advanced technological settings (Schmidt et al., 2018).

The application of biochar to arable soils is particularly interesting for considerations of early deployment because it is a market-ready technology including low-tech options for small landholders as well as high-tech variants for larger scales (Cornelissen et al., 2016; Smith, Adams, et al., 2019). Furthermore, biochar used as soil amendment has been shown to improve soil conditions and increase crop yields significantly in many regions (Jeffery et al., 2017; Melo et al., 2022; Ye et al., 2020).

As it holds true for all biomass-based NETs, the source of the feedstock is the most critical factor for the environmental impact of PyCCS. The land and water footprints of PyCCS feedstock production is thus minimal if based on residues from cropland or forestry (Woolf et al., 2010), but can be substantial if based on dedicated plantations (Werner et al., 2018). However, estimating globally available crop residues involves significant uncertainties (Wirsenius, 2000). An additional option for sustainable feedstock production can be applied for PyCCS through biomass input from dedicated fast-growing crops produced in land-neutrality: When reaching a significant level of biochar-mediated yield increases, the same amount of food can be produced on less land (calorie-neutral). Thus, a fraction of the cropland can be dedicated to fast-growing crops supplying PyCCS without requiring additional land (land-neutral). Grounding on these assumptions, LCN-PyCCS may produce NEs without further transgressions of the nitrogen PB and without additional pressures on the PBs of land-system change, biosphere integrity and freshwater use.

1.3 Assessed research questions

Adopting a supply-driven perspective on multiple land-based NETPs, which integrates critical terrestrial Earth system processes, this global assessment aims to answer the following questions:

- ***(1)*** *How much NEs could be provided from dedicated biomass plantations for BECCS outside of current agricultural areas under the constraint that further transgressions of PBs are to be avoided?*
- **(2)** *To which degree could these NE potentials be increased through parallel reforestation on pasture areas and LCN-PyCCS on cropland?*

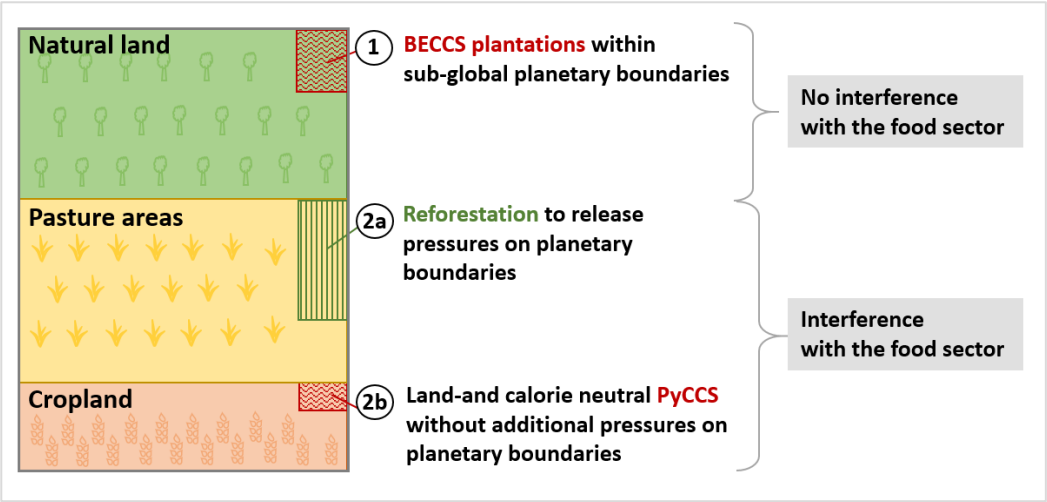

Figure 1: Overview of the three analysis parts on PB-compatible NE potentials

While (1) only considers areas outside of current agricultural areas, (2) assesses the extended option space for NEs upon potential reductions in future agricultural land demand (Figure 1). It thereby assesses the increased opportunities for climate change mitigation depending on feasible future land and resource sparing developments within the food system, through reduced or more efficient livestock production (2a) and biochar-mediated yield increases (2b). The analysis is grounded on model development to (i) enhance the representation of biomass plantations within LPJmL, incl. fertilization and nitrogen flows (see Deliverable 3.1, and section 2.2.1.2 in this report) and (ii) improvements in spatially explicit modelling of PBs (see 2.2.2), thus contributing to the NEGEM agenda of deriving realistic and responsible NETP potentials.

2 Methods

2.1 Analysis set-up

To assess spatially explicit NE potentials for BECCS, reforestation and PyCCS, we simulate biomass yields and carbon (C) sequestration in forests with the state-of-the-art dynamic global vegetation model LPJmL (see 2.2.1). For each of the analysis parts, we define three scenarios by varying key assumptions to provide lower, medium and optimistic estimates for NE potentials. For BECCS and PyCCS, this relates to a range of CDR efficiencies for conversion of simulated biomass harvest to net NEs, computed based on the MONET framework (see 2.3.1 and D7.1/D7.2). PyCCS scenarios are complemented by varying assumed yield increases through biochar (impacting the available area for biomass plantations) as well as the assumptions on plantation management (see 2.3.3). For reforestation, we define three scenarios for the global reforested pasture extent based on literature estimates of rededication potentials (see 2.3.2.1). In contrast to IAM scenarios, we thus systematically assess an opportunity space rather than specific storylines of future socio-economic development.

When quantifying NE potentials, it is crucial to define a fixed evaluation period for all assessed NETPs in order to ensure comparability. We here chose an evaluation period of 40 years, i.e. the potential of a *first major* CDR deployment wave. As the assumed evaluation period impacts the simulated yearly NE potentials (i.e. planting a forest as a slowly stabilizing C sink once vs. harvesting a biomass plantation for BECCS every year), all results have to be interpreted against the background of the assumed 40-year evaluation period. For example, yearly BECCS potentials increase the longer the evaluation timeframe, as land use change emissions are in relative terms smaller, the more years with continuous harvests are included. For reforestation on the other side, C accumulation rates decline over longer timeframes, with eventually saturating carbon pools (this is further discussed in 4.4).

Building the ground for the approaches to BECCS, reforestation and PyCCS (details in 2.3), the modelling basis, including details on relevant processes in LPJmL, as well as the PB concept and the representation of regional boundaries in this study are presented in the following.

2.2 Modelling basis

2.2.1 LPJmL

2.2.1.1 General model description

The LPJmL model is suited to assess climate and land use change impacts on the terrestrial biosphere, agricultural/biomass production, as well as the C, N and water cycle by way of spatially-explicit, process-based biogeochemical modelling, at daily time steps and a spatial resolution of 0.5° x 0.5°. The version LPJmL5-NEGEM, employed in this analysis, has been prepared in subtask 3.1.1 and is described in D3.1. Since that report, three major updates were additionally achieved: 1) the implementation of input-driven fertilization of biomass plantations; 2) the representation of woody lignocellulosic biomass crops with N dynamics; and 3) the improved representation of N demand for herbaceous biomass crops. Further, extensive descriptions and validations of the biogeochemical dynamics can be found in Schaphoff, von Bloh, et al. (2018) and von Bloh et al. (2018).
LPJmL simulates key ecosystem functions of vegetation by representing eleven natural plant functional types (PFTs) (Sitch et al., 2003), 13 crop functional types (CFTs) plus managed grassland (Bondeau et al., 2007), and three types of fast-growing second-generation energy crops (Beringer et al., 2011; Heck et al., 2016). These bioenergy functional types (BFTs) are separated in herbaceous types, i.e. C4 grass, and woody types parametrized as short rotation coppice of eucalypt in tropical climates and poplar and willow in temperate and boreal climates.

While the distribution of natural PFTs is a result of simulated competition for light, water and nutrients, the land cover of crops and pasture is prescribed by a scenario-specific land use input, including the extent of irrigated vs. rainfed areas. For irrigated areas, cell- and CFT-specific irrigation water demand is internally computed based on the soil water deficit and is requested for withdrawal from local renewable freshwater resources (river discharge, lakes and reservoirs), taking into account the system-specific inefficiencies of surface, sprinkler or drip irrigation (Jägermeyr et al., 2015; prescribed by the land use input). Total irrigation water withdrawals per grid cell are constrained by local water availability, after reductions through prescribed water withdrawals for households, industry and livestock (Tab. S1). For simulation of river discharge, surface and subsurface runoff accumulate along the river network, with respective reductions through anthropogenic water withdrawals.

In LPJmL5-NEGEM, the representation of the N cycle accounts for N-limited plant growth and ecosystem productivity through photosynthesis and respiration rates depending on N availability (von Bloh et al., 2018). Thus, if the plant's N demand cannot be fulfilled by N uptake, the water-limited photosynthesis rate is reduced correspondingly. N-uptake, in turn, is determined by soil mineral N-concentration, soil properties, fine root mass and plant demand for N, based on Smith et al. (2014). N in soils is represented by distinct pools for the two main reactive forms, NO_3^- and NH_4^+, and N of soil organic matter. Sources of N input to those pools include the dynamically modelled decomposition of plant biomass and biological N fixation as well as atmospheric deposition and fertilization that are prescribed by the scenario's input data (Table S1). The model accounts for mineralization of soil organic matter, immobilization, (de-)nitrification and plant uptake within the N pools and simulates losses to the atmosphere via (de-)nitrification (N_2; N_2O) or volatilization (NH_3) as well as NO_3 losses to renewable freshwater resources in runoff and leaching.

2.2.1.2 Improvements in representing biomass plantations

As the assessment of realistic potentials of biomass-based NETPs is a crucial part of the NEGEM agenda, we focused on enhancing the representation of the above described C, N and water flows for the three BFTs in subtask 3.1.1. Following the implementation by Beringer et al. (2011), herbaceous biomass plantations are assumed to be mowed once the above-ground C storage reaches 350 gm^{-1}, but at least once a year. The woody BFTs are harvested in an 8-year-cycle with a maximum plantation lifetime of 40 years before clearance. As reported in D3.1, we validated the simulated yields in simulations without N dynamics for all BFTs and integrated the herbaceous BFT in the range of crops represented with N dynamics in LPJmL5-NEGEM.

Since D3.1, we have also parametrized woody lignocellulosic biomass crops for representation of N limitation on plantations, in addition to simulated water and C pools and fluxes. The BFT-specific parameters relevant for the N flows (maximum N uptake rate $N_{up;root}$, increase in N demand k_{store}, N recover fraction at turnover k_{turn}) shown in Table 1 were adapted from the respective natural archetypes of tropical broadleaved evergreen trees for the tropical type (eucalypt) and broadleaved summergreen trees for the non-tropical BFT (willow/poplar) . As the minimum canopy conductance (g_{min}) and maximum water transport capacity E_{max} required higher thresholds in the N-limited version of LPJmL (von Bloh et al., 2018), we increased these parameters for the woody BFTs linearly according to the shift in the respective natural archetype, see Table 1. The comparison of the simulated biomass yields from this updated LPJmL5-NEGEM version to the observations shows a reasonable fit (Figure 2). However, the model seems to limit eucalypt biomass production to a level that is exceeded in the observations. This limitation needs to be assessed in more detail.

Table 1 List of BFT-specific parameters. Maximum nitrogen uptake rate ($N_{up;root}$), increase in nitrogen demand (k_{store}), nitrogen recover fraction at turnover (k_{turn}), minimum canopy conductance (g_{min}), maximum water transport capacity (E_{max}) used in the LPJmL5-NEGEM model.

parameter	$N_{up;root}$	k_{store}	k_{turn}	g_{min}	E_{max}
Unit	gN kgC^{-1}	--	%	mm s^{-1}	mm day^{-1}
Herbaceous BFT	5.1	1.30	30	0.80	8
Woody BFT – non-tropical	2.8	0.15	30	0.40	7
Woody BFT – tropical	2.8	0.15	80	0.64	10

Furthermore, we have improved the representation of the N demand for the herbaceous BFT with a revised C to N ratio of the aboveground biomass set to 92. This is based on miscanthus and switchgrass entries in the Phyllis2 database on the composition of biomass and waste (Phyllis2, 2022). In comparison to simulations with the previous C to N ratio of 34, corresponding to non-lignocellulosic grass compositions, the N demand of the herbaceous BFT is significantly lower with the revised value. This is in line with the literature reporting relatively low fertilizer requirements for miscanthus and switchgrass (Cadoux et al., 2012). Yet, the performance of the model in representing biomass yields, assessed by the comparison to observed yields from Li et al. (2018), does not change significantly with the revised C to N ratio and is still in a reasonable range of uncertainty Figure 2.

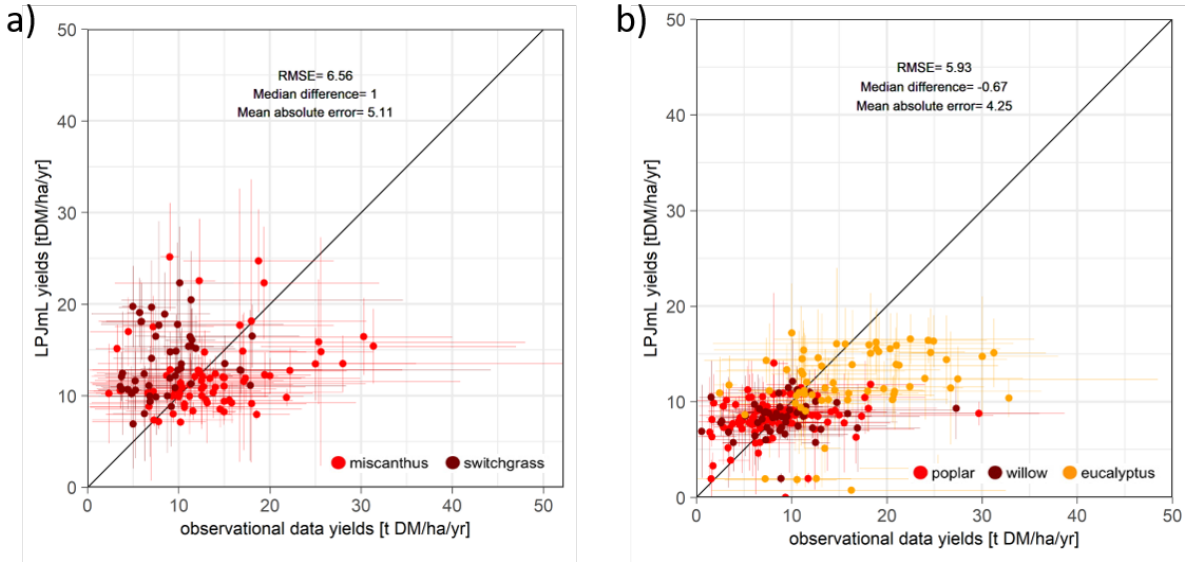

Figure 2: Scatterplots of observed and LPJmL-simulated BFT yields in the respective grid cell for a) herbaceous and b) woody BFTs. Model uncertainty is derived from a simulated minimum featuring low fertilization (woody: the amount of N harvest from a preliminary simulation with unlimited N, herbaceous: half of the respective N harvest) combined with rainfed conditions and a maximum characterized by high fertilization (woody: four times the amount of N harvest from a preliminary simulation with unlimited N, herbaceous: twice the respective N harvest) and optimal water supply averaged over 40 years, whereas observation uncertainty reflects dependencies on plantation management.

An additional significant update of the LPJmL5-NEGEM model was achieved by implementing a fertilizer module for biomass plantations to assess the effects of fertilization in a more comprehensive way than the prior evaluation capacity ranging from the total absence of fertilizer input to unlimited N supply. First, the cell- and BFT-specific fertilizer input prescribed for each year is split into two equal applications. Subsequently, the timing

of these two applications is based on the phenological state of leaves throughout the year. The first rate is applied when the sum of unitless daily phenological states, ranging from 0 (no leaf development) to 1 (fully unfolded leaf), reaches 30 as an early-season proxy when plants begin to grow and require N. The second half of the fertilizer is applied when this value meets the threshold of 50, to match the time in the year where a second application may enhance mid-season productivity.
With this implementation, different levels of plantation fertilization can be assessed. In this study, we consider high and low levels of BFT-specific fertilizer application, separated for rainfed and irrigated conditions (assuming drip irrigation with high conveyance efficiency). Cell-specific fertilization levels for each biomass plantation type are derived from simulated harvested N under unlimited N supply, thus taking into account the strong dependence of fertilizer requirements on spatially-explicit soil properties, water availability and climate conditions. Considering nitrogen use inefficiencies (e.g. limited plant uptake, N losses from the soil), the N input assumed for high fertilizer scenarios needs to be significantly higher than the harvested N under unlimited N supply. The high fertilizer input is thus here estimated to be the fourfold amount of harvested N for the woody BFT and the double amount for the herbaceous BFT, representing distinct uptake capacities of the different plant types. Lower levels of fertilization are estimated by assuming application rates equal to the amount of the harvested N for the woody BFT and half the amount for the herbaceous BFT. To circumvent unrealistically high fertilization levels, these rates derived from dynamic LPJmL5-NEGEM simulations are capped to literature-based maximum thresholds of 300 kg N $ha^{-1}yr^{-1}$ (the 99^{th} percentile in Li et al. (2018)).

2.2.1.3 Simulation protocol

Preceding the LPJmL simulations for the analysis, an equilibrium of the distribution of natural vegetation as well as C and N stocks was achieved by recycling 1901-1930 climate in a 10,000-year spin-up of potential natural vegetation. Subsequently, we introduced the influence of agriculture on the C and N cycle with a second spin-up period of 390 years followed by simulations of the historical land use change until 2015, the reference land use for our scenarios of BECCS, PyCCS and reforestation. The evaluation of PB states and NE potentials, then, required simulations of three major categories: the simulation of the reference scenario with current land use (2015), the simulation of potential biomass yields with different management options as well as adapted land use patterns according to the NETP scenarios (see 2.3).

To account for current climate variability, we keep the land use pattern and management for the different scenarios constant over a 40-year evaluation period (i.e. the pattern and management of the land use reference for the year 2015, or the adapted patterns of the BECCS, reforestation and PyCCS scenarios) and shuffle 1986-2015 climate, atmospheric CO2 concentration and N deposition (see below and Tab. S1). For the assessment of the N-PB (see 2.2.2.2), an additional simulation with potential natural vegetation is required for the evaluation of N flows at preindustrial levels of N deposition, where the NO_3 and NH_4 deposition data of 1901–1930 are recycled, accordingly.

The model is driven by climate data (Harris et al., 2020), NO_3 and NH_4 deposition rates (Lamarque et al., 2013) and atmospheric CO_2 concentration (NOAA ESRL, 2019) as specified in the appendix and Tab. S1. Further, the agricultural reference scenario is based on the CFT-specific extent of cropland and pasture, including the fraction of irrigated areas (Ostberg, 2022, in prep.), as well as fertilizer and manure input (Elliott et al., 2015; Zhang et al., 2017) as described in more detail in the appendix.

2.2.2 Planetary boundaries: Framework and definitions

In our assessment of environmentally restricted NE potentials, we employ limits from the PB framework accounting for key Earth system functions. While scientists continue their warning that tipping points within the Earth system and its subsystems could already be reached within this century and cause major transition that could threaten the existence of humankind (Lenton et al., 2019; Steffen et al., 2018), the PB framework suggests limits to the anthropogenic disruption of Earth system functioning (Rockström et al., 2009; Steffen et al., 2015). The desired safe conditions within those limits are defined as the stable conditions of the Holocene (Rockström et al., 2009), the conditional frame in which humanity has evolved and thrived (Van der Leeuw, 2008). Thus, in the PB framework, thresholds of unacceptable human-induced global environmental changes for nine key Earth system processes are described as non-linear transitions away from the Holocene state. Following the precautionary principle, boundaries are positioned at a safe distance to the thresholds determined by the uncertainty in representing the respective processes in science. In addition to global thresholds, sub-global boundaries are defined for some PBs to account for the spatial heterogeneity of many processes and the different scales at which some PB-relevant processes operate. Thus, transgressions of these sub-global boundaries can impact Earth system functioning at a planetary scale through (i) interactions with other processes, e.g. large-scale deforestation impacting continental-scale rainfall patterns and global climate, or (ii) aggregate effects of destabilized processes at the regional scale, e.g. exceedance of sustainable water withdrawals in many locations can lead to collapse of aquatic ecosystems. Acknowledging the strong regional patterning of current terrestrial PB transgressions (Gerten et al., 2020), we focus our analysis of PB-limited BECCS potentials on these sub-global definitions of the four major terrestrial PBs, i.e. freshwater use, N flows, land-system change and biosphere integrity.

2.2.2.1 Planetary Boundary for Freshwater Use

While diverse approaches for the freshwater PB are currently being discussed (Gleeson et al., 2020; Wang-Erlandsson et al., 2022), the sub-global control variable for freshwater use as defined in Steffen et al. (2015) refers to the minimum river flow required to maintain at least a “fair” ecological status within rivers. These “environmental flow requirements” (EFRs) are here determined for each grid cell based on the variable monthly flow (VMF) method (Pastor et al., 2014; Steffen et al., 2015), which sets limits to water withdrawals based on flow regime dependent percentages of pristine monthly flow (see Table 1 for more details on flow regime classification and percentages). Pristine river flow, as reference for EFR calculations, is simulated with potential natural vegetation under current climate (1986-2015) and in the absence of anthropogenic land use and water withdrawals (see 2.2.1.3). Current transgressions of the PB for freshwater use in the agricultural baseline simulation thus result from anthropogenic water withdrawals and, to a smaller degree, from changes in river flow due to land use change induced alterations of runoff. In all cells where mean annual flow is <1 m^3s^{-1}, EFR computation is omitted. EFR estimates as simulated with LPJmL and the VMF method have been validated against local case study estimates in Jägermeyr et al. (2017).

As proposed in Jägermeyr et al. (2017) and Gerten et al. (2020), the status of the PB for freshwater use for each cell is expressed as the transgression-to-uncertainty ratio averaged over months with a transgression. The uncertainty span in turn is defined by varying EFR shares by ±15%, with the lowest values constituting the cell-specific sub-global PB (see Table 2). Grid cells with a ratio between 5 and 75% are allocated to the zone of uncertainty; higher ratios are defined as high risk (beyond zone of uncertainty); lower ratios as “safe”.

2.2.2.2 Planetary Boundary for Nitrogen flows

To address the main concerns associated with anthropogenic modification of the N cycle, such as eutrophication of aquatic and terrestrial ecosystems as well as pollution of groundwater, several regional control variables for the PB for N have been proposed (de Vries et al., 2013). We here focus the analysis on limits to surface water eutrophication as (i) Steffen et al. (2015) argue that eutrophication of aquatic surface waters is the major concern being addressed within the PB for biogeochemical flows and (ii) it has been shown that thresholds addressing surface water eutrophication are generally strictest (Chang et al., 2021; de Vries et al., 2021). Complying with these thresholds is therefore likely to result in acceptable levels of terrestrial eutrophication and groundwater pollution.

Specifically, we define the regional N boundary based on critical N concentrations in runoff (through surface and subsurface runoff and leaching N flows) from agricultural and natural land to surface waters as suggested by de Vries et al. (2021). N loads in runoff are dynamically simulated within LPJmL based on a process-based representation of N transformations and losses in the soil and depend on climatic and soil conditions as well as on the soil management, e.g. fertilization or plant cover (von Bloh et al., 2018). As denitrification in groundwater is not yet implemented in LPJmL, we apply a global denitrification factor of 0.71 derived from (Bouwman et al., 2013) to simulated cell specific N loads, as suggested in Gerten et al. (2020). A concentration of 1 mg N l^{-1} has been suggested as critical threshold (see Table 2) based on ecological and toxicological effects of inorganic N pollution (Camargo & Alonso, 2006; Poikane et al., 2019), with the upper end of uncertainty set to 2.5 mg N l^{-1} based on national surface water quality standards and objectives (de Vries et al., 2021).

By defining the PB based on N thresholds in runoff, we capture potential transgressions in all tributary streams and argue that, if thresholds in runoff are complied with, any downstream transgression would also be prevented. To specifically capture anthropogenically increased N loads, we subtract N loads from a simulation with potential natural vegetation and low N deposition (1901-1930 = first 30 years available in the used input dataset, see 2.2.1.3) from the agricultural baseline simulation. Thereby, we exclude any potential transgressions due to natural processes as simulated in LPJmL. Also, we omitted the calculation of the N PB status in all cells with arid climate (annual precipitation ÷ potential evapotranspiration <0.2 (UNEP, 1997)) due to negligible leaching (Skujiņš, 1981). It should be noted that our approach intends to focus on the agricultural impact on surface water eutrophication by taking into account N losses from soils, exclusively. As in Chang et al. (2021) and de Vries et al. (2021), additional N inputs to surface waters from direct atmospheric deposition and point sources such as sewage or aquaculture, as well as instream-retention are not accounted for.

2.2.2.3 Planetary Boundary for Land-system change

As proposed in Steffen et al. (2015), the land-system change PB is defined based on remaining forest cover (i.e. non-deforested areas) to acknowledge the importance of forests in climate regulation. At a sub-global level, biome-specific thresholds for minimum forest cover have been defined for tropical, temperate, and boreal forest ecosystems (see Table 2). For tropical and boreal forests, these thresholds are stricter because of substantial climate feedbacks through changed evapotranspiration (tropical forest) and albedo (boreal forest) with potential impacts beyond the region of forest loss through teleconnections. We here estimate pristine forest cover based on a simulation with potential natural vegetation under current climate (1986-2015) and assign cells to tropical, temperate, and boreal forest based on foliage projected cover of simulated plant functional types (see 2.2.2.5 for more details). The status of the PB for land-system change is then determined for each biome and continent by subtracting current pasture and cropland areas (see Table S1) from pristine forest cover and averaging the remaining forest cover in all cells belonging to the respective biome. To account for the uncertainties associated with the geographic extent of potential natural forest biomes, we additionally calculate the status of the land-system change PB based on spatially-explicit forest biome extents from Olson et al. (2001) (see 2.2.2.5).

2.2.2.4 Planetary Boundary for Biosphere Integrity

In the PB framework, biosphere integrity is addressed by two key roles of biosphere in the Earth system: 1) the genetic diversity providing genetically unique material to ensure further evolution, adaption and resilience of life on Earth; and 2) the functional diversity of species connected in a complex network of functional traits to ensure ecosystem stability. For both components Steffen et al. (2015) proposed interim control variables, because no measure for the global impact of biosphere degradation has been developed until today. While genetic diversity is assessed by the global extinction rate, the functional diversity is evaluated by the Biodiversity Intactness Index (BII) at biome level. Our analysis of NE potentials restricted by PBs considers the latter, as a spatially explicit assessment can only be applied for this component. The BII measures the average abundance of originally present species relative to abundance in an undisturbed habitat (Scholes & Biggs, 2005). In order to stay within the safe operating space of functional biosphere integrity, a BII of 90% species abundance must be maintained within biomes (Steffen et al., 2015) (Table 2).

Our assessment of the current status of the PB of functional biosphere integrity is based on the latest product of a global quantification of the BII from Newbold et al. (2016) with information on species abundance at a resolution of 30 arc seconds. Newbold et al. (2016) derived the spatially-explicit BII from a statistical model based on among-site comparisons of species abundance at 18,659 sites from the PREDICTS database (Hudson et al., 2014) that were scored for four putative pressures: land use and use intensity, human population density and proximity to roads. We aggregated the BII data to the LPJmL grid of 0.5° x 0.5° and assessed its mean values over biomes (see 2.2.2.5).

Table 2: Overview on applied control variables and thresholds for terrestrial planetary boundaries. Values within brackets refer to the zone of uncertainty used for the calculation of the current status of PBs in 3.1.1.

Earth System Process	Control Variable	Threshold for Planetary Boundary (zone of uncertainty)	Sub-global assessment Unit	Reference
Change in biosphere Integrity	Biodiversity Intactness Index (BII)	Maintain BII at 90% (90-30%) or above	Biomes, for each continent	Steffen et al. 2015, Newbold et al. 2016
Biogeochemical Flows (N cycle)	N in runoff to surface water as proxy for dissolved inorganic N concentrations in surface water	1 mgN l^{-1} (1-2.5 mgN l^{-1})	LPJmL grid cells	De Vries et al. 2013, 2021
Land-System Change	Area of forested land as % of potential forest for each biome	Tropical: 85% (85-60%) Temperate: 50% (50-30%) Boreal: 85% (85-60%)	Forest biomes, for each continent	Steffen et al. 2015
Freshwater Use	Blue water withdrawal as % of mean monthly river flow	low-flow months (MMF < 0.4 x MAF): 25% (25-55%); intermediate-flow months (MMF > 0.4 x MAF & MMF ≤ 0.8 x MAF): 40% (40-70%) high-flow months (MMF > 0.8 x MAF): 55% (55-85%)	LPJmL grid cells	Steffen et al. 2015, Pastor et al. 2014

2.2.2.5 *Classification of biomes*

Given (i) the uncertainty associated with geographic distribution of natural biomes and (ii) the impact of the biome classification on both the biosphere integrity and the land-system change PBs (the geographic extent over which the status is averaged has a strong influence), we use two independent biome classifications for forest extents and PB status calculations:

a. An LPJmL derived classification based on simulated distribution of plant functional types under potential natural vegetation, adapted to the new model version from Ostberg et al. (2013) and Ostberg et al. (2015) (Figure 3a and more details on the adaptions in the appendix). While being well validated against satellite derived biomes, not yet fully understood N feedbacks lead to minor anomalies in biome distribution in LPJmL5-NEGEM (e.g. dominance of boreal deciduous forest over evergreen forest), which are being addressed by further model development
b. The widely used biome extents from Olson et al. (2001) (Figure 3b, for details on processing of the shapefiles see appendix)

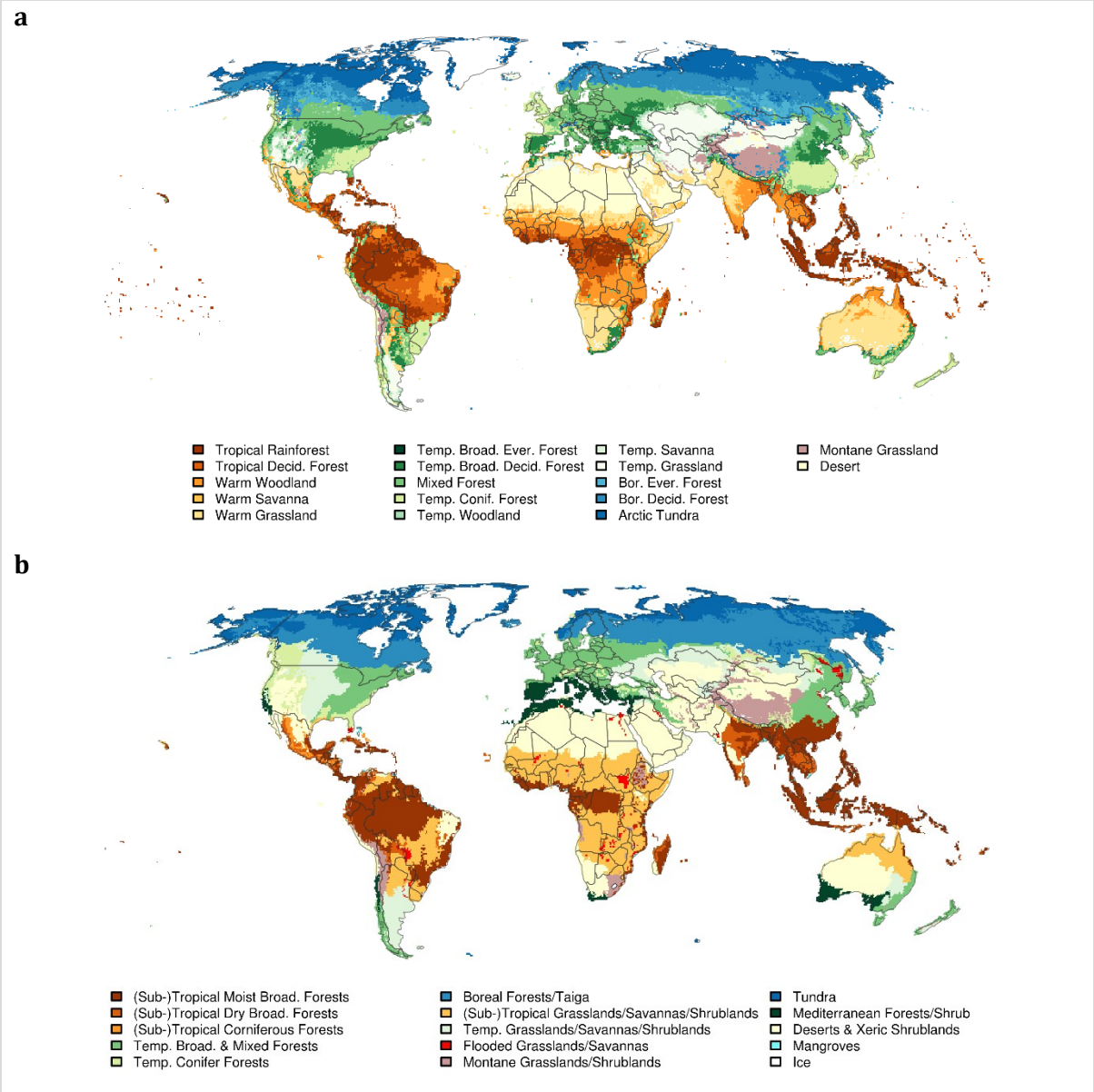

Figure 3: Biome distribution based on geographic distribution of natural plant functional types in LPJmL(a) and Olson et al. (2001) (b)

2.2.3 CO_2 removal efficiencies from the MONET framework

While LPJmL is a start-of-the-art tool for simulating spatially-explicit harvest on biomass plantations, we rely on the Modelling and Optimisation of Negative Emissions Technology (MONET) framework (see NEGEM Deliverables D7.1 and D7.2), Chiquier et al. (2022, in review)) to convert LPJmL harvest to net NEs by accounting for the CDR efficiency of BECCS and PyCCS along the supply chain. The CDR efficiency (CEff) of BECCS and PyCCS as determined with MONET can be defined as the fraction of CO_2 captured (*i.e.,* CO_2 biogenically sequestrated via photosynthesis during the biomass growth) that is permanently removed from the atmosphere, once the CO_2 emissions arising along the value chain of BECCS and PyCCS have been accounted for. The CEff η^{CDR} can be expressed as follows, considering CO_2 captured $CO_2^{Captured}$ and CO_2 leaked over the supply chain CO_2^{Leaked}:

$$\eta^{CDR} = \frac{CO_2^{Captured} - CO_2^{Leaked}}{CO_2^{Captured}}$$

For BECCS, upstream CO_2 emissions as considered within MONET arise from biomass cultivation, harvest, processing, and transport, and downstream CO_2 emissions are associated with the capture, transport and storage of CO_2 into geological reservoirs. While the percentage of biogenic C that is captured and sequestrated can vary significantly depending on the BECCS energy conversion pathway, we here assume BECCS to be a biomass-to-electricity pathway, with a CCS rate ranging from 90% to 98% (Bui et al., 2021). Other key factors for the CEff include the CO_2 intensity of the energy system (i.e., electricity, fuels (diesel) and natural gas for the drying of biomass), and the transport distance of the biomass from the farm to the BECCS plant.

To represent a range for potential future CEff, we consider the three following scenarios with variations in key parameters along the supply chain:

- Optimistic scenario: The CCS rate is assumed to be 98%, the energy system is almost entirely decarbonised (electricity is CO_2 neutral, fuels are replaced by 90% of biofuels, and natural gas for biomass drying is also replaced by 90% of wood), and the biomass is transported over short distances (100 km), representing a relatively high density of BECCS plants.
- Medium scenario: The CCS rate is assumed to be 95%, the energy system is partially decarbonised (a third of the current CO_2 intensity for electricity (475 g CO_2/kWh in 2018 according to (IEA, 2019)), fuels are replaced by 50% of biofuels, and natural gas is also replaced by 50% of wood), and the biomass is transport over longer distances (250 km).
- Lower scenario: The CCS rate is assumed to be 90%, the energy system is scarcely decarbonised (two third of the current CO_2 intensity for electricity, fuels are replaced by 10% of biofuels only, and natural gas is also replaced by 10% of wood), and the biomass is transport over long distances (500 km).

Depending on 1) the scenario and 2) the type of biomass used, *i.e.* miscanthus (for herbaceous biomass) or willow (for woody biomass), the CEff of BECCS η_{BECCS}^{CDR} is shown in Table 3.

For PyCCS, upstream CO_2 emissions arise from biomass cultivation, harvest, processing, and transport, and downstream CO_2 emissions are associated with the conversion of biomass into biochar at the pyrolysis plant, and the transport and application of biochar on soil. In this study we exclusively assume biochar storage in agricultural soils because PyCCS is suggested to be applied as a decentralized NET without requiring infrastructures for geological storages. Scenarios of high technological development and investment could, however, alternatively assume the additional storage of further pyrolysis products (bio-oil and permanent pyrogases) in geological storages to enhance the overall CO_2 capture efficiency.

Table 3: CDR efficiency for the three defined BECCS and PyCCS scenarios

	CDR efficiency					
	BECCS				PyCCS	
	herbaceous biomass		woody biomass		herbaceous biomass	
	%	$t\ CO_2$ removed/t biomass DM	%	$t\ CO_2$ removed/t biomass DM	%	$t\ CO_2$ removed/t biomass DM
Scenario 1 (optimistic)	92%	1.60	88%	1.57	24%	0.42
Scenario 2 (medium)	84%	1.45	73%	1.31	23%	0.40
Scenario 3 (lower)	80%	1.37	66%	1.18	22%	0.38

The PyCCS feedstock in our analysis are fast-growing lignocellulosic grasses, parametrized as miscanthus and switchgrass in LPJmL (see 2.2.1.2). They suit as representatives for low maintenance biomass production for the biochar supply of agricultural land enabling the LCN-PyCCS approach. The C, ash and lignin content of lignocellulosic grasses was collected from the Phyllis2 database (Phyllis2, 2022) and averaged over all miscanthus and switchgrass entries (excluding entries for ensilaged biomass).

For the pyrolysis process, we assumed parameters for slow pyrolysis with the highest heating temperature at 500°C to ensure relatively high biochar yields at the same time as high shares of recalcitrant biochar. The feedstock- and temperature-specific biochar yields (23% of ash-free dry matter feedstock biomass) and C content of the char (82% of ash-free dry matter biochar) were calculated based on formulas from Woolf et al. (2021). For the permanence of biochar, we apply the conservative estimate of 74% C remaining in the soil after 100 years based on an annual decay rate of 0.3% per year for biochar with H/C ratios <0.4 from the findings of Camps-Arbestain et al. (2015). Overall, this results in a CO_2 capture efficiency of 28% of the feedstock C.

In addition to the settings in the pyrolysis process, the net CEff derived by MONET depends on the transport distance of the biomass and the biochar (see biochar implementation described in D7.2). Here, we set the mean distance of all scenarios to 55 km – the length across the latitudes of 0.5°x 0.5° LPJmL grid cells, which we assume to be self-sufficient in biochar supply, representing a decentralized approach to NE production. Additional factors for the CEff are the CO_2 footprint of the energy supply and the biofuel share in the transport sector. In this regard, all three LCN-PyCCS scenarios are aligned with the assumptions in the corresponding BECCS scenario (Table 3).

2.3 Assessing planetary boundary limited NETP potentials

2.3.1 BECCS

To derive maximum NE potentials from plantation-based BECCS constrained by regional PBs, we first define the areas potentially available for biomass plantations of dedicated energy crops. We then optimize the geographic distribution of biomass plantations on these areas to maximize NE provision while not leading to further transgressions of regional PBs for N flows, freshwater use, land-system change and biosphere integrity (see Figure 4 for an overview of the approach). As an update to Heck et al. (2018), N flows are dynamically modelled within LPJmL, which allows to (i) better represent the N PB (see 2.2.2.2), (ii) differentiate the geographically explicit effect of biomass plantations on the N PB depending on fertilization levels (see 2.2.1.2), and (iii) include emissions of the greenhouse gas nitrous oxide (N_2O) in the calculation of net NEs (see 2.3.1.2).

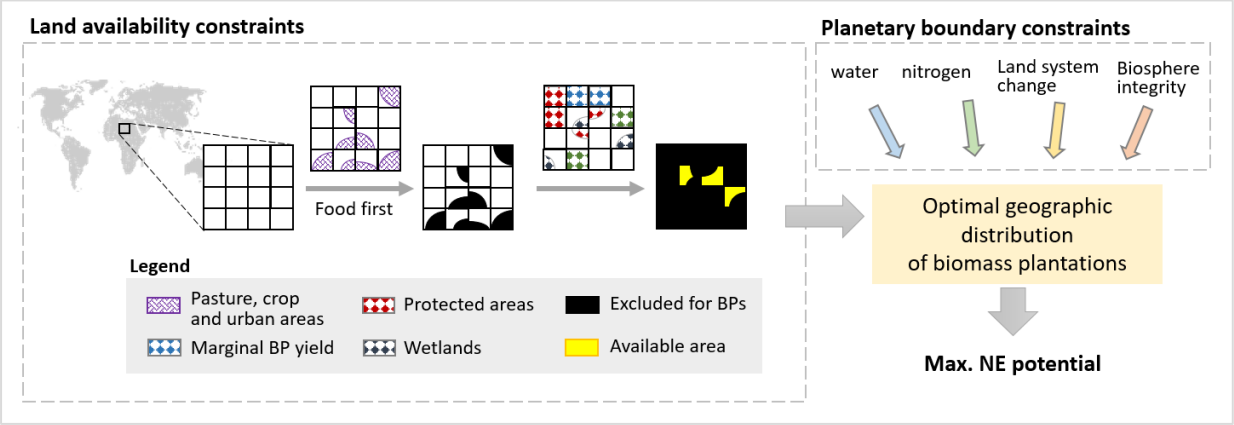

Figure 4: Conceptual overview on the approach to derive maximum negative emission potentials from plantation-based BECCS as constrained by land availability and planetary boundaries. BPs = 2nd generation biomass plantations for BECCS.

2.3.1.1 Land availability constraints for biomass plantations

We exclude all agricultural and urban areas for the year 2015 (Hurtt et al., 2020), thus only allowing for conversion of natural vegetation to biomass plantations. Further, we block all protected areas according to IUCN&UNEP-WCMC (2015) and wetlands from Lehner and Döll (2004), given the counteractive climate effect of draining wetlands (see Figure 5a). To only consider areas with economically reasonable yields on biomass plantations, we apply a yield threshold of 5 t DM ha^{-1} yr^{-1} (Hastings et al., 2009). This results in different masks depending on the biomass plantations type (biograss (bg) or biotree (bt), rainfed (rf) or irrigated (irr), low or high fertilization (l/hF)). Figure 5b displays the simulated biomass yields for each of the eight biomass plantation types as well as the blocked areas below the yield threshold.

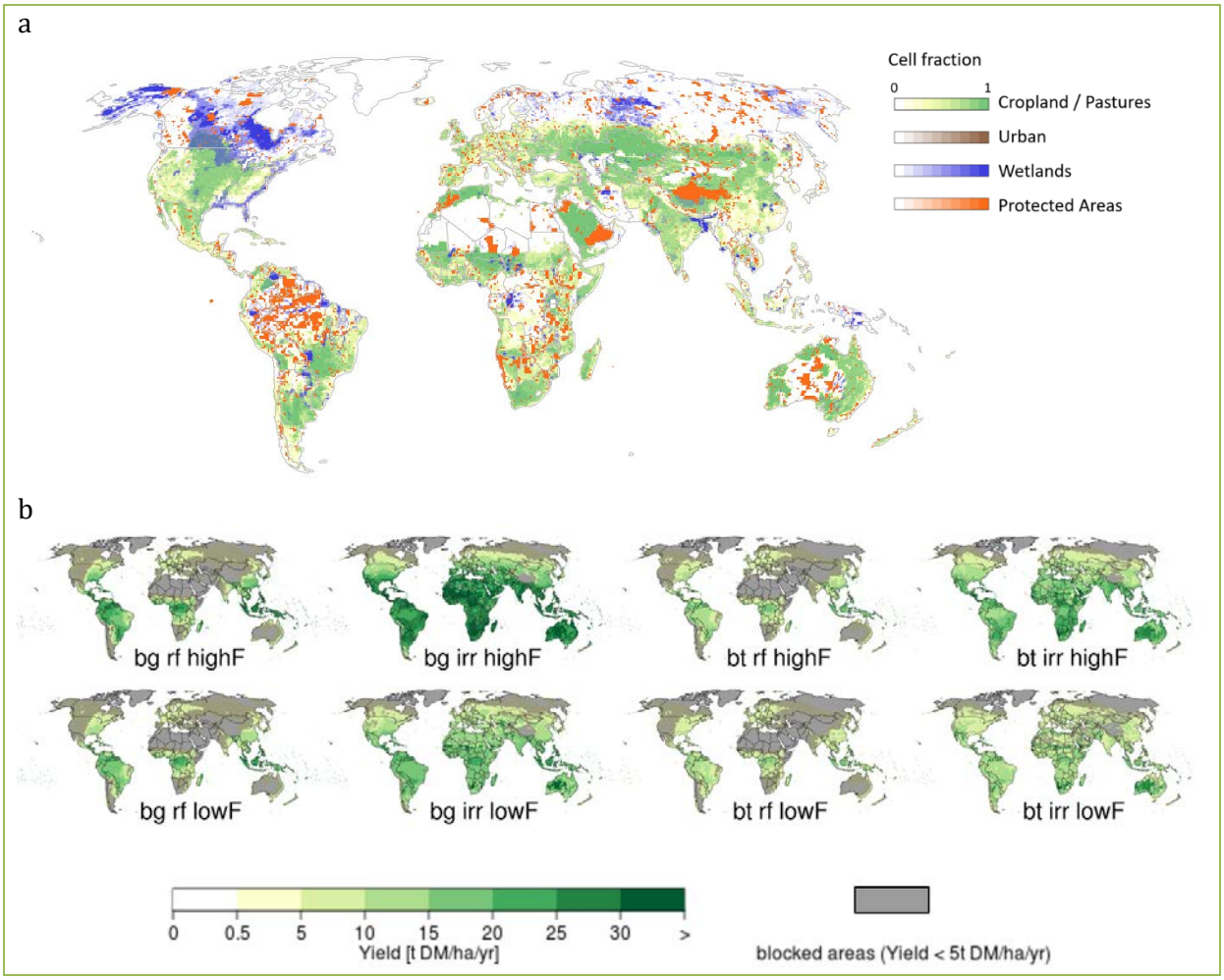

Figure 5: Geographical distribution of land availability constraints for biomass plantations. (a) Cell fractions blocked for biomass plantations due to agricultural use, urban areas, wetlands and protected areas. (b) Dry matter (DM) yield of the eight biomass plantations configurations (Ø 1986-2015 climate) as well as blocked cells with yields below the harvest threshold of 5t DM $ha^{-1}yr^{-1}$. bg = biograss (herbecous biomass plantation), bt = biotree (woody biomass plantation), rf = rainfed, irr = irrigated, highF = high fertilization, lowF = low fertilization.

2.3.1.2 Optimization of geographic distribution of biomass plantations under planetary boundary constraints

The optimization model developed in Heck et al. (2018) was refined and expanded to distribute biomass plantations in available 0.5° cells or cell fractions outside of agricultural baseline areas (see 2.3.1.1), considering eight biomass plantation configurations (herbaceous and woody, each rainfed and irrigated, each high and low fertilization). Based on the upgraded LPJmL model with N flows, the management spectrum on biomass plantations could thus be expanded in comparison to Heck et al. (2018) by including fertilization scenarios (high and low) within the optimization. To optimize geographic distribution of biomass plantations under PB constraints, we first calculated potential net NE for each grid cell (j = 1…n) and biomass plantation type ($p \in \{bg_{rf_{hF}}, bg_{rf_{lF}}, bg_{irr_{hF}}, bg_{irr_{lF}}, bt_{rf_{hF}}, bt_{rf_{lF}}, bt_{irr_{hF}}, bt_{irr_{lF}}\}$) by multiplying the 40 year harvest from biomass plantations (H_j^p) with the biomass-feedstock specific carbon removal efficiency ($CEff^p$) and subtracting (i) land use change emissions (LUC_j^p) and (ii) additional N_2O emissions (in CO_2-eq; $N20_j^p$):

$$netNE_j^p = H_j^p * CEff^p - LUC_j^p - N20_j^p$$

H, LUC and $N2O$ were obtained from global simulations with biomass plantations in LPJmL and with fertilization levels and irrigation as described in 2.2.1.2. LUC through biomass plantations were calculated based on the 40-year average difference in C pools (soil, litter, vegetation) between the specific biomass plantation type and natural vegetation. $N2O$ in turn, converted to CO_2 equivalents, was determined by subtracting cumulative 40-year emissions from potential natural vegetation from nitrous oxide emissions on biomass plantations, thereby providing the additional emissions caused by cultivation of biomass (depending on fertilization level / irrigation / feedstock type).
We apply elaborate scenarios of $CEff$ for biomass to electricity conversion, by taking into account a detailed representation of the BECCS supply chain in the MONET framework (see 2.2.3) and differentiating between herbaceous and woody feedstocks. Also, we do not only account for fossil energy use along the supply chain, but also for additional nitrous oxide emissions, thus better representing potential net NEs than in Heck et al. (2018).

To maximise net NE provision under regional boundary constraints (C_{PB}^{reg}) of freshwater use (W), nitrogen flows (N), land-system change (L) and biosphere integrity (B), a linear weighted sum optimization was then performed based on the R package lpSolveAPI (Heck et al., 2018; Konis & Schwendinger, 2020). The geographic distribution of cell fractions (f_j^p) for the respective biomass plantation types is thus optimized as follows:

$$\max_{f_j \in C_{PB}^{reg}} \left(\sum_{j=1}^{n} \sum_{p} f_j^p \cdot netNE_j^p \right)$$

with the regional constraints C_B^{reg}, C_W^{reg}, C_N^{reg} and C_L^{reg}.
We chose to maximise net NEs in contrast to harvest in Heck et al. (2018), assuming that NE provision and not biomass supply is economically rewarded.

Regional boundary constraints

Net NE provision is maximised under regional boundary constraints, by allowing land use expansion for biomass plantations where regional thresholds according to the PB framework are not transgressed by current agricultural land use and expanding up to the point they are reached.

Freshwater Use
For the freshwater PB constraint, the available water for irrigation of biomass plantations ($Wavail$) in each cell j is calculated for each month, after subtracting (i) agricultural water withdrawals, (ii) withdrawals for household, industry and livestock as well as monthly EFRs in line with the PB definition (see 2.2.2.1). A maximum irrigated cell fraction for each biomass plantation type (p) is then defined based on the smallest monthly (m) ratio between cell-specific $Wavail$ and irrigation water demands of biomass plantations, if the entire cell was covered by irrigated bioenergy crops ($WirrigBP$). Thus, the month with the "strictest" irrigation water constraint determines the maximum irrigated cell fraction ($maxIrrig$) in order to ensure provision of EFRs in all months of the year (omitting months with WirrigBP = 0):

$$maxIrrig_j^p = \min_{m \in 1...12} \left(\frac{Wavail_{j,m}}{WirrigBP_{j,m}^p} \right)$$

In the optimization, water availability for irrigation of biomass plantations is additionally limited at the cell and river basin level: Maximum monthly water availability in each cell, averaged over the irrigation period, is reduced by upstream irrigation withdrawals from biomass plantations (minus return flows) to account for upstream-downstream effects. At the basin level, a constraint is introduced, which limits water withdrawals in each basin to the water availability in the respective final drainage cell.

Nitrogen

For the regional optimization constraint C_N^{reg}, biomass plantations can be allocated to cells until the regional maximum yearly N load in runoff according to the boundary threshold ($PB_{threshold}$=1 mg N l^{-1}) is reached. The maximum allowable additional N load in runoff from biomass plantations is calculated for each cell j as follows, based on the yearly runoff $runoff_{LU}$ and N load within runoff (N_{LU}) in the agricultural baseline:

$$N\ budget_j = runoff_{LU\,j} \cdot PB_{threshold} - N_{LU\,j}, \text{ set to 0 if <0}$$

In all cells with a transgression in the agricultural baseline, no biomass plantations can be added; in cells with arid climate, the constraint is not applied (see 2.2.2.2). Total added N load from all biomass plantation types within a cell j must be smaller than the remaining $N\ budget_j$, so that combined N loads from the agricultural baseline and the biomass plantations do not transgress the regional threshold for runoff.

Land-system change

The regional constraint for land-system change takes effect at the level of major forest biomes (temperate, tropical, boreal) for each continent (see 2.2.2.5). Conversion of forests to biomass plantations is only allowed to the extent that deforestation from both the agricultural baseline and biomass plantations do not exceed the biome-level boundaries as defined by the PB. Thus, in cells where the land-system change boundary is already transgressed in the year 2015 agricultural baseline, allocation of biomass plantations is disallowed.

Biosphere integrity

Under the optimization constraint for biosphere integrity, natural vegetation can be converted to biomass plantations (p ∈ biomass plantation types; f_j^p= cell shares of biomass plantation types) as long as the BII averaged per biome and continent is ≥90%:

$$\frac{1}{n} \cdot \sum_{j=1}^{n} \sum_{p} \left(BII_{LU\,j} - f_j^p \cdot\ BIIeffect_p \right) \geq 90\%$$

with j encompassing all cells belonging to a biome (b).

For the agricultural baseline, we assume the spatially explicit BII as published by (Newbold et al., 2016) (BII_{LU}). To estimate reductions of BII through added biomass plantations ($BIIeffect_p$), we account for land use and land use intensity as the most important explanatory variables of the Newbold model. Yet, the spatial resolution of our analysis is not compatible with the representation of effects from human population density and proximity to roads as assessed in Newbold et al. (2016). Thus, for the fraction of the grid cell that is assessed for conversion to biomass plantations, we reduce the BII by the statistically quantified abundance difference weighted by the respective effected area. For woody bioenergy crops, we assume a BII reduction of 34% on plantations as published in Newbold et al. (2016) for intense use of forest plantations. For herbaceous biomass plantations, we take the average BII reduction for second generation biofuel crops from (Tudge et al., 2021). While Tudge et al. (2021) also provide specific entries for perennial grasses, the data base does not include any miscanthus or switchgrass entries and only very limited data (e.g. no data on the effect on vertebrates). Therefore, the average BII reduction across all second-generation biofuel crops was taken (29%). It is important to note, that both

current BII and BII effects of biomass plantations are highly uncertain. For the latter, we cannot capture a spatially explicit effect of biomass plantations on BII, nor a management specific BII impact, due to a lack of available data.

Final net NE potentials

To ensure consistency in biogeochemical and hydrological modelling, the land use patterns obtained from the optimization model were simulated with LPJmL for 40 years with shuffled climate from 1986-2015 and a 0.5° resolution, thereby covering a full plantation lifecycle of simulated woody biomass plantations. Upon clearing of natural vegetation, timber is assumed to be harvested for wood products and not for BECCS because of the higher material quality. Timber products from this one-time harvest are however not considered for NEs, assuming that they are eventually fully converted to CO_2 ("committed emissions"). In total, net NE potentials for six scenarios were determined as described above (for two different biome classification (see 2.2.2.5), impacting the biosphere and land-system PB constraint, and three CEff scenarios (see 2.2.3).

2.3.2 Reforestation

Potentially providing co-benefits for climate change mitigation, biodiversity, water regulation and human health amongst others (Beatty et al., 2022; Ellison et al., 2017), reforestation is discussed as important cornerstone for "sustainable" CDR by integrating a range of interrelated sustainability targets (Griscom et al., 2017; Smith, Adams, et al., 2019; Soto-Navarro et al., 2020). To harness this potential with regard to PB compatible NE potentials, we here deliberately define reforestation as the restoration of natural forest ecosystems (i.e. only including areas where forests would naturally grow (see 2.2.2.3), assuming planting of native species and excluding harvesting).

We calculate NE potentials through reforestation by (A) defining targeted area scenarios, (B) generating spatially explicit reforestation patterns by prioritizing non-fragmented forest restoration in proximity to remaining forest cover, and (C) simulating NEs based on changes in C pools (Figure 6). Details on each of the steps are provided in the following.

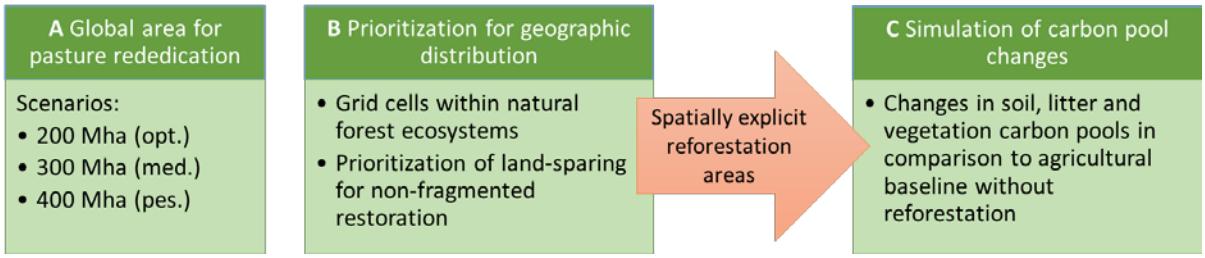

Figure 6: Approach to derive negative emission potentials through reforestation.

2.3.2.1 Assumptions on global areas for pasture rededication (A)

Considering only reforestation and not afforestation, agricultural areas on previously forested land constitute potential target areas. While future reductions in cropland are unlikely, pasture areas may however be released through diet changes towards less livestock products and/or efficiency increases in animal husbandry (Griscom et al., 2017; OECD & FAO, 2020). Thus, global permanent meadows and pasture areas have already declined

between 2000 and 2019 by 6% (IPCC, 2022). At the same time, population growth may counteract these trends, and drastic large-scale diet changes, although desirable from an environmental perspective, might be considered unlikely. In line with the aim of NEGEM to assess realistic and responsible NE pathways, we therefore evaluate three scenarios aiming to span the range of cautious literature estimates on pasture rededication potentials (see Table 4): 200 Mha (lower scenario), 300 Mha (medium scenario) and 400 Mha (optimistic scenario). We deliberately chose estimates without land-based climate change mitigation as strong decreases in pasture areas in these scenarios are often based on highly ambitious assumptions regarding agricultural intensification (Chavas, 2008; Humpenöder et al., 2018). Our scenarios for rededicated pasture extent are also well in line with a recent publication on forest restoration opportunities in close proximity to intact or degraded closed forests (344 Mha; Littleton et al. (2021)) as well as with "The Bonn Challenge", an international initiative with the goal to bring 350Mha of degraded or deforested areas into restoration until 2030 (https://www.bonnchallenge.org/).

Table 4: Literature estimates on potential decreases in the extent of global pasture areas.

Decrease in pasture areas	Details on scenario	References
~290 Mha	Land use change between 2010 and 2050 in the SSP1 scenario (SSP=shared socio-economic pathway), simulated with the IMAGE model; no consideration of land-based climate mitigation	van der Esch et al. (2017)
SSP1: mean across models = ~180 Mha, highest estimate = 388 Mha SSP2: mean across models = ~30 Mha *increase,* highest estimate = 362 Mha decrease	Land use change between 2010 and 2050 for SSP1 and SSP2 as simulated by 6 integrated assessment models (AIM, GCAM, GLOBIOM, IMAGE-MAGNER, MAgPIE, IMPACT); no climate impact and mitigation elements such as afforestation or BECCS included	Stehfest et al. (2019)
408 Mha	Land use change between 2015 and 2100 in the SSP2-RCP4.5 scenario, simulated with the GLOBIOM model; no perennial crops for BECCS	Hurtt et al. (2020)
490 Mha	Land use changes through measures to increase the C sequestration on farmland (diet change, yield growth, increased feeding efficiency and waste reduction), simulated with a biomass-balance model; in comparison to reference land use for 2050 (TREND Scenario in Erb et al. (2012))	Smith et al. (2013)
"close to 200 Mha"	Reducing meat consumption in households with the highest levels of per capita consumption today to the global average level	IEA (2021)

2.3.2.2 Prioritization for spatially explicit reforestation areas (B)

To generate spatially explicit reforestation patterns, we first exclude all pasture areas in cells without natural forest growth according to (a) the LPJmL-based biome classification and (b) the biome classification from Olson et al. (2001) (see 2.2.2.5 and Figure 3). By applying these two independent biome classification schemes, we take into account the uncertainty associated with defining natural forest areas. Given the importance of intact forest landscapes for conservation (Betts et al., 2017) and to minimize fragmentation, we then prioritize cells for (always complete) reforestation with high shares of remaining forest (Gerten et al., 2020): Cells are ranked according to the mean share of remaining forest within the cell itself and the eight neighbouring cells. We then iteratively select the cells with highest remaining forest cover until the targeted area according to the scenario (i.e. 200, 300 or 400 Mha) is reached cumulatively. By prioritizing the proximity to larger forest areas, reforested areas "can form buffer zones and corridors between forested areas, increasing resilience and recovery in both intact forests and adjacent reforested land" (Littleton et al., 2021, p. 13).

2.3.2.3 Simulation of negative emission potentials (C)

To simulate NE potentials from reforestation, we compare C pools in vegetation, litter and soil between an LPJmL run with reduced pasture areas according to the spatially explicit reforestation patterns (B) and the agricultural baseline run (see 2.2.1.3). On reforestation areas, natural vegetation is simulated to regrow on former pasture

areas, undergoing establishment and competition among plant functional types as implemented in a process-based manner within LPJmL. While this approach is well suited to derive the maximum C sequestration in mature forests, the temporal evolution of C pool changes in a managed forest is not well represented due to the absence of an explicit reforestation module with planted tree saplings of higher age instead of slow establishment of competing small plants. Therefore, we derive maximum C pool changes in mature forests from our simulations and apply biome specific adjustment factors to calculate C sequestration after 40 years. The adjustment factors are based on Braakhekke et al. (2019), who implemented a forest plantation module in an earlier LPJmL version without N dynamics, accounting for increased stemwood C growth rates in planted forests. We thus use the share of maximum stemwood C reached after 40 years in forest plantations as simulated in Braakhekke et al. (2019) as proxy, differentiating between tropical, temperate and boreal forests, and multiply it with here simulated C pool changes (tropical: 55%, temperate: 50%, boreal: 13%). This total C sequestration within the first 40 years is downscaled to yearly C sequestration rates, referring to the average rate over the assessed timeframe.

2.3.3 LCN-PyCCS

In addition to BECCS and reforestation, we assess further potentials for CDR without additional transgressions of the four assessed PBs following the LCN-PyCCS approach.

We apply LPJmL to simulate the potential rainfed biomass yields on (sub-)tropical cropland redistributed to PyCCS feedstock production and subsequently calculate the NE potentials for three different scenarios. They feature three levels of biochar-mediated yield increases in the (sub-)tropics (10%, 15% and 20%) combined with the corresponding lower to upper assumptions on the fertilization of biomass crops and, accordingly, the lower to upper estimates of PyCCS C sequestration efficiencies derived from MONET (22%, 23% and 24%). The range of yield increases assumed after biochar application as fertilizer enhancer is based on recent meta-analyses (Bai et al., 2022; Melo et al., 2022) and described in more detail in the appendix. The medium values for yield increases (15%), fertilization (simulated input = N harvest in simulation of unlimited N supply, see 2.2.1.2) and CEff (23%) mark the standard scenario, while the others draw a range from less efficient to optimized systems.

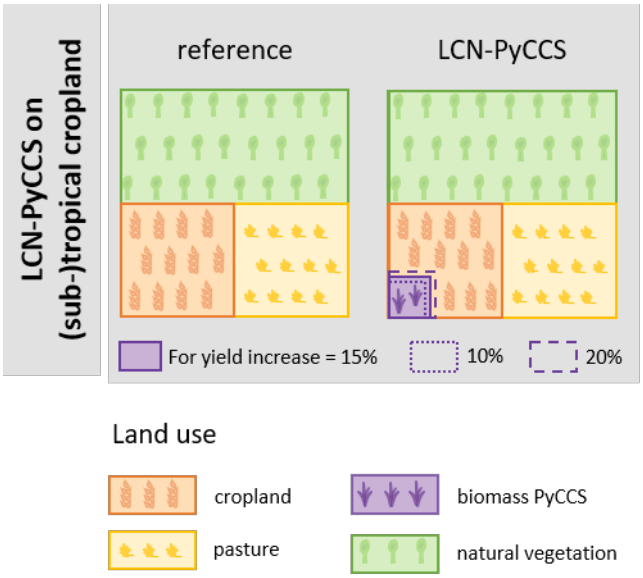

Figure 7: Visualization of land use allocation in a generic LPJmL grid cell for the reference scenario and the LCN-PyCCS scenarios of three different levels of biochar-mediated yield increases (10%, 15%, and 20%).

For the assessment of LCN-PyCCS potentials in the three scenarios of distinct levels of yield increases (10%, 15% and 20%), we assumed biochar-mediated yield increases exclusively on cropland within tropical and subtropical regions of the Köppen-Geiger classification. We selected the (sub-)tropics as our focus region for LCN-PyCCS as the soils have shown the largest response to biochar applications (Jeffery et al., 2017; Ye et al., 2020), while the regions are also characterized by wider yield gaps in general (Mueller et al., 2012). Through the yield increases, a fraction of the cropland (9%, 13%, and 17% corresponding to 10%, 15% and 20% yield increase, respectively) can be dedicated to PyCCS feedstock production to provide self-sufficient biochar supplies plus NE while maintaining calorie production (Figure 7). To emphasize the advantage of LCN-PyCCS as a decentral approach, we model each cell in the (sub-)tropics as closed systems of agriculture without trade of biochar. Thus, in order to supply sufficient biochar for the remaining cropland in the system (i.e. 1t ha^{-1}), the biochar yield needs to be particularly high if yield increases are relatively low, because the lower the yield increase, the smaller the area of land dedicated to feedstock production.

After a preliminary simulation of potential biomass yields, we exclude the cells from the analysis in which the areas dedicated to PyCCS feedstock production cannot provide enough biomass to supply the remaining cropland in the cell with sufficient biochar. However, the simulated yields strongly depend on the prescribed N-input and the response of herbaceous lignocellulosic biomass crops to specific levels of fertilization in LPJmL5-NEGEM could not be validated, due to a lack of the respective observational data. Thus, we additionally test the LCN-PyCCS approach with simulations of unlimited N supply to address the effect of uncertainties in the fertilization response. These represent cases of optimal fertilization which might be possible if the farmer is particularly invested in producing biochar to increase crop yields and the land's C sink.

Further, we block those cells where the N-PB was either already transgressed in the agricultural baseline scenario or where the fertilization of introduced biomass crops would lead to a transgression. The biomass yields of the cells confirmed as suitable for the LCN-PyCCS approach after this filtering are combined with the corresponding CEff to calculate the NE potential.

3 Results

3.1 BECCS potentials constrained by planetary boundaries

3.1.1 Current planetary boundary transgressions: Severe constraints on NE provision through BECCS

All four terrestrial PBs already show severe and widespread transgressions with boundary-specific regional patterns (see Figure 8). Most extensive PB transgressions were calculated for the biosphere integrity PB (based on biome-wise averaged BII from Newbold et al. (2016), see 2.2.2.4), with only boreal biomes and tropical forest ecosystems still classified as "safe" (BII >90%). In all other biomes, estimated reductions in local terrestrial biodiversity through land use and related pressures exceed the boundary threshold, entering a stage of increased risk (Newbold et al., 2016). However, due to a lack of knowledge on the relationship between BII and the functioning of the Earth system, it is unclear at what point the Earth system stability is critically affected and which BII value marks the zone of high risk. Further, historic deforestation has led to transgressions of the land-system change boundary in all tropical forest biomes except for Oceania, as well as in temperate forests in South America and Africa according to the applied land use dataset (2015) as well as LPJmL derived forest biomes. Despite high overall deforestation, temperate forests in Europe, North America and East Asia on the other hand are still classified as "safe", which also reflects less strict boundary thresholds for these biomes (see 2.2.2.3). In contrast to Gerten et al. (2020) and Steffen et al. (2015), deforestation in boreal forest biomes does not lead to an exceedance of the land-system change boundary in our analysis. This reflects (i) uncertainty in current land use extent as well as pristine forest area, and (ii) differences in how forest biomes were defined (e.g. assumptions on minimum tree cover for forests). To account for the latter, we additionally calculated the biosphere integrity PB (also depending on biome classifications) and land-system change boundary statuses based on biome extents from Olson et al. (2001) (see Figure S1). Except for temperate forests in South America, the regional patterns of land-system change boundary transgressions are robust independent of the two different biome classifications. For the biosphere integrity boundary, both biome classifications overall lead to very similar results, except for a disagreement with regard to the biosphere integrity in temperate forests in East Asia (see Fig. S1).

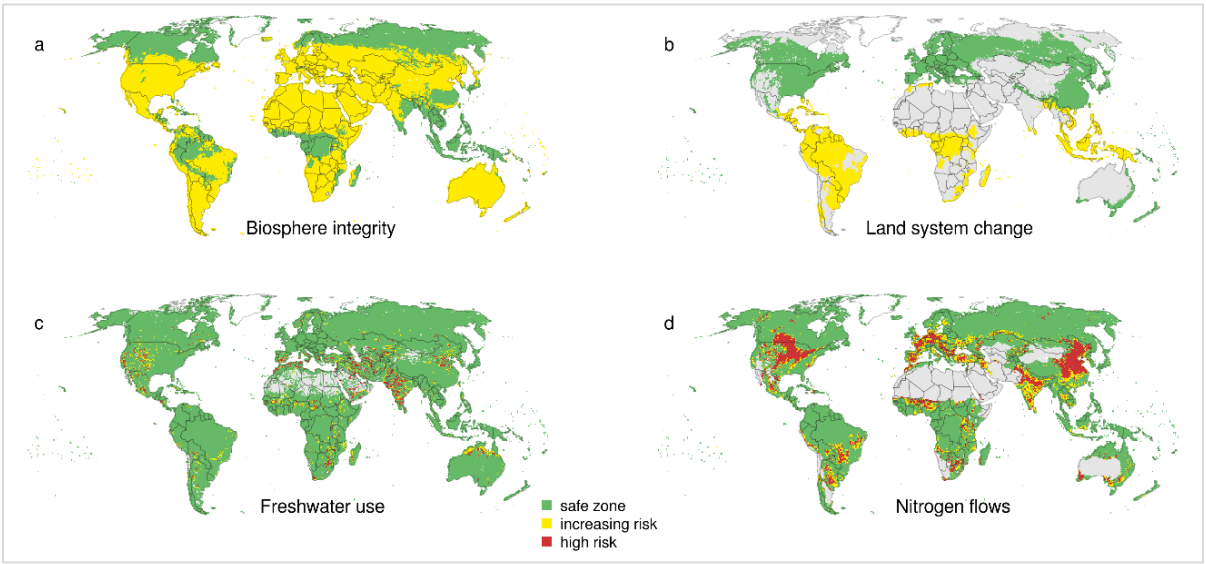

Figure 8: Simulated geographic distribution of the four terrestrial planetary boundaries' status for current agricultural land use (a: 2005 land use; b-d: 2015 land use, averaged over 1986-2015 climate). The status for the biosphere integrity and land-system change boundary is based on the LPJmL derived biome classification (see 2.2.2.5). For the respective maps based on the biome classification from Olson et al. (2001) see Fig. S1. Cells where the boundary definitions do not apply are displayed in grey (land-system change: all non-forest biomes, freshwater use: discharge < 1m/s, nitrogen flows: annual precipitation ÷ potential evapotranspiration < 0.2 (arid climate)).

Regarding freshwater use, EFRs are strongly transgressed in irrigation hotspots such as in Central and South Asia, the Mediterranean and the Great Plains in North America. This is well in line with previous simulations (Gerten et al., 2020), but transgression magnitude is lower in some locations in our analysis. This is due to (i) the updated land use dataset for 2015 (in comparison to 2005 in Gerten et al. (2020)) with less irrigated areas due to a changed data basis and (ii) the N limitation in crop growth now implemented in LPJmL5, which may reduce crop water demand. Finally, regional N boundaries in leaching are greatly exceeded in regions with intense agricultural use and fertilization, such as the corn belt in North America, Western Europe, North India, large parts of Eastern China as well as the Pampa and Cerrado regions in South America, among others. While large uncertainties are inherent to globally estimating regional PB transgressions, the overall picture is robust and independent of modelling approaches (Campbell et al., 2017; Gerten et al., 2020; Steffen et al., 2015): Large parts of the world face severe and often multiple terrestrial PB transgressions today, leading to increased risks for abrupt and irreversible environmental changes.

3.1.2 BECCS potentials constrained by planetary boundaries

As current PB transgressions already call for radical transformations in the food system to get back into the "safe space" (Gerten et al., 2020; Willett et al., 2019), current agricultural production only leaves very little regional opportunities to expand land use within PB constraints. To estimate the maximum NE potentials through BECCS from dedicated energy crops without increased risks through PB transgressions, we optimized distribution of biomass plantations for maximal net NE provision under the condition that biomass plantations may only be added around the agricultural baseline up to the point that regional boundaries are reached.

As a result of the optimization, biomass plantations are primarily allocated in high latitudes of the northern hemisphere, filling a small gap between unsuitable bioclimatic conditions and blocked areas due to PB transgressions (see Figure 9). This mirrors strong PB constraints, particularly regarding biosphere integrity, as well as area availability constraints due to other land uses and bioclimatic limits to economically viable biomass production. Additional areas are identified for potential conversion to biomass plantations in tropical Oceania, and, if biomes are derived from LPJmL, in South-East Asian woodlands. That the resulting areas for biomass plantations may seem unrealistic to actually be cultivated, e.g. given their sparse road infrastructure (e.g. Ibisch et al., 2016), only emphasizes the difficulties in reconciling NE provision from plantation-based BECCS with PBs (Heck et al., 2018). Also, the remaining areas for biomass plantations will have to be evaluated further in terms of other sustainability dimensions, e.g. the protection of remaining natural forests (see below).

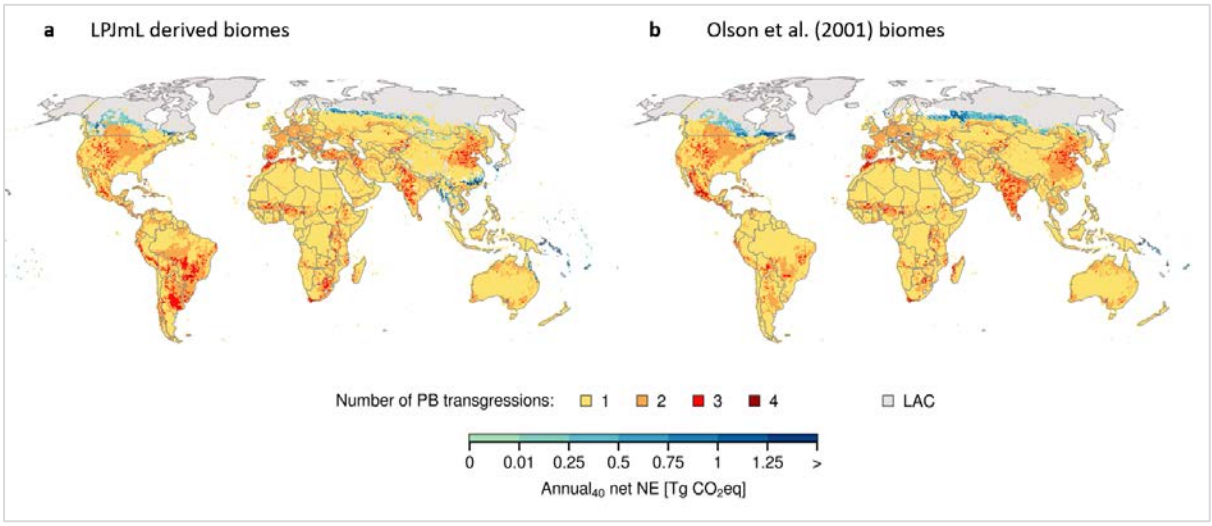

Figure 9: Geographic distribution of net negative emission (NE) potentials from BECCS constrained by planetary boundaries and land availability based on (a) the LPJmL derived biome classification and (b) the Olson et al. (2001) biome extents for biome-specific PB constraints. Land use patterns for biomass plantations result from an optimization model to maximize net NEs from biomass plantations around the agricultural baseline (2015) under PB constraints. Potential yields, water demand and N leaching a.o. from biomass plantations, as input to the optimization, were simulated with LPJmL for 1986-2015 climate. Cells with yields <5t dry matter $ha^{-1}yr^{-1}$ are blocked as well as protected areas and wetlands (Displayed in grey; LAC = land availability constraints).

Regarding the biomass plantation type, herbaceous plantations dominate over woody plantations in all optimization scenarios due to higher simulated yields in most locations (Figure 10 and Figure 5). Also, the optimized land use patterns are predominantly composed of irrigated plantations with more low than high fertilization. As the sparse remaining areas for biomass plantations are found in relatively water abundant regions with minor freshwater PB constraints, irrigated plantations with higher yields prevail. In contrast, the N boundary takes effect in more, primarily boreal, cells.

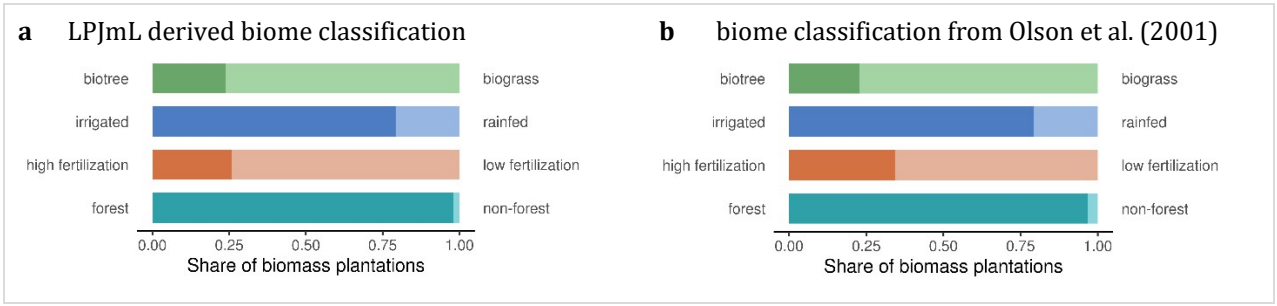

Figure 10: Characteristics of optimized biomass plantation distribution for medium CEff in the LPJmL derived biome classification (a) and the biomes from Olson et al (2001) (b). The bottom bar refers to the share of biomass plantations that is allocated in forest vs. non-forest ecosystems.

Globally aggregating the net NEs from the optimized distribution of biomass plantations results in a net CO_2eq removal of 1.18 Gt per year [for $CEff_{med}$, 1.07-1.43 $GtCO_2$-eq yr^{-1} with $CEff_{low}$ and $CEff_{opt}$]. This is in the following referred to as *annual*$_{40}$ potential, as the annual results depend on the assumed evaluation period of 40 years, reflecting the near-term political decision horizon. If biome extents from Olson et al. (2001) are used, the net annual$_{40}$ NEs are slightly lower with 1.13 $GtCO_2$-eq yr^{-1} [1.02-1.36 $GtCO_2$-eq yr^{-1}] (see Figure 9). While roughly 2 $GtCO_2$-eq are harvested per year, the CDR is reduced through (i) land use change emissions, i.e. reduced C pools

in biomass plantations as compared to natural vegetation (~0.3 $GtCO_2$-eq yr^{-1}), (ii) additional N_2O emissions through fertilization of biomass plantations (~0.1 $GtCO_2$-eq yr^{-1}) and (iii) losses along the supply chain through fossil fuel use and lost CO_2 in the capture and storage process (0.2-0.6 $GtCO_2$-eq yr^{-1} depending on the CEff, see Figure 11).

It is important to note that a large part of the net NE is provided from biomass plantations, which need >10 years to compensate for the initial reductions in C pools (44/31% for LPJmL derived / Olson et al. 2011 biomes, see *carbon debt* bars in Figure 11). Given the timely urgency to reduce atmospheric CO_2 concentrations and the risks associated with overshoot scenarios, this might be considered a severe caveat. Also, nearly all allocated biomass plantations replace natural forests (see Figure 10). However, it might be highly risky to convert forest ecosystem to biomass plantations for two reasons. First, other assessments conclude that the land-system change boundary for boreal forest biomes (Gerten et al., 2020; Steffen et al., 2015) as well as for temperate Asian forests is already transgressed (Steffen et al., 2015). Second, remaining intact forest landscapes have been shown to have a particularly high importance for biodiversity conservation (Betts et al., 2017) as well as for maintaining the natural C sink (Jung et al., 2021; Noon et al., 2022; Soto-Navarro et al., 2020). Therefore, a primacy of protecting all remaining forest areas has been strongly advocated (Cook-Patton et al., 2021). If all biomass plantations in forest ecosystems were excluded from our results, the maximum $annual_{40}$ net NE potential for the medium CEff scenario drastically declines by more than 90% to only 0.02 and 0.11 $GtCO_2$-eq yr^{-1} based on Olson et al. (2001) biomes and LPJmL derived biomes, respectively.

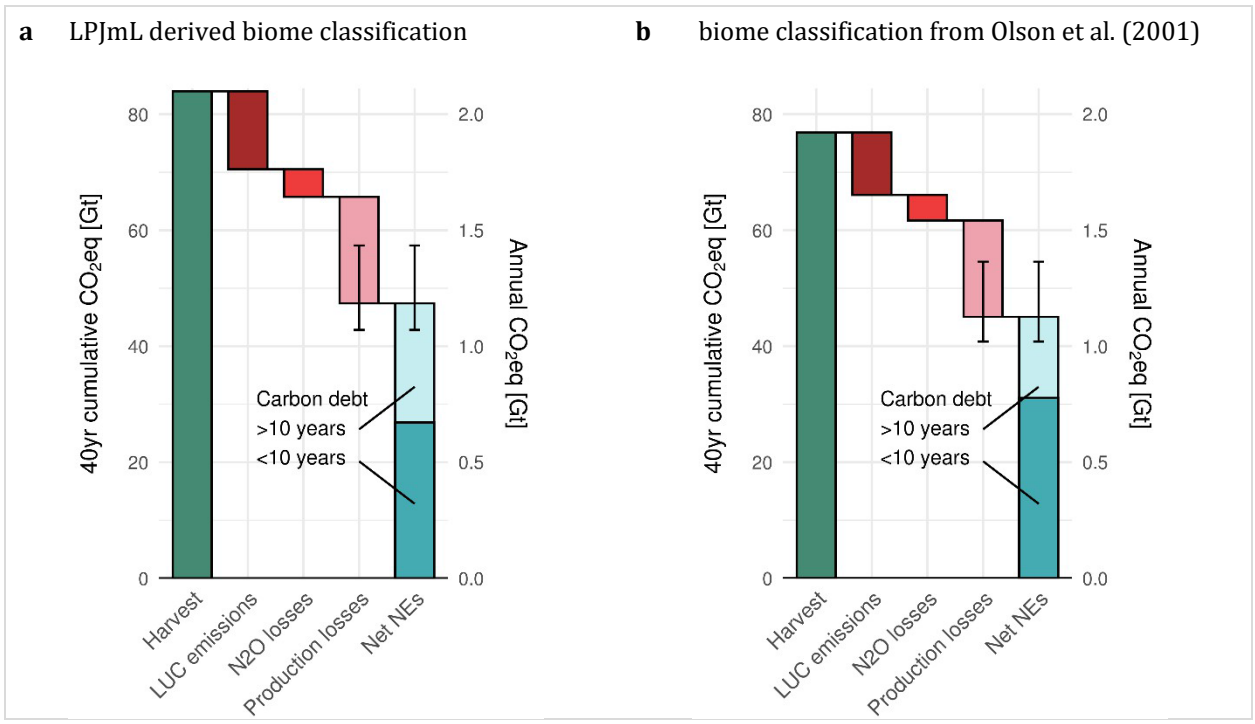

Figure 11: Global net NE from optimized distribution of biomass plantations constrained by PBs, calculated as harvested biomass from plantations, minus land use change emissions through reduced carbon pools on plantations, minus additional N_2O emissions through fertilization on plantations (in CO_2eq), minus CO_2 losses along the BECCS supply chain through fossil fuel use and in the carbon capture and storage process (see 2.2.3). Error bars for net NEs and losses along the supply chain reflect lower and optimistic CEff scenarios. The darker/lighter net NE bar indicates cumulative NE from all biomass plantations where losses of carbon pools through conversion of natural vegetation ("carbon debt") are compensated for within less/more than 10 years, respectively.

3.2 Reforestation potentials releasing pressures on planetary boundaries

In contrast to dedicated biomass plantations for BECCS, forest restoration on pasture areas may release pressures on PBs, but is bound to future land sparing developments or efforts within the food system. Prioritizing reforestation in cells with high remaining forest cover within neighbouring cells, remote pasture areas in cells with marginal anthropogenic land use are selected first in the scenario of 200 Mha reforestation (see grey shading in Figure 12a, b). In the 300 and 400 Mha rededication scenarios, less pristine areas in temperate Europe, North America and East Asia as well as in tropical South America are added amongst others, with higher pasture area shares and thus larger reforestation areas per cell (see Figure 10a, b). We generated spatially explicit reforestation patterns both by only considering pasture areas within cells classified as forest according to (i) the LPJmL derived biome classification and (ii) the biome extents from Olson et al. (2001). However, reforestation patterns have generally high agreement independent of the applied forest definition.

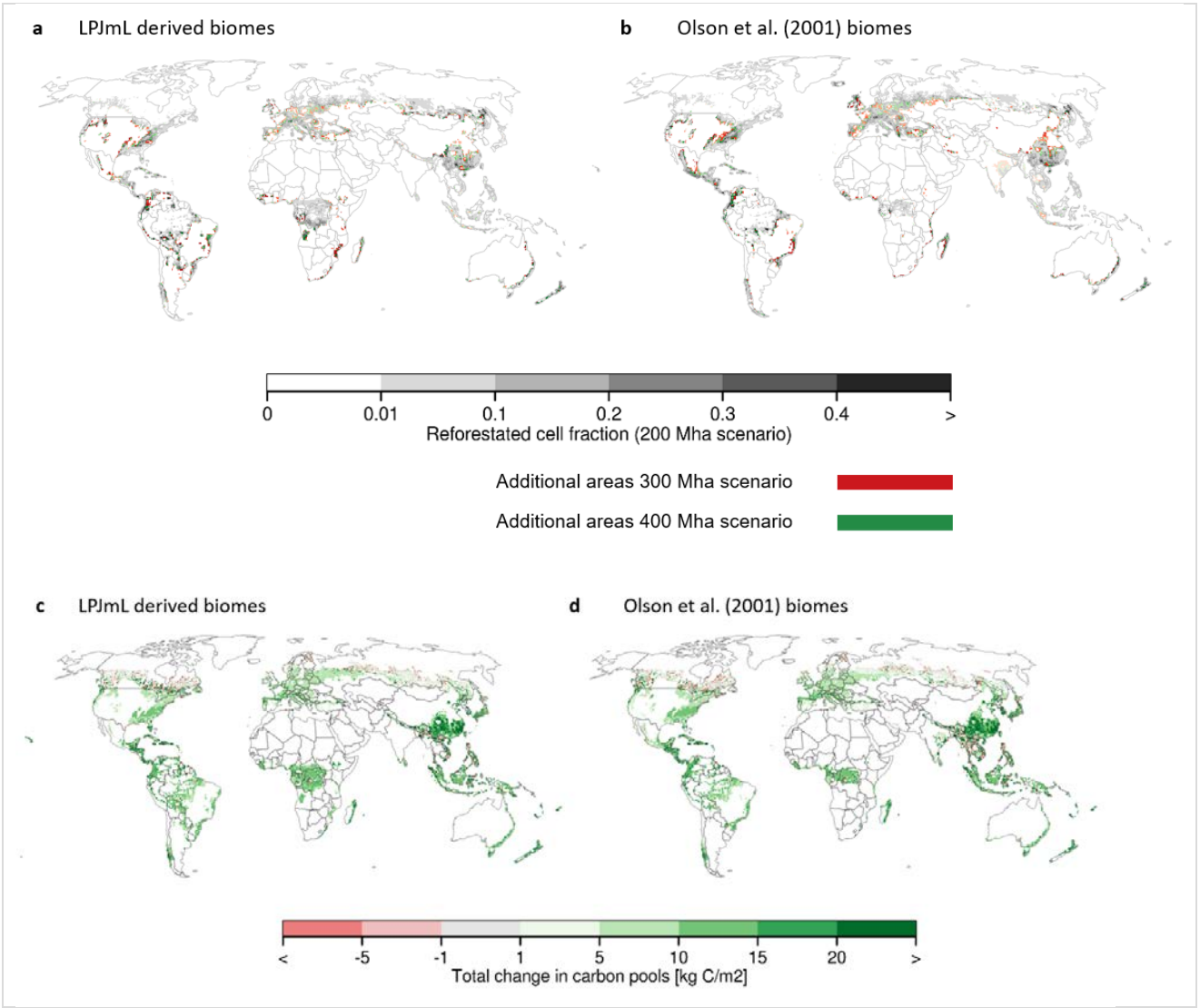

Figure 12: Geographic distribution of reforested cell fractions according to the three reforestation scenarios (a, b) and changes in carbon pools on reforested areas within 40 years (c, d), each for LPJmL derived forest biomes as well as forest biome extents from Olson et al. (2001).

Potential C pool changes on reforested areas, as simulated with LPJmL, are highest in tropical forests, with gradually decreasing C sequestration in higher latitudes (see Figure 12c, d). Within the tropics, the annual$_{40}$ C sequestration is 3.15 Mg ha^{-1}yr^{-1} on average, in comparison to 2.2 Mg ha^{-1}yr^{-1} in temperate and 0.3 Mg ha^{-1}yr^{-1} in boreal forests. These numbers compare well with previous assessments (e.g. 4.8 Mg ha^{-1}yr^{-1} for the tropics and 2 Mg ha^{-1}yr^{-1} for temperate regions assumed in Griscom et al. (2017)), but potentials within the tropics might be somewhat underestimated. In some, predominantly northernmost, cells, C pools are simulated to decrease through reforestation of pasture areas, which points to the fact that tree planting on grazing land in areas with slow tree growth and high soil C pools may not always lead to overall C sequestration within decadal timescales (Friggens et al., 2020; see also D3.6 for uncertain climate effects of reforestation in Nordic countries).

Aggregating total C sequestered within 40 years to the biome level shows that most C is removed in tropical American forests and Asian temperate or tropical forests in our scenarios (see Figure 13). While most reforestation areas in Asia are located in southern China, the respective cells are classified as temperate forest according to LPJmL derived biomes, in contrast to (sub-) tropical forest according to Olson et al. (2001). This emphasizes the dependence of the biome-specific results on assumed biomes and their extents (see 2.2.2.5). Averaged over the two biome classifications, 43% of reforestation areas are in the tropics, 50% in temperate and 7% in boreal forests in the 300 Mha scenario. The identified spatially explicit reforestation patterns resemble forest restoration opportunities determined in previous assessments, but put less emphasis on the tropics, where 70-80% of restoration opportunities are identified in Griscom et al. (2017) and Littleton et al. (2021), both based on a map of forest condition from Potapov et al. (2011) and under exclusion of boreal forest restoration.

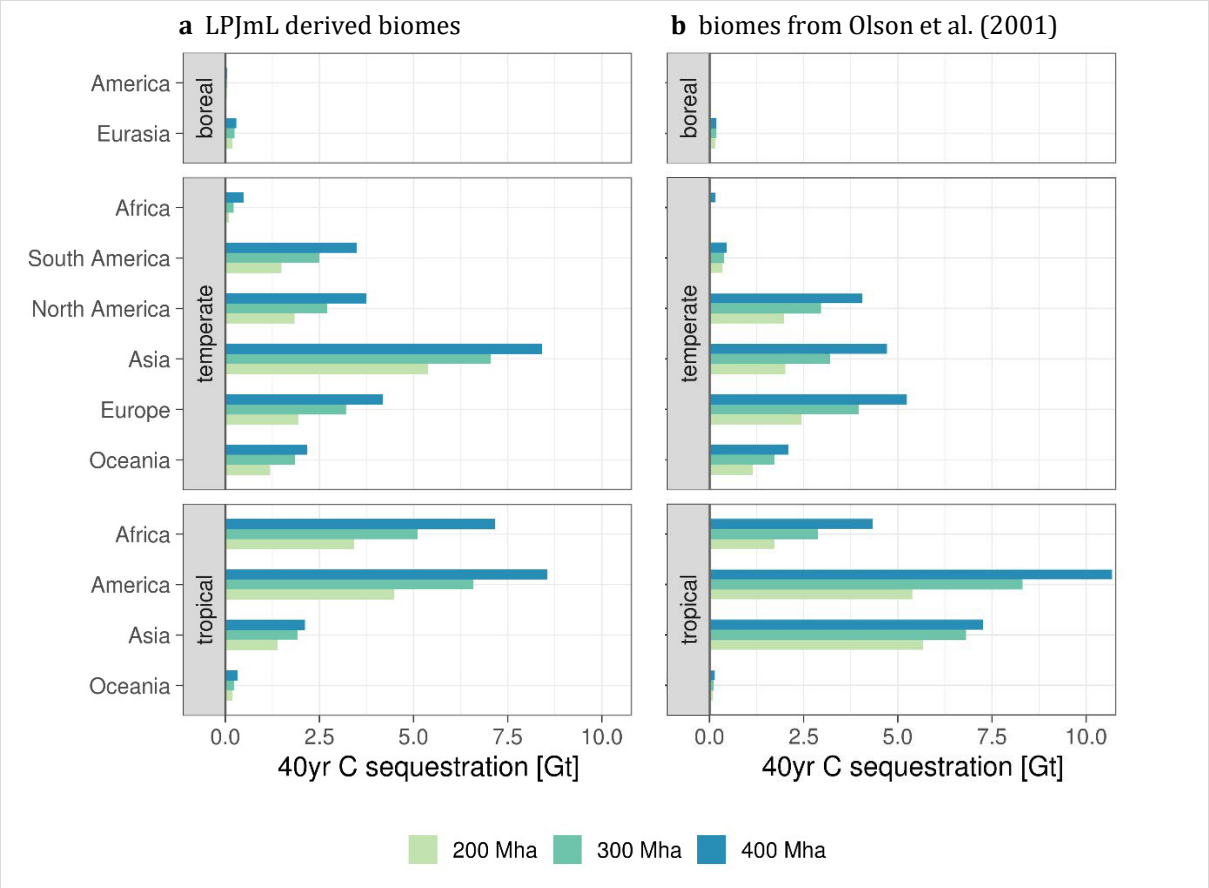

Figure 13: Simulated total carbon (C) sequestration through reforestation within 40 years for different forest ecosystems and reforestation extents (i.e. rededication of 200, 300 or 400 Mha of pasture areas).

At the global level, reforestation on 200, 300 or 400 Mha could significantly contribute to NE provision. In the medium scenario (300 Mha), ~30 GtC are removed from the atmosphere and stored within vegetation, soil and litter within 40 years (translating to ~114 $GtCO_2$-eq). Whereas most C is globally stored within the vegetation (~20 GtC), increases in soil C (~7 GtC) and litter C pools (~4 GtC) are also simulated to contribute to overall NEs (see Figure 14). In the optimistic scenario (400 Mha), total stored C could be increased to ~40 GtC or ~147 $GtCO_2$-eq; in the lower scenario (200 Mha), ~21 GtC is sequestered on reforestation areas. Importantly however, these potentials for reforestation on 200, 300 or 400 Mha should be considered as upper ceiling given that potential disruptions through climate change, such as increases in fire frequency or droughts, have not been included here. Against the background of already observed increased tree dye-off events through hotter droughts (Hammond et al., 2022), overall C sequestration potentials on simulated reforestation areas are likely smaller.

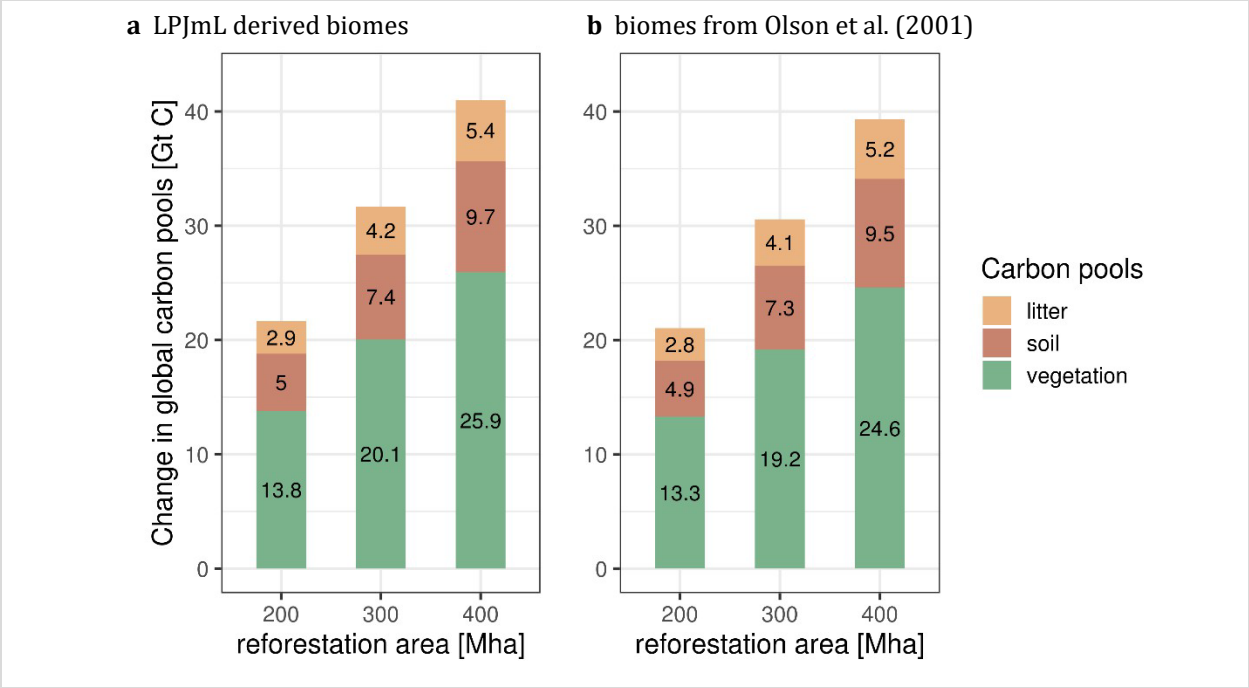

Figure 14: Globally aggregated increases in litter, soil and vegetation carbon pools through reforestation on allocated pasture areas. Results are based on changes in global carbon pools between LPJmL simulations with 2015 land use vs. reduced land use with reforestation on pasture areas.

Reforestation, defined as restoration of forest ecosystems with native species and little anthropogenic interference, e.g. no or very limited timber harvesting, may release pressures on the land-system change and biosphere integrity boundaries. Given the definition of the land-system change boundary as remaining forest cover, any forest restoration naturally contributes to increasing resilience with regard to this PB. Especially in tropical forest biomes, where boundary thresholds are exceeded, the reforestation simulated here could get the biomes closer to the "safe" zone (see Figure 15). Depending on the applied biome extents, the identified reforestation areas may even shift the state of the South American rainforest from the "zone of uncertainty" to the "safe operating space". In any case, forest restoration in the Amazon rainforest may provide particular

benefits in terms of increased resilience, as it recently has been shown that the Amazon rainforest may be close to a tipping point with potential large-scale tree dye-off (Boulton et al., 2022).

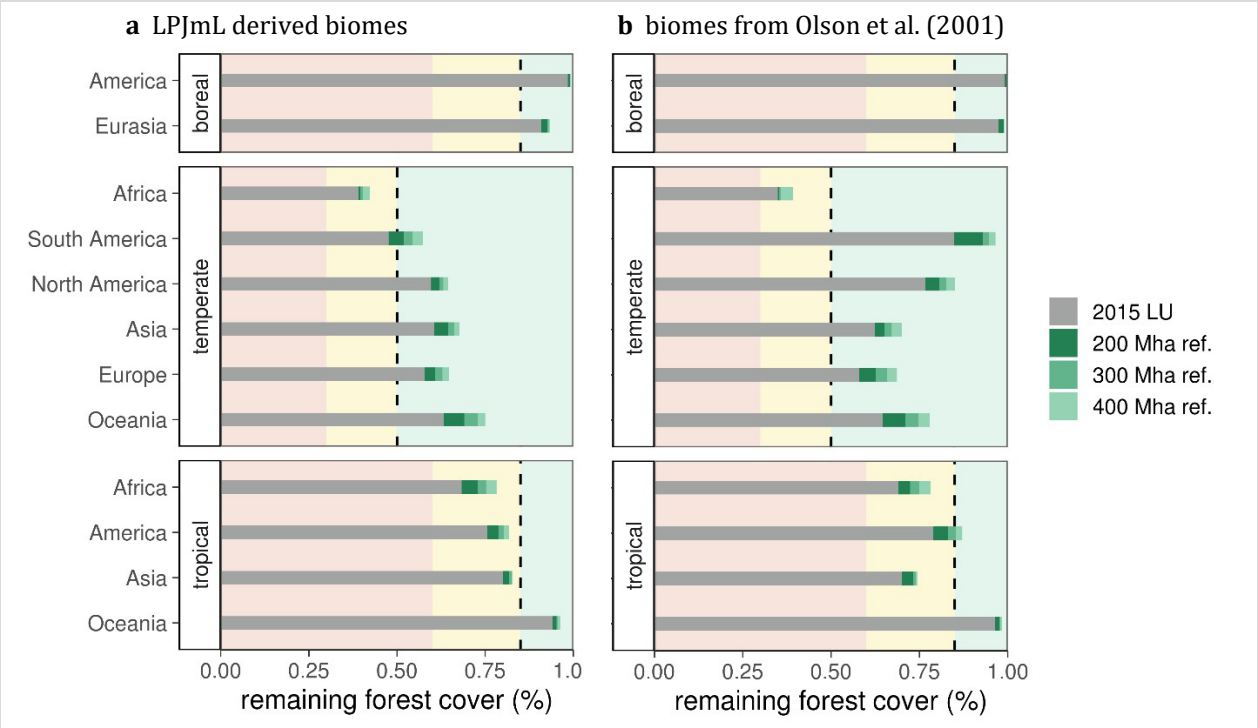

Figure 15: Impact of reforestation scenarios on biome-specific land-system change relative to PB thresholds. Background colour indicates the safe, increasing risk and high-risk zone according to the biome-specific thresholds defined in Steffen et al. (2015). For tropical and boreal biomes, the thresholds are stricter, given stronger climate feedbacks and teleconnections of these biomes (see 2.2.2.3).

3.3 Land- and calorie-neutral PyCCS potentials without additional planetary boundary transgressions

For the LCN-PyCCS approach we find that the suitable area is relatively small, when the fertilizer rate is prescribed according to the scenario. The area of potential biochar feedstock production extents to 5 Mha in the medium scenario and 23 Mha in the optimistic scenario, while the approach is not compatible with the low fertilization and yield increases of 10% in the lower scenario. The lower the yield increase, the smaller the fraction of cropland dedicated to PyCCS feedstock production and the higher the demand for biomass to provide sufficient biochar for the remaining cropland. Moreover, when a small yield increase is combined with low fertilization, the biomass production is limited even further. If the biomass yields in a grid cell are, however, sufficient to serve the LCN-PyCCS approach, the area that is allocated for feedstock production depends on the prevailing cropland extent and the scenario-specific yield increases defining the fraction of cropland that can be dedicated to biomass crops (Figure 16a).

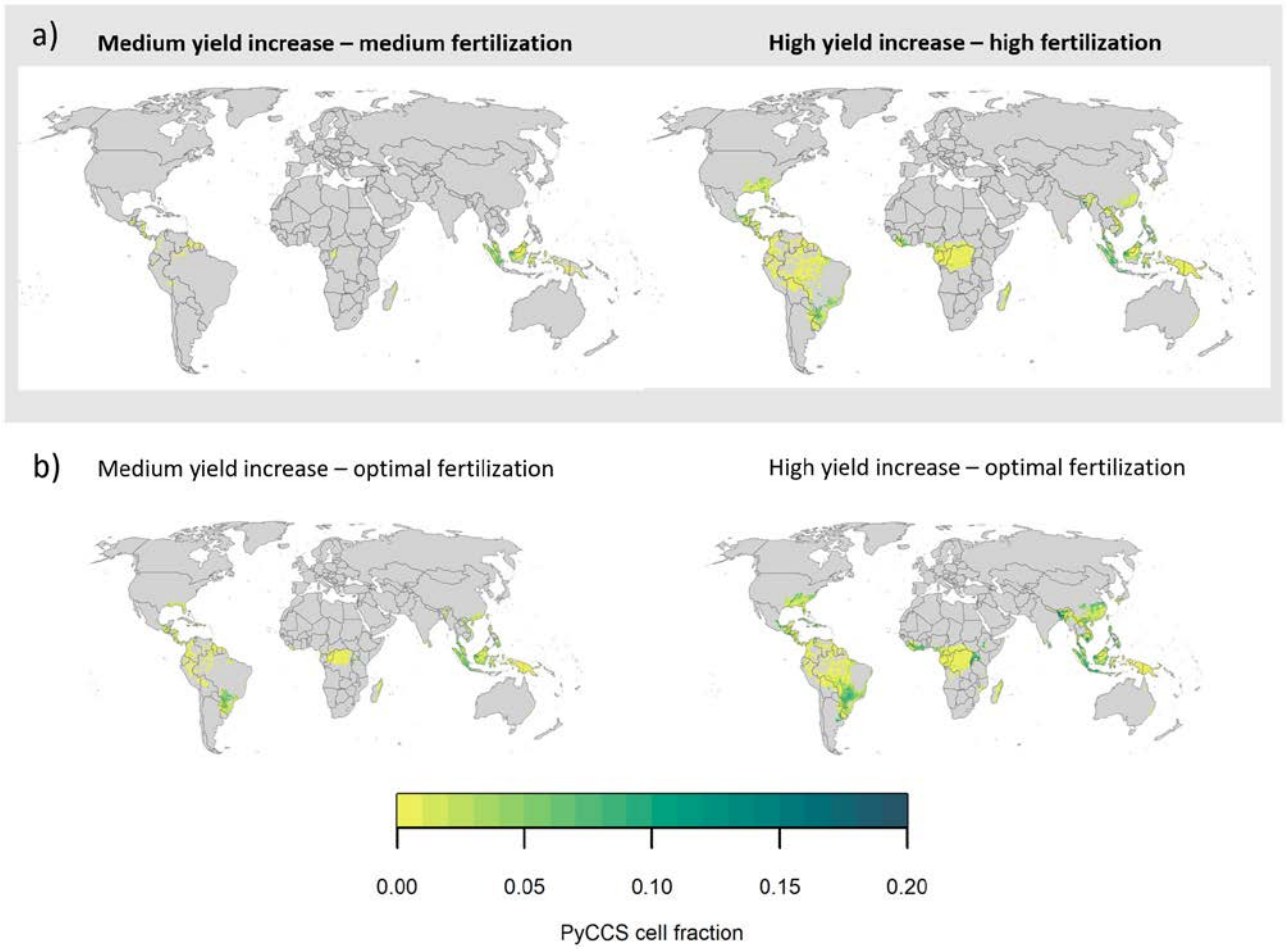

Figure 16: Geographic distribution of cell fractions allocated for LCN-PyCCS feedstock production a) in the medium scenario (medium yield increase - medium fertilization), the optimistic scenario (high yield increase - high fertilization) and b) for simulations of optimal fertilization with different levels of yield increases (medium yield increase – optimal fertilization and high yield increase – optimal fertilization).

Corresponding to the small spatial extent of potential feedstock production, the CDR potentials of LCN-PyCCS are relatively low. The medium scenario results in annual sequestration rates of about 0.05 $GtCO_2$ yr^{-1} while the optimistic scenario may reach levels of 0.21 $GtCO_2$ yr^{-1}. Over the assessed 40-year time horizon, these sum up to 2.00 $GtCO_2$ and 8.43 $GtCO_2$, respectively. As a relatively strict yield threshold needs to be reached by grid cells in order to be included in the LCN-PyCCS approach, most of the suitable areas barely exceed it and the distribution pattern shows similar NE rates across the different regions of application (Figure 17a).

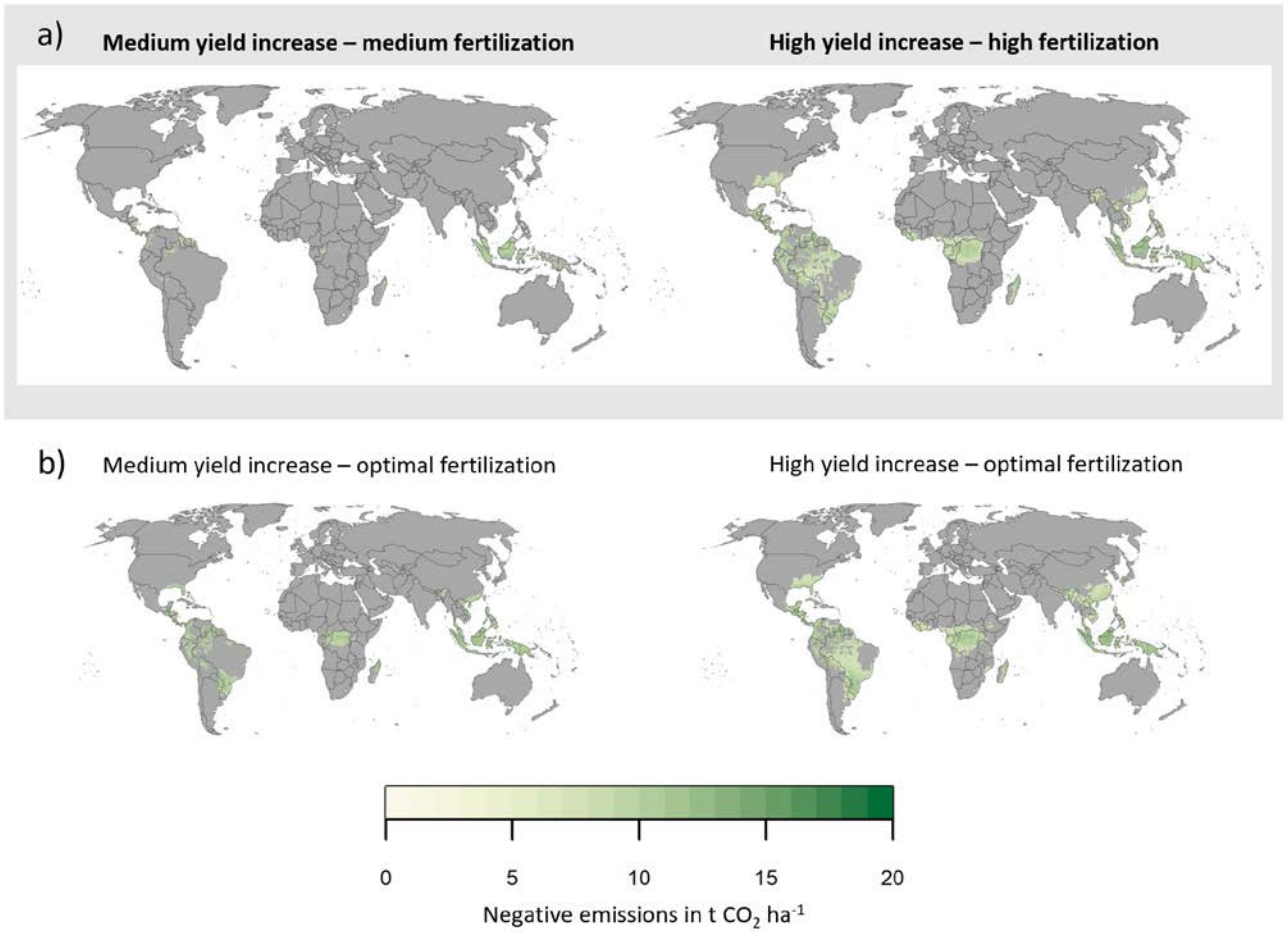

Figure 17: Geographic distribution of negative emission potentials relative to the area of biomass feedstock production for LCN-PyCCS a) in the medium scenario (medium yield increase - medium fertilization), the optimistic scenario (high yield increase - high fertilization) and b) for simulations of optimal fertilization with different levels of yield increases (medium yield increase – optimal fertilization and high yield increase – optimal fertilization).

To evaluate the dependency of the results on the simulated N-limited yields, we additionally assess the NE potentials without N limitation on biomass plantations. The yields for herbaceous biomass crops are simulated to be significantly higher in the simulations with unlimited N supply that represent optimal fertilization. Accordingly, more areas produce enough biomass to supply the cropland with sufficient biochar and become suitable for the approach in this setting (Figure 16b). Based on the higher biomass yields, about 16 Mha of land could be provided for PyCCS feedstock production in the medium scenario with a quantified NE potential of about 0.17 $GtCO_2$ per year and 6.64 $GtCO_2$ over the 40-year time period. In the optimistic scenario, LCN-PyCCS might reach extents up to 49 Mha and CDR levels of about 0.45 $GtCO_2$ per year and 18.00 $GtCO_2$ over 40 years.

3.4 Synthesis

In a first step, we here simulated the maximum amount of NE from dedicated biomass plantations for BECCS under the constraints that further transgressions of PBs are to be avoided and, that no current agricultural land is converted. Depending on the assumptions on the CEff along the BECCS supply chain, this PB-friendly annual$_{40}$ net NE potential is calculated to range between 1.0 and 1.4 $GtCO_2$-eq yr^{-1}, with 1.16 $GtCO_2$-eq yr^{-1} for the medium CEff. These limited potentials represent an ambitious upper ceiling where all regional opportunity spaces to expand land use within PBs are generously exploited up to the limit and come at the background of already severe and widespread PB transgressions through current agriculture. Further, the simulated remaining areas for biomass plantations are in questionable locations, for both economic reasons (e.g. sparse road infrastructure), in terms of timely delivery of NEs (many locations with long compensation times for land use change emissions) and with regard to other sustainability goals (i.e. preservation of all remaining forest areas). If deforestation of natural forests was excluded, BECCS potentials would decrease to close to 0, emphasizing the difficulties in reconciling plantations-based BECCS with sustainability targets.

We secondly further assessed the degree to which these very limited potentials could be sustainably increased through reforestation on pasture areas and PyCCS on arable land, under the condition that future land demand for food production decreases due to dietary changes and higher efficiencies in the livestock sector and biochar-mediated yield increases on cropland. While land-and-calorie neutral PyCCS potentials are low in our assessment (mostly due to constraints on yields from biomass plantations; 0-0.2 $GtCO_2$-eq yr^{-1}), reforestation on 300 Mha (200-400 Mha) pasture areas ("medium scenario") may remove on average up to 2.9 $GtCO_2$-eq annually (2.0-3.7 $GtCO_2$-eq yr^{-1}), summing up to 114 $GtCO_2$-eq within 40 years (78-147 $GtCO_2$-eq).

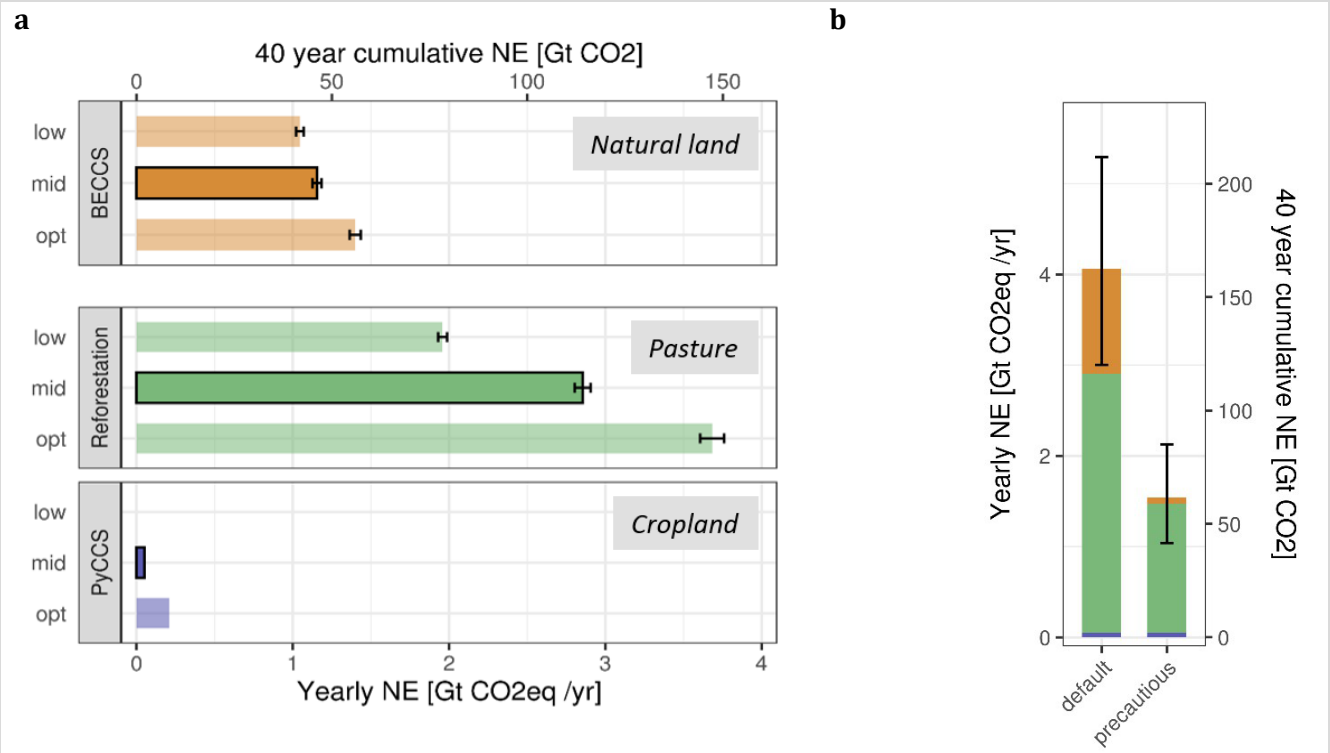

Figure 18: (a) Simulated results for BECCS on natural land, reforestation on pasture areas and PyCCS on cropland, all referring to three scenarios (low, medium and optimistic assumptions). For BECCS and reforestation, the displayed results were averaged for the two applied biome classifications (LPJmL-derived and Olson et al. (2001)), with the error bar reflecting the range. (b) Additive overall NE potential from BECCS, reforestation and PyCCS for the medium scenario (the error bar reflects the range between lower and optimistic scenario). The right bar visualizes the explorative NE potential if (i) deforestation for BECCS was excluded and (ii) it is assumed that 50% NEs from reforestation are non-permanent due to climate change effects amongst others. All results were derived from simulations with 1986-2015 climate and refer to an evaluation period of 40 years.

While reforestation might not only significantly contribute to NE provision, large co-benefits could also be unlocked through potential increases in the resilience of natural forest ecosystems. On the other hand, the simulated NE potentials do not take into account potential disruptions through climate change such as increased fire frequencies and other extreme events, which could considerably decrease actual NEs.

Under the very generous assumptions that (i) biomass plantations for BECCS may replace current forest ecosystems and (ii) climate change effects on biomass plantations and reforestation are not considered, the three assessed NETPs analysed here could add up to ~4 $GtCO_2$-eq per year in the medium scenario (~160 $GtCO_2$-eq over 40 years) without additional PB transgressions (see Figure 18b). If however forest ecosystems were excluded from conversion to biomass plantations, and we tentatively assume that up to 50% of C sequestered within reforestation sites is not permanently stored because of poor subsequent management, wildfires, plundering, extreme weather events and other effects of climate change, the cumulative PB-compatible $annual_{40}$ NE potentials would significantly decline to up to 1.5 $GtCO_2$-eq yr^{-1} (1.0-2.1 $GtCO_2$-eq yr^{-1}, see Figure 18b).

4 Discussion

We employed the global biosphere model LPJmL to estimate PB-compatible NE potentials from plantations-based BECCS, reforestation and PyCCS. While simulated C, water and N fluxes have been extensively validated (e.g. Schaphoff, Forkel, et al., 2018), further model development is ongoing, especially with regard to improved N demand and uptake routines as well global PFT distribution. Also, fertilizer demand of biomass plantations is to be further evaluated, to ensure adequate representation of management on N flows. These ongoing developments will contribute to updates of the results throughout the NEGEM project. Against the background of the uncertainties inherent to global modelling of the biosphere, we first discuss and contextualize the findings for the three assessed NETPs in the following. We then summarize key findings and policy relevant messages, also pointing to further steps for assessing environmentally sustainable NE potentials.

4.1 NEs from plantations-based BECCS without further PB transgressions

The here calculated maximum NE supply from plantation-based BECCS within regional safe zones of four terrestrial PBs is ~ 1.2 $GtCO_2$-eq yr^{-1}. This is significantly higher than the estimates in Heck et al. (2018) (0.2 $GtCO_2$-eq yr^{-1} for the more efficient biomass-to-hydrogen conversion pathway). It is however important to note that the estimates are not directly comparable, as (i) Heck et al. (2018) refer to BECCS potentials within regional safe zones for 2050 based on several simulated agricultural baselines in line with uncertain storylines of specific SSPs and (ii) the calculations for the N and biosphere integrity boundaries have been updated here (see 2.2.2). While we avoided the high uncertainties related to future projections of the food system and its resource demand by using current agricultural land use as baseline, PB-compatible BECCS potentials might be limited even stronger if resource and land demand for food production increased, thereby further shrinking the opportunity space for NEs. Also, the dependency of the results on the defined regional boundary constraints points to uncertainties in PB assessment. The currently published PB definitions are to be understood as “work-in-progress” and are subject to continuous debate and improvement (e.g. Wang-Erlandsson et al. (2022) for the water PB). Besides the definition of the control variable and its threshold, the spatial unit applied for estimating regional PB statuses matters. To address this uncertainty, we calculated the biosphere integrity and land-system change PB constraints both by averaging over LPJmL-derived biomes as well as the widely used biome distribution published in Olson et al. (2001), with overall little impact on global results.

Despite remaining uncertainties in PB definitions and input data, the key message – that plantation-based BECCS through conversion of natural vegetation can only marginally contribute to NE provision if regional safe zones are adhered to – holds true for both, the here updated assessment as well as for Heck et al. (2018). All the more, it is important to emphasize, that any NE provision from plantation-based BECCS is difficult to reconcile with PBs given that *global* control variables for three of the four terrestrial PBs (land-system change, biosphere integrity, N flows) are transgressed through current agriculture. In a strict sense, any further conversion of natural vegetation thus puts additional pressures on the biosphere, potentially associated with increased risks for abrupt and irreversible environmental changes at the planetary scale. The here quantified potentials from BECCS should thus be cautiously interpreted as an upper ceiling, assuming that all remaining opportunity spaces for land use expansion within regional safe zones were optimally exploited.

Except for Heck et al. (2018), previous studies on plantation-based BECCS or bioenergy under environmental constraints generally find larger potentials. However, to our knowledge, all other studies considered less environmental dimensions, e.g. only sustainable irrigation (Ai et al., 2021), biodiversity protection and sustainable irrigation (Frank et al., 2021), or biodiversity protection and exclusively rainfed plantations (Wu et

al., 2019). In general, the more environmental protection targets are considered, the smaller the opportunity space for plantation-based BECCS, emphasizing societal decisions and weighting of what to protect or which risks to avoid. This is also reflected by the much reduced BECCS potential in our assessment, if – in addition to the PB constraints – deforestation for biomass plantations is prohibited. Importantly, as pointed out here and in previous studies, ensuring biosphere integrity by protecting biodiversity is the key limiting factor for plantation-based BECCS (Frank et al., 2021; Heck et al., 2018). As it has been argued that biosphere integrity is, next to climate change, one of the two core PBs, integrating the other boundaries (Steffen et al., 2015), it may however be considered highly risky to combat climate change at the cost of biosphere integrity. Not only substantial shifts in climate, but also in the biosphere may be capable of pushing the Earth system out of its Holocene state (Steffen et al., 2015).

When comparing our results to 1.5°C- or 2°C-compatible IAM-based scenarios (classified as C1, C2 or C3) considered in the recently published IPCC report on climate change mitigation (Working Group III report as part of the 6th assessment report (AR6), IPCC (2022)), we find that the here quantified maximum annual$_{40}$ NE from plantation-based BECCS is significantly lower than most of the projected annual BECCS NE rates in year 2050 (less than half of the C1-C3 median of 2.75 $GtCO_2$ yr^{-1}, IPCC (2022), see Figure 19). This difference in sequestration rates is even more pronounced in the second half of the century for which most AR6 scenarios assume a strong increase in CDR by BECCS (median of 8.96 $GtCO_2$ yr^{-1} in 2100). That magnitude is all the more remarkable as it would entail an additional anthropogenic C sink larger than the current net land sink (terrestrial C sink – land use change emissions) and almost as large as the current ocean sink (Friedlingstein et al., 2021). This strong reliance on BECCS can partially be explained by the limited coverage of the various NETPs in IAMs. The large majority of the models represent BECCS and A/R, whereas enhanced weathering and direct air capture have been included by only a few IAMs so far (Byers et al., 2022; Realmonte et al., 2019; Strefler et al., 2021).

Yet, while the BECCS potentials that we quantified lie at the lower end of projected NE demands for Paris-compatible IAM scenarios, they are compatible with illustrative mitigation pathways (IMPs) that include severe transformations in society and economy. Thus, the BECCS capacity of our medium scenario is higher than the BECCS demands in 2050 for the IMP characterized by gradual strengthening of the current climate policies until 2030 with coordinated and rapid decarbonization actions thereafter (i.e. Gradual Strengthening (GS)), and the IMP with a focus on shifting pathways towards Sustainable Development Goals, including poverty reduction and broader environmental protection next to deep GHG emissions cuts (i.e. Shifting Pathways (SP)) (see Figure 19F). Further, the very low potentials of BECCS when excluding forest conversion for biomass plantations are most compatible with the IMP focussing on Low Demand (LD) that avoids BECCS and relies only on CDR from the AFOLU sector (agriculture, forestry and other land use). This IMP is characterized by efficient use of resources as well as large-scale shifts in consumption. Thus, there is evidence from IAM assessments that BECCS rates of the magnitude quantified in this study could be compatible with the climate targets of the Paris agreement, however, only if the stringent decarbonization measures in combination with the comprehensive socioeconomic transformations assumed in these scenarios are successful. Importantly, PBs should however also be considered in the design of decarbonisation measures, ideally contributing to reversing current terrestrial PB transgressions, in addition to reduced pressure on the climate change PB (e.g. Algunaibet et al., 2019).

A similar conclusion can be drawn when comparing the quantified NE potential of BECCS restricted by the PBs (1.16 $GtCO_2$ yr^{-1}) to the maximum NE supply from BECCS of 1.3 $GtCO_2$ yr^{-1} in 2050 simulated in the recently published scenario of net zero emissions (NZE) by 2050 from the International Energy Agency (IEA, 2021). BECCS rates of these (comparatively low) magnitudes can only support the net zero target, if radical decarbonization measures are implemented early and stringently as described for the IEA NZE scenario. For example, the NZE scenario implies immediate and massive increases in renewable energies with annual additions of solar and wind capacities quadrupling until 2030, rapid electrification necessitating a 2.5-fold increase of total global electricity

generation until 2050, and zero traditional use of solid biomass for cooking by 2030, amongst others. In this context, it is also important to note, that bioenergy is not only considered for BECCS but also for provision of renewable energy as a substitution to fossil fuels in the NZE scenario, as well as in many IAM scenarios (Bauer et al., 2020).

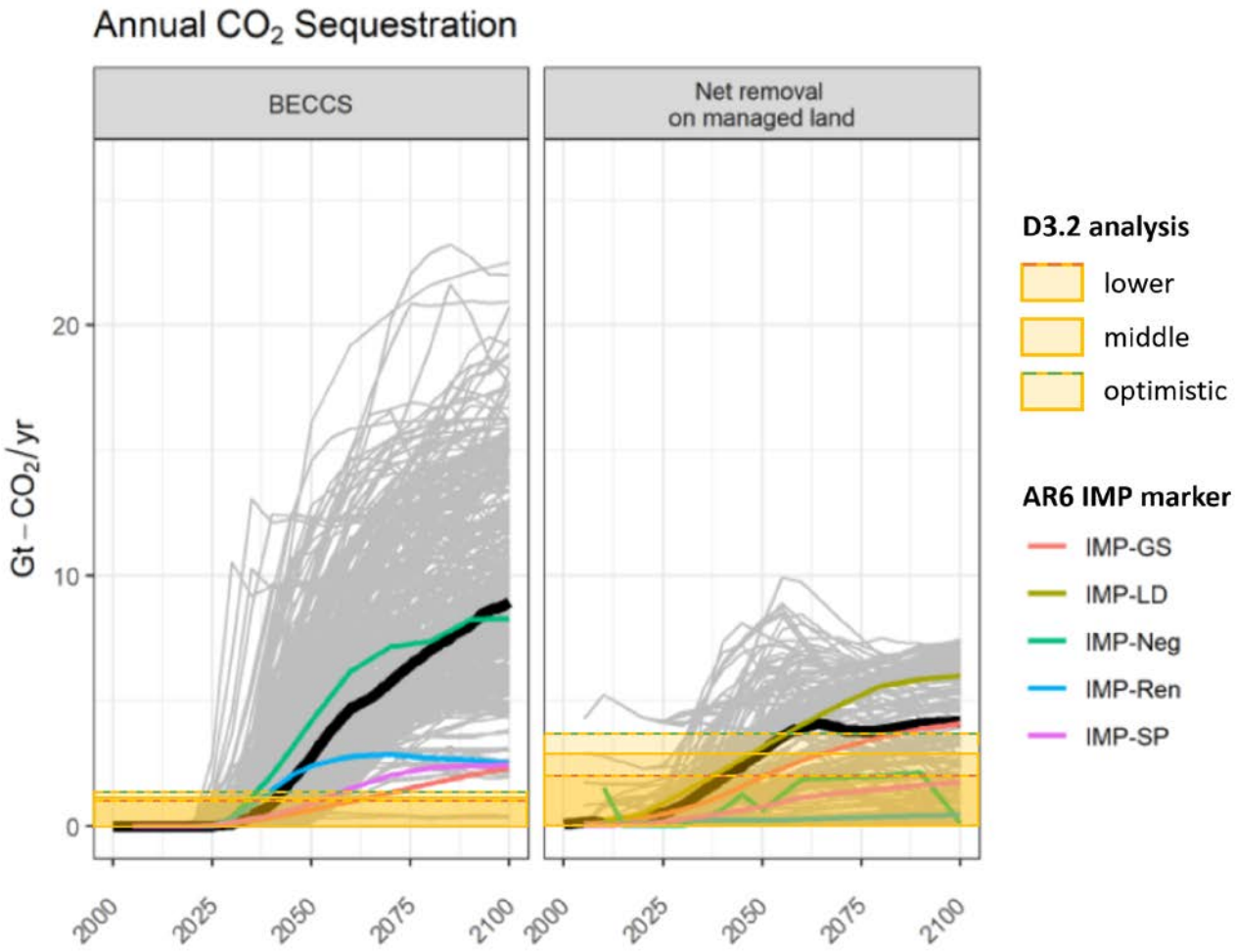

Figure 19: Annual sequestration from BECCS and AFOLU in the IPCC AR6 IAM scenarios likely limiting warming to 2°C or lower (lines) and annual 40-year sequestration potential for BECCS and reforestation quantified in the lower, medium and optimistic scenario of this analysis (transparent yellow boxes). The black line indicates the median of all the IPCC AR6 scenarios in categories C1-C3, while the IMPs are highlighted with colours, as shown in the legend (GS = "Gradual Strengthening", Neg = "Net Negative Emissions", Ren = "Renewables", LD = "Low Demand", SP = "Shifting Pathways"). Figure adapted from IPCC (2022).

When comparing our BECCS estimates to other modelling studies, it is important to consider that we focused on PB-compatible BECCS capacities from dedicated biomass plantations outside of current agricultural areas. However, many IAMs assume to complement these feedstocks with agricultural and forestry residues (Hanssen et al., 2020), or biogenic point sources e.g. from pulp and paper industries or municipal solid waste (Pour et al., 2018; Rosa et al., 2021). While these feedstocks can provide substantial sustainability advantages, particularly because of the avoided land competition with food and nature, (i) the feedstock availability is uncertain and limited (Hanssen et al., 2020; IPCC, 2022) and (ii) residues and waste cannot be considered freely available in the light of competing uses or benefits, such as e.g. soil C built-up against land degradation or the replacement of animal feed from purpose grown crops in the case of agricultural residues (Kalt et al., 2020; Van Zanten et al., 2018). Nevertheless, residues and waste may to some degree contribute to the provision of PB-compatible BECCS

(IPCC, 2022). Additionally, a few IAMs simulate, in addition to forestry residues, the use of logs from managed forests as feedstock for BECCS (Rose et al., 2022). However, this requires thorough assessment of (i) alternative wood uses and (ii) the impacts of harvesting on C stocks within forests, with potential decreases upon intensive management (see 4.2).

Also, while we excluded all current agricultural areas for energy crops, it is frequently assumed that low-productivity pasture areas are available in future, but this neglects that these marginal areas might be particularly exposed to climate change risks and often exhibit little infrastructure for transport and processing of biomass (IPCC, 2019). Additionally, economic reasons and empirical evidence indicate that biomass plantations will rather expand into highly productive grassland, thereby potentially adding pressure on food security (Kalt et al., 2020) and PBs. We therefore focused on reforestation on pasture areas, which may be more likely realized in remote areas, with potentially less interference with the food system and synergies with regard to PB maintenance as well as other nature restoration targets. Nonetheless, further analyses are needed that thoroughly examine the potentials of plantation-based BECCS on pasture areas as constrained by PBs and dependant on developments in the food sector.

4.2 NEs from reforestation on pasture areas

To expand the marginal NE capacities from plantations-based BECCS compatible with PBs, we simulated scenarios of 200, 300 and 400 Mha forest restoration on pasture areas. The calculated annual$_{40}$ potential of 2.0, 2.9 and 3.7 $GtCO_2$-eq yr^{-1}, respectively, is in the range of previous estimates for a scenario reflecting national forest restoration commitments from Cook-Patton et al. (2020) (5.9 $GtCO_2$-eq yr^{-1} from 349 Mha, but referring to a 30-year timeframe) as well as an intact forest restoration scenario from Littleton et al. (2021) (1.82 $GtCO_2$-eq yr^{-1} from 344 Mha, 2030-2070). The wide range of potentials from similar targeted areas mirrors uncertainties in C sequestration rates per ha as well as differences in scenario assumptions on prioritized areas and/or input data on potential or degraded forest cover. With regard to simulated C sequestration rates, we are in the range of previous studies, but might underestimate rates within the tropics (see 3.2; see e.g. Griscom et al. (2017) and Koch and Kaplan (2022)). Also, the rates depend on the considered timeframe, with higher annual increases within the first decades. To scale maximum C accumulation within planted forests to the 40-year political decision horizon chosen within this study, we applied biome-specific factors from Braakhekke et al. (2019). Future model development might however focus on representing human supported reforestation in a process-based manner within LPJmL to reflect grid-cell specific temporal dynamics. In this context, it is important to stress that our analysis marks the upper ceiling of potential C sequestration on the selected reforested areas as impacts of climate change and the corresponding risks of reversibility of C sinks from heat stress, tree die-off and increased fire disturbance (e.g. Hammond et al., 2022; UNEP, 2022) are not considered. In NEGEM these effects will be addressed in task D3.4 where the impacts of climate extremes will be evaluated for different terrestrial NETPs (see 4.5).

We here deliberately chose to prioritize restoration of intact forest landscapes in line with a “land-sparing paradigm”, but acknowledge that there are eligible alternative prioritization schemes depending on the restoration target, e.g. a focus on reforestation in areas with high deforestation shares reflecting a “land-sharing paradigm” (Fischer et al., 2008; Phalan et al., 2011), which might alter the annual potential through changes in the geographic location of targeted reforestation areas. Further, to capture uncertainties in potential natural forest cover, we applied two independent forest definitions (LPJmL derived vs. natural forest extents from Olson et al. (2001)). Regardless, both potential forest cover as well as current extent of degraded forest through anthropogenic land use are subject to considerable uncertainties (e.g. Grantham et al., 2020).

Regarding the net climate effect of reforestation, we here focused on CO_2 fluxes only, but reductions in albedo might lead to net warming effects of reforestation in boreal biomes (e.g. Bala et al., 2007; Bonan, 2008; Pongratz et al., 2011; see als D3.6; Sonntag et al., 2016; see also D3.6). While a strict focus on the climate change PB thus argues for an exclusion of boreal forest restoration (as assumed in Littleton et al. (2021) and Griscom et al. (2017)), we here did not exclude boreal biomes a priori given the integrative consideration of four additional PBs in this study and the positive impact of reforestation on these. Despite the small targeted areas within the boreal biomes based on our prioritization scheme (5-9% depending on the rededicated area and biome classification), the consideration of albedo changes might thus however reduce the overall net climate cooling effect of the simulated reforestation scenarios.

Also, given the PB-perspective in this analysis as well as the evaluation period of 40 years, we excluded any harvesting in reforested areas, but refer to forest restoration with no or little anthropogenic disturbance. We thus did not assess potential effects of harvesting for BECCS or long-lived wood products on overall CDR potentials. While forest management could increase the CDR potential on longer timescales, this effect is highly uncertain as unsustainable harvesting levels can decrease C stocks and resilience within forests. Furthermore, intensive management might introduce additional pressures on PBs, e.g. through use of fertilizers or habitat fragmentation resulting from maintenance infrastructure. Nevertheless, sustainable harvesting on reforested areas may contribute to CDR on longer time-scales, when C accumulation rates within natural forests decline, e.g. by providing feedstocks to BECCS to circumvent the PB trade-offs from dedicated energy crops For a thorough assessment of the trade-off between increased harvesting vs. increases in the forests' C sink as well as impacts of forest-related NETPs on ecosystem services in the Nordics, see D3.6.

The range of annual CDR potential from reforestation over the assessed 40-year time horizon lies well within the assumptions for the 2050-level of AFOLU in "Paris-compatible" C1-C3 scenarios of the AR6, with our medium scenario mean of 2.85 $GtCO_2$ yr^{-1} matching the C1-C3 median of 2.98 $GtCO_2$ yr^{-1} (IPCC, 2022). In these IAM scenarios of the AR6, the CDR increase of the AFOLU sector (re-/afforestation CDR minus land use change emissions) over the century is projected to be less strong than for BECCS, showing final rates that are only 0.5 $GtCO_2$ yr^{-1} above the upper range of the scenarios of our assessment (see Figure 19).

As even scenarios of the two IMPs with relatively low emissions (LD + SP) and partly even no BECCS demand (LD), rely on CDR from land management, the role of CDR to compensate residual emissions to achieve net zero emissions becomes evident. This is also addressed in the IEA report on pathways to net zero emissions (NZE). While the balancing in the NZE IEA scenario focuses on what is achievable within the energy and industry sector, the report further debates contributions to a net zero balance in the AFOLU sector, concluding that especially the non-CO_2 greenhouse gases (5-6 Gt $GtCO_2$-eq yr^{-1}) are hard to abate and would require NETP deployment. In this regard, the potentials quantified for reforestation, here, could potentially cover the compensation of about half of these emissions.

In general, the identified NE potentials through reforestation strongly depend on the available pasture area. The here chosen scenarios (200, 300, 400 Mha), derived from literature on pasture reduction potentials, show similar ranges than simulated forest expansion in C1-C3 scenarios of the AR6 in 2050. If compared to studies on the maximum biophysical potential of reforestation, roughly half of the overall potentially available areas (678 Mha according to Griscom et al. (2017)) is covered. The scenario of 400 Mha forest restoration provides up to ~40% of the estimated maximum NE potential of ~9-10 $GtCO_2$-eq yr^{-1}, which may be achieved if all pasture areas in forest ecosystems were reforested (Cook-Patton et al., 2020; Griscom et al., 2017). While exploiting half of the biophysical potential might seem politically more realistic, this emphasizes that even higher NE potentials could be achieved upon comprehensive sustainability transitions within the food system, including large-scale diet

changes and/or increases in feeding efficiencies. This is also in line with the higher NE rates from managed land in 2100 as simulated in the IMP-LD scenario characterised by large shifts in consumption patterns amongst others (see Figure 19).

Overall, forest restoration (not to be confused with afforestation of non-native tree monocultures) would not only benefit climate targets but could significantly contribute to getting back into the „safe operating space" for biosphere integrity. By consolidating international targets regarding both climate change mitigation and nature restoration, it could help to reach the proposed 2030 target of the UN Convention on Biological Diversity of protecting 30% of terrestrial land surface. For example, restoring and protecting 200-400 Mha would lift the current terrestrial protected area coverage of ~16.6% (UNEP-WCMC et al., 2020) to ~ 18-20%. In the context of Europe, the EU attempts to address this synergy with its pledge to plant three billion additional trees by 2030, aiming to increase C storage in biodiversity-friendly forests.

4.3 NE contribution of LCN-PyCCS

In comparison to BECCS and reforestation, LCN-PyCCS provides only a relatively small contribution to overall NE potentials in this assessment. For this specific land- and calorie-neutral approach we assessed here, the requirements are particularly strict: systems must be self-sufficient in biochar supply and can only derive feedstock from biomass plantations on cropland allocated through accounting of biochar-mediated yield increases. Thus, LCN-PyCCS is strongly dependent on high biomass yields because yield thresholds need to be met to supply sufficient biochar. This becomes evident with the larger extent of suitable area and correspondingly higher NE potentials quantified in the supplementary scenarios of unlimited N supply that are characterized by significantly higher yields. Earlier LPJmL-based analyses of LCN-PyCCS without any consideration of N dynamics showed even higher biomass yields and NE potentials around 0.44 $GtCO_2\ yr^{-1}$ for a similar scenario of 15% biochar-mediated yield increases on cropland (Werner et al., 2022, in revision). Yet, this study used different assumptions on cropland extent and biochar application rates which in total detracts from comparability. While this earlier assessment simulated biomass production without N limitation, the scenarios of unlimited N supply tested in this study can still be restricted in N uptake depending on fine root mass, soil temperature and porosity. Especially on plantations without irrigation systems, the root development required for a sufficient N uptake of the plants can be restrained by limited water supply.

However, it is unclear which yield levels are more representative for lignocellulosic grasses, because observational data is particularly rare for the tropics, which builds the focus region of the LCN-PyCCS assessment and which is also where the yield differences between simulations in-/excluding N dynamics reach their maximum. Furthermore, there is currently no systematic observational dataset available that could be used to evaluate the fertilizer response of biomass crops on LPJmL, according to the best of our knowledge. However, as the N content in harvested biomass is likely to be overestimated in LPJmL, due to the incomplete representation of N translocation from shoots to rhizomes at senescence, which is typical for miscanthus for example (Cadoux et al., 2012; Christian et al., 2006), the model is likely to overestimate the fertilizer requirements for herbaceous bioenergy crops. Yet, a deeper analysis and corresponding calibration of the fertilization response is needed to adequately address the effect of plantation management on the N cycle that is a crucial component of the Earth system.

At the same time the reliance of the LCN-PyCCS approach on particularly high biomass yields indicates that other feedstock sources need to be organized for PyCCS in order for this NETP to play a significant role in contributing NEs at a global scale. Diverse feedstock options of low environmental impact are explored for residues from cropland or forestry (Laird et al., 2009; Woolf et al., 2010), invasive species (Ahmed et al., 2020), hedgerow pruning, street-wood management and municipal waste (Randolph et al., 2017). Yet, the estimates of globally

available crop residues include significant uncertainties (Wirsenius, 2000), while the other sources are not assessed at a global scale yet.

In addition to further feedstock sources, the NE potential of PyCCS could be increased substantially by considering the storage of the bio-oil and permanent-pyrogases; i.e. by sequestering a larger fraction of the initial biomass C (Schmidt et al., 2018). The technology of storing these pyrolysis products in geological deposits is however much more advanced and not yet tested on a reliable scale. Thus, we have chosen the state-of-the-art PyCCS practice of biochar application on agricultural soils to represent PyCCS CEff in our assessment of near-term NETPs potentials.

While this analysis only accounts for the sequestration potential of the biochar and yield increases, the potential overall contribution of PyCCS to the challenge of shifting the land use sector from a greenhouse gas source into a sink is not fully represented. Biochar enriched soils have shown to enhance the build-up of soil organic C (Bai et al., 2019; Blanco-Canqui et al., 2020; Weng et al., 2017) and reduce soil acidity (Chintala et al., 2014; Yuan et al., 2011), nitrate leaching (Borchard et al., 2019; Hagemann et al., 2017) as well as N_2O and CH_4 emissions (Borchard et al., 2019; He et al., 2017; Jeffery et al., 2016), which in total enhances soil quality, cuts down management costs and lowers agricultural greenhouse gas emissions (Kammann et al., 2017; Lehmann et al., 2021). Further, the increased water and nutrient holding capacities of soils after biochar application (Borchard et al., 2019; Razzaghi et al., 2020) can also reduce the pressure on the PBs of freshwater use and N flows.

4.4 Quantified NE potentials in the context of general challenges for NETPs

Leaving CDR requirements in draw-down scenarios and compensation for delays and idleness of mitigation action aside, CDR will still be required to realize net zero targets as the emissions that are hard to abate would need to be compensated. Assuming that, despite ambitious decarbonization, 10% of today's CO_2 emissions would remain as hard-to-abate emissions until mid-century, the overall potentials quantified as upper ceiling potentials for the assessed NETPs in this study could compensate these residual emissions for the assessed timeframe of 40 years. However, this net zero approach is only sufficient if decarbonization measures are successful and if the system is pushed to its limits, i.e. focussing on the interference with the four PBs as assessed in this study, disregarding other restoration and nature protection goals. Also, this conclusion specifically refers to the assessed evaluation period of 40 years. On longer timescales, the additional yearly C accumulation on reforested areas, which contribute the lion's share of the simulated overall NE potential in this assessment, declines until C pools eventually stabilize in mature forests. This points to the fact that additional PB-compatible NETPs will be required for long-term net zero greenhouse gas emissions.

Even though the overall NE potential of about 4 $GtCO_2$-eq yr^{-1} seems relatively low in comparison to NE demands in the majority of IAM scenarios, it still compares to more than half of the current net C sink of the entire global land surface (Friedlingstein et al., 2021). That would mean to create an additional anthropogenic sink of the magnitude of half of the existing natural (net) land sink. Thus, the deployment of the NETPs up to the quantified maxima would be a form of bio-geoengineering at a planetary scale that would require a vast global effort for a successful implementation. Furthermore, this is a burden we lay on the future generations, especially when even more CDR would be required to compensate any further delay of stringent decarbonization. Thus, even a world with a stabilized climate in the future would most likely be an Earth system that is severely manipulated by humans – well deserving the title "Anthropocene".

4.5 Further steps

As a contribution to exploring the safe operating space in the Anthropocene, we set out to analyse PB-compatible potentials for three major NETPs, BECCS, reforestation and LCN-PyCCS. While plantation-based BECCS is difficult to reconcile with PBs, reforestation and LCN-PyCCS may have synergies with regard to PBs and other sustainability targets. Future research might further expand the portfolio of assessed NETPs, given that constrained potentials of individual technologies and practices may add up to increase overall PB-compatible potentials (Fuss et al., 2018). With regard to PBs, particularly promising NETPs with synergies for PBs as well as other sustainability targets include BECCS from residues and waste, improved forest management, agroforestry and wetland restoration amongst others (Griscom et al., 2017), which are addressed in detail for the Nordic region in D3.6 and on a global level in NEGEM's sister project LANDMARC (EU Horizon 2020 Research and Innovation Programme, grant agreement No 869367).

In the context of NEGEM, the following three aspects deserve particular attention within further WP3 research:

- *Interdependence of NETP potentials with developments within the food system:* Potential PB-compatible NE capacities depend to a large degree on developments within the food system, i.e. future land availability for land-based climate change mitigation (Erb et al., 2012; Kalt et al., 2020). Further scenarios could systematically analyse the availability of pasture areas for reforestation and/or BECCS depending on developments within the food system (i.e. diet changes; increases in feeding efficiency) and more closely examine trade-offs between climate mitigation and food security with respect to land and water resources (Deliverable 3.7).
- *More thorough analysis of NETP's impact on biosphere integrity:* Biosphere integrity, as the second core PB, needs specific attention when assessing environmental impacts of NETPs. In the context of Deliverable 3.3, key measures for biosphere integrity will be evaluated and/or developed, going beyond the current PB definition, to better capture this second pillar of Earth system stability within NETP assessment.
- *Impacts on climate change and extreme events on NETP potentials:* We here excluded effects of climate change and derived maximum NE potentials under current climate conditions. Potential reductions of the here quantified NE capacities through extreme events will be addressed more closely in Deliverable 3.4.

5 Key findings and policy relevant messages

Taking a supply-constrained perspective is crucial when assessing responsible and realistic NE potentials as aimed for within NEGEM. We here specifically addressed the environmental dimension, focussing on four terrestrial PBs – for land-system change, biosphere integrity, freshwater use and N cycling – and estimated that maximum global NEs from plantation-based BECCS outside of agricultural areas are constrained to ~1.2 $GtCO_2$-eq yr^{-1} (referring to an evaluation period of 40 years). While this covers only 43% or 13% of the median BECCS rates assumed in 1.5°/2°-compatible IAM scenarios in 2050 or 2100, respectively, the potential will further be reduced to almost zero if deforestation for BECCS plantations is precluded. This emphasizes that any conversion of natural vegetation to biomass plantations is extremely difficult to reconcile with PBs and other environmental targets, given that agriculture is already today the major driver of PB transgression and therefore a major anthropogenic pressure on the Earth system. A more holistic perspective on Earth system stability, which does not only consider climate change, but all relevant Earth system components, thus calls for a very cautious consideration of plantations-based BECCS, contrasting common assumptions in demand-driven and cost-optimizing IAMs.

The constrained NE capacities through BECCS might however be significantly increased through reforestation on pasture areas, with a further annual NE rate of 2–3.7 $GtCO_2$-eq yr^{-1} depending on the amount of rededicated pasture area and excluding climate change effects on C stocks within forests. This might not only contribute to climate change mitigation, but also to reducing pressures on terrestrial PBs and achieving international nature restoration targets, i.e. the Bonn Challenge on forest restoration or the 2030 targets of the UN Convention on Biological Diversity. These NE potentials and its co-benefits are particularly dependant on dietary changes towards less livestock products, as a key prerequisite for reduced pasture demand.

While we here estimated only very limited NE potentials from plantation-based LCN-PyCCS, the approach may be more efficient when considering other sources for biochar production, like residues and invasive species. Additional NETPs with synergies for several environmental targets, i.e. agroforestry or improved forest management, might further contribute to expand PB-compatible NE potentials.

Although the PB-compatible potentials estimated here are at the lower end of estimated NE rates assumed in IAM scenarios compatible with the Paris agreement, they are in line with mitigation scenarios putting a strong emphasis on rapid decarbonisation, reduced energy demand and/or achievement of sustainable development goals. This underpins that climate change mitigation does not have to come at the cost of other crucial Earth system components, but that rapid socioeconomic transformations are needed to prevent further PB transgressions.

Our analysis focused on global PB compatible NETP potentials, derived from geographically explicit simulations with the dynamic global vegetation model LPJmL. It thereby contributed to a more holistic consideration of limits and opportunities for BECCS, reforestation and PyCCS with regard to environmental dimensions relevant for Earth system stability. From the perspective of the EU, these results have to be interpreted in a more regional context of political, social and technological feasibility as produced by the NEGEM project as a whole. For this, the assessment of the environmental dimension will feed into further Europe specific NEGEM scenarios to derive country-specific portfolios and realistic and responsible NE pathways for the EU, which take into account the individual country's characteristics (e.g. low reforestation potential and high availability of forestry residues for BECCS in the Nordic countries, see D3.6). However, as CDR is a topic where Europe can likely only partially rely on sequestration on its own territory, additionally requiring a realistic assessment and subsequent use of global potentials overall, this analysis clearly shows that there are both opportunities and limitations originating from the overarching objective of re-stabilizing the Earth system in its current interglacial-like state. This requires

consideration of other environmental dimensions relevant to the state of the Earth system in addition to merely carbon sequestration. The EU's assumptions about realistic CDR potentials beyond its territory should therefore be squarely founded on consideration of all planetary boundaries, not just the climate targets. Moreover, land-based potentials are highly contingent on developments in land use more generally, against the backdrop of growing demand for an ever larger and more affluent population. The EU should therefore not adopt overly optimistic assumptions about large-scale land-based mitigation for achieving high levels of CO_2 emissions compensation. Our analysis shows that CDR from BECCS, reforestation and PyCCS rather is a contribution to climate change mitigation that goes hand in hand with sufficiently ambitious decarbonisation targets, but requires careful management and considered deployment to be feasible and realistic.

For preparing this report, the following deliverable/s have been taken into consideration:

D#	Deliverable title	Lead Beneficiary	Type	Dissemination level	Due date (in MM)
D3.1	Upgraded LPJmL5 version	PIK	R	PU	M12
D7.1	MONET-EU tool	ICL	R	PU	M12
D7.2	Extended MONET-EU	ICL	R	PU	M17

References

Aerts, R., & Honnay, O. (2011). Forest restoration, biodiversity and ecosystem functioning. *BMC Ecology*, *11*(1), 29. https://doi.org/10.1186/1472-6785-11-29

Ahmed, A., Abu Bakar, M. S., Hamdani, R., Park, Y.-K., Lam, S. S., Sukri, R. S., Hussain, M., Majeed, K., Phusunti, N., Jamil, F., & Aslam, M. (2020). Valorization of underutilized waste biomass from invasive species to produce biochar for energy and other value-added applications. *Environmental Research*, *186*, 109596. https://doi.org/https://doi.org/10.1016/j.envres.2020.109596

Ai, Z., Hanasaki, N., Heck, V., Hasegawa, T., & Fujimori, S. (2021). Global bioenergy with carbon capture and storage potential is largely constrained by sustainable irrigation. *Nature Sustainability*. https://doi.org/10.1038/s41893-021-00740-4

Algunaibet, I. M., Pozo, C., Galan-Martin, A., Huijbregts, M. A. J., Mac Dowell, N., & Guillen-Gosalbez, G. (2019). Powering sustainable development within planetary boundaries. *Energy & Environmental Science*, *12*(6), 1890-1900. https://doi.org/10.1039/c8ee03423k

Anderson, K., & Peters, G. (2016). The trouble with negative emissions. *Science*, *354*(6309), 182-183. https://doi.org/10.1126/science.aah4567

Bai, S. H., Omidvar, N., Gallart, M., Kämper, W., Tahmasbian, I., Farrar, M. B., Singh, K., Zhou, G., Muqadass, B., Xu, C.-Y., Koech, R., Li, Y., Nguyen, T. T. N., & van Zwieten, L. (2022). Combined effects of biochar and fertilizer applications on yield: A review and meta-analysis. *Science of The Total Environment*, *808*, 152073. https://doi.org/https://doi.org/10.1016/j.scitotenv.2021.152073

Bai, X., Huang, Y., Ren, W., Coyne, M., Jacinthe, P.-A., Tao, B., Hui, D., Yang, J., & Matocha, C. (2019). Responses of soil carbon sequestration to climate-smart agriculture practices: A meta-analysis. *Global Change Biology*, *25*(8), 2591-2606. https://doi.org/https://doi.org/10.1111/gcb.14658

Bala, G., Caldeira, K., Wickett, M., Phillips, T. J., Lobell, D. B., Delire, C., & Mirin, A. (2007). Combined climate and carbon-cycle effects of large-scale deforestation. *Proceedings of the National Academy of Sciences*, *104*(16), 6550-6555. https://doi.org/doi:10.1073/pnas.0608998104

Bauer, N., Rose, S. K., Fujimori, S., van Vuuren, D. P., Weyant, J., Wise, M., Cui, Y., Daioglou, V., Gidden, M. J., Kato, E., Kitous, A., Leblanc, F., Sands, R., Sano, F., Strefler, J., Tsutsui, J., Bibas, R., Fricko, O., Hasegawa, T., Klein, D., Kurosawa, A., Mima, S., & Muratori, M. (2020). Global energy sector emission reductions and bioenergy use: overview of the bioenergy demand phase of the EMF-33 model comparison. *Climatic Change*, *163*(3), 1553-1568. https://doi.org/10.1007/s10584-018-2226-y

Beatty, C., Stevenson, M., Pacheco, P., Terrana, A., Folse, M., & Cody, A. (2022). *The Vitality of Forests. Illustrating the Evidence Connecting*

Forests and Human Health.

Bednar, J., Obersteiner, M., & Wagner, F. (2019). On the financial viability of negative emissions. *Nature Communications*, *10*(1), 1783. https://doi.org/10.1038/s41467-019-09782-x

Beringer, T., Lucht, W., & Schaphoff, S. (2011). Bioenergy production potential of global biomass plantations under environmental and agricultural constraints. *GCB Bioenergy*, *3*, 299-312. https://doi.org/10.1111/j.1757-1707.2010.01088.x

Betts, M. G., Wolf, C., Ripple, W. J., Phalan, B., Millers, K. A., Duarte, A., Butchart, S. H. M., & Levi, T. (2017). Global forest loss disproportionately erodes biodiversity in intact landscapes. *Nature*, *547*(7664), 441-444. https://doi.org/10.1038/nature23285

Blanco-Canqui, H., Laird, D. A., Heaton, E. A., Rathke, S., & Acharya, B. S. (2020). Soil carbon increased by twice the amount of biochar carbon applied after 6 years: Field evidence of negative priming. *GCB Bioenergy*, *12*(4), 240-251. https://doi.org/10.1111/gcbb.12665

Bonan, G. B. (2008). Forests and Climate Change: Forcings, Feedbacks, and the Climate Benefits of Forests. *Science*, *320*(5882), 1444-1449. https://doi.org/doi:10.1126/science.1155121

Bondeau, A., Smith, P. C., Zaehle, S., Schaphoff, S., Lucht, W., Cramer, W., Gerten, D., Lotze-Campen, H., Muller, C., Reichstein, M., & Smith, B. (2007). Modelling the role of agriculture for the 20th century global terrestrial carbon balance. *Global Change Biology*, *13*, 679-706. https://doi.org/10.1111/j.1365-2486.2006.01305.x

Borchard, N., Schirrmann, M., Cayuela, M. L., Kammann, C., Wrage-Mönnig, N., Estavillo, J. M., Fuertes-Mendizábal, T., Sigua, G., Spokas, K., Ippolito, J. A., & Novak, J. (2019). Biochar, soil and land-use interactions that reduce nitrate leaching and N2O emissions: A meta-analysis. *Science of The Total Environment*, *651*, 2354-2364. https://doi.org/https://doi.org/10.1016/j.scitotenv.2018.10.060

Boulton, C. A., Lenton, T. M., & Boers, N. (2022). Pronounced loss of Amazon rainforest resilience since the early 2000s. *Nature Climate Change*, *12*(3), 271-278. https://doi.org/10.1038/s41558-022-01287-8

Bouwman, A. F., Beusen, A. H. W., Griffioen, J., Van Groenigen, J. W., Hefting, M. M., Oenema, O., Van Puijenbroek, P. J. T. M., Seitzinger, S., Slomp, C. P., & Stehfest, E. (2013). Global trends and uncertainties in terrestrial denitrification and N2O emissions. *Philosophical Transactions of the Royal Society B: Biological Sciences*, *368*(1621), 20130112. https://doi.org/doi:10.1098/rstb.2013.0112

Boysen, L. R., Lucht, W., & Gerten, D. (2017). Trade-offs for food production, nature conservation and climate limit the terrestrial carbon dioxide removal potential. *Global Change Biology*, *23*(10), 4303-4317. https://doi.org/10.1111/gcb.13745

Braakhekke, M. C., Doelman, J. C., Baas, P., Müller, C., Schaphoff, S., Stehfest, E., & van Vuuren, D. P. (2019). Modeling forest plantations for carbon uptake with the LPJmL dynamic global vegetation model. *Earth Syst. Dynam.*, *10*(4), 617-630. https://doi.org/10.5194/esd-10-617-2019

Bui, M., Zhang, D., Fajardy, M., & Mac, D. N. (2021). Delivering carbon negative electricity, heat and hydrogen with BECCS – Comparing the options. *International Journal of Hydrogen Energy*, *46*, 15298-15321. https://doi.org/10.1016/j.ijhydene.2021.02.042

Byers, E., Krey, V., Kriegler, E., Riahi, K., Schaeffer, R., Kikstra, J., Lamboll, R., Nicholls, Z., Sanstad, M., Smith, C., van der Wijst, K.-I., Lecocq, F., Portugal-Pereira, J., Saheb, Y., Strømann, A., Winkler, H., Auer, C., Brutschin, E., Lepault, C., Müller-Casseres, E., Gidden, M. J., Huppmann, D., Kolp, P., Marangoni, G., Werning, M., Calvin, K., Guivarch, C., Hasegawa, T., Peters, G., Steinberger, J. K., Tavoni, M., von Vuuren, D., Forster, P., Lewis, J., Meinshausen, M., Rogelj, J., Samset, B., Skeie, R., & Al Khourdajie, A. (2022). *AR6 Scenarios Database hosted by IIASA* Version 1.0). https://doi.org/10.5281/zenodo.5886912

Cadoux, S., Riche, A. B., Yates, N. E., & Machet, J.-M. (2012). Nutrient requirements of Miscanthus x giganteus: Conclusions from a review of published studies. *Biomass and Bioenergy*, *38*, 14-22. https://doi.org/https://doi.org/10.1016/j.biombioe.2011.01.015

Camargo, J. A., & Alonso, Á. (2006). Ecological and toxicological effects of inorganic nitrogen pollution in aquatic ecosystems: A global assessment. *Environment International*, *32*(6), 831-849. https://doi.org/https://doi.org/10.1016/j.envint.2006.05.002

Campbell, B. M., Beare, D. J., Bennett, E. M., Hall-Spencer, J. M., Ingram, J. S. I., Jaramillo, F., Ortiz, R., Ramankutty, N., Sayer, J. A., & Shindell, D. (2017). Agriculture production as a major driver of the Earth system exceeding planetary boundaries. *Ecology and Society*, *22*(4), Article 8. https://doi.org/10.5751/ES-09595-220408

Camps-Arbestain, M., Amonette, J. E., Singh, B., Wang, T., & Schmidt, H. P. (2015). A biochar classification system and associated test methods. *Biochar for Environmental Management: Science, Technology and Implementation*, 165-193.

Chang, J., Havlík, P., Leclère, D., de Vries, W., Valin, H., Deppermann, A., Hasegawa, T., & Obersteiner, M. (2021). Reconciling regional nitrogen boundaries with global food security. *Nature Food*, *2*(9), 700-711. https://doi.org/10.1038/s43016-021-00366-x

Chavas, J.-P. (2008). On the economics of agricultural production*. *Australian Journal of Agricultural and Resource Economics*, *52*(4), 365-380. https://doi.org/https://doi.org/10.1111/j.1467-8489.2008.00442.x

Chintala, R., Mollinedo, J., Schumacher, T. E., Malo, D. D., & Julson, J. L. (2014). Effect of biochar on chemical properties of acidic soil. *Archives of Agronomy and Soil Science*, *60*(3), 393-404. https://doi.org/10.1080/03650340.2013.789870

Chiquier, S., Patrizio, P., Sunny, N., Bui, M., & Mac Dowell, N. (2022). A comparative analysis of the efficiency, timing and permanence of CO2 removal options [in review]. *Energy Environ. Sci.*

Christian, D. G., Poulton, P. R., Riche, A. B., Yates, N. E., & Todd, A. D. (2006). The recovery over several seasons of 15N-labelled fertilizer applied to Miscanthus×giganteus ranging from 1 to 3 years old. *Biomass and Bioenergy*, *30*(2), 125-133. https://doi.org/https://doi.org/10.1016/j.biombioe.2005.11.002

Cook-Patton, S. C., Drever, C. R., Griscom, B. W., Hamrick, K., Hardman, H., Kroeger, T., Pacheco, P., Raghav, S., Stevenson, M., Webb, C., Yeo, S., & Ellis, P. W. (2021). Protect, manage and then restore lands for climate mitigation. *Nature Climate Change*, *11*(12), 1027-1034. https://doi.org/10.1038/s41558-021-01198-0

Cook-Patton, S. C., Leavitt, S. M., Gibbs, D., Harris, N. L., Lister, K., Anderson-Teixeira, K. J., Briggs, R. D., Chazdon, R. L., Crowther, T. W., Ellis, P. W., Griscom, H. P., Herrmann, V., Holl, K. D., Houghton, R. A., Larrosa, C., Lomax, G., Lucas, R., Madsen, P., Malhi, Y., Paquette, A., Parker, J. D., Paul, K., Routh, D., Roxburgh, S., Saatchi, S., van den Hoogen, J., Walker, W. S., Wheeler, C. E., Wood, S. A., Xu, L., & Griscom, B. W. (2020). Mapping carbon accumulation potential from global natural forest regrowth. *Nature*, *585*(7826), 545-550. https://doi.org/10.1038/s41586-020-2686-x

Cornelissen, G., Pandit, N. R., Taylor, P., Pandit, B. H., Sparrevik, M., & Schmidt, H. P. (2016). Emissions and Char Quality of Flame-Curtain "Kon Tiki" Kilns for Farmer-Scale Charcoal/Biochar Production. *Plos One*, *11*(5), e0154617. https://doi.org/10.1371/journal.pone.0154617

de Vries, W., Kros, J., Kroeze, C., & Seitzinger, S. P. (2013). Assessing planetary and regional nitrogen boundaries related to food security and adverse environmental impacts. *Current Opinion in Environmental Sustainability*, *5*, 392-402. https://doi.org/http://dx.doi.org/10.1016/j.cosust.2013.07.004

de Vries, W., Schulte-Uebbing, L., Kros, H., Voogd, J. C., & Louwagie, G. (2021). Spatially explicit boundaries for agricultural nitrogen inputs in the European Union to meet air and water quality targets. *Science of The Total Environment*, *786*, 147283. https://doi.org/https://doi.org/10.1016/j.scitotenv.2021.147283

Elliott, J., Müller, C., Deryng, D., Chryssanthacopoulos, J., Boote, K. J., Büchner, M., Foster, I., Glotter, M., Heinke, J., Iizumi, T., Izaurralde, R. C., Mueller, N. D., Ray, D. K., Rosenzweig, C., Ruane, A. C., & Sheffield, J. (2015). The Global Gridded Crop Model Intercomparison: data and modeling protocols for Phase 1 (v1.0). *Geosci. Model Dev.*, *8*(2), 261-277. https://doi.org/10.5194/gmd-8-261-2015

Ellison, D., Morris, C. E., Locatelli, B., Sheil, D., Cohen, J., Murdiyarso, D., Gutierrez, V., Noordwijk, M. v., Creed, I. F., Pokorny, J., Gaveau, D., Spracklen, D. V., Tobella, A. B., Ilstedt, U., Teuling, A. J., Gebrehiwot, S. G., Sands, D. C., Muys, B., Verbist, B., Springgay, E., Sugandi, Y., & Sullivan, C. A. (2017). Trees, forests and water: Cool insights for a hot world. *Global Environmental Change*, *43*, 51-61. https://doi.org/https://doi.org/10.1016/j.gloenvcha.2017.01.002

Erb, K.-H., Haberl, H., & Plutzar, C. (2012). Dependency of global primary bioenergy crop potentials in 2050 on food systems, yields, biodiversity conservation and political stability. *Energy Policy*, *47*, 260-269. https://doi.org/https://doi.org/10.1016/j.enpol.2012.04.066

Erb, K.-H., Kastner, T., Plutzar, C., Bais, A. L. S., Carvalhais, N., Fetzel, T., Gingrich, S., Haberl, H., Lauk, C., Niedertscheider, M., Pongratz, J., Thurner, M., & Luyssaert, S. (2018). Unexpectedly large impact of forest management and grazing on global vegetation biomass. *Nature*, *553*(7686), 73-76. https://doi.org/10.1038/nature25138

Fischer, J., Brosi, B., Daily, G. C., Ehrlich, P. R., Goldman, R., Goldstein, J., Lindenmayer, D. B., Manning, A. D., Mooney, H. A., Pejchar, L., Ranganathan, J., & Tallis, H. (2008). Should agricultural policies encourage land sparing or wildlife-friendly farming? *Frontiers in Ecology and the Environment*, *6*, 380-385. https://doi.org/10.1890/070019

Foley, J. A., DeFries, R., Asner, G. P., Barford, C., Bonan, G., Carpenter, S. R., Chapin, F. S., Coe, M. T., Daily, G. C., Gibbs, H. K., Helkowski, J. H., Holloway, T., Howard, E. A., Kucharik, C. J., Monfreda, C., Patz, J. A., Prentice, I. C., Ramankutty, N., & Snyder, P. K. (2005). Global Consequences of Land Use. *Science*, *309*, 570-574. https://doi.org/10.1126/science.1111772

Frank, S., Gusti, M., Havlík, P., Lauri, P., DiFulvio, F., Forsell, N., Hasegawa, T., Krisztin, T., Palazzo, A., & Valin, H. (2021). Land-based climate change mitigation potentials within the agenda for sustainable development. *Environmental Research Letters*, *16*(2), 024006. https://doi.org/10.1088/1748-9326/abc58a

Friedlingstein, P., Jones, M. W., O'Sullivan, M., Andrew, R. M., Bakker, D. C. E., Hauck, J., Le Quéré, C., Peters, G. P., Peters, W., Pongratz, J., Sitch, S., Canadell, J. G., Ciais, P., Jackson, R. B., Alin, S. R., Anthoni, P., Bates, N. R., Becker, M., Bellouin, N., Bopp, L., Chau, T. T. T., Chevallier, F., Chini, L. P., Cronin, M., Currie, K. I., Decharme, B., Djeutchouang, L., Dou, X., Evans, W., Feely, R. A., Feng, L., Gasser, T., Gilfillan, D., Gkritzalis, T., Grassi, G., Gregor, L., Gruber, N., Gürses, Ö., Harris, I., Houghton, R. A., Hurtt, G. C., Iida, Y., Ilyina, T., Luijkx, I. T., Jain, A. K., Jones, S. D., Kato, E., Kennedy, D., Klein Goldewijk, K., Knauer, J., Korsbakken, J. I., Körtzinger, A., Landschützer, P., Lauvset, S. K., Lefèvre, N., Lienert, S., Liu, J., Marland, G., McGuire, P. C., Melton, J. R., Munro, D. R., Nabel, J. E. M. S., Nakaoka, S. I., Niwa, Y., Ono, T., Pierrot, D., Poulter, B., Rehder, G., Resplandy, L., Robertson, E., Rödenbeck, C., Rosan, T. M., Schwinger, J., Schwingshackl, C., Séférian, R., Sutton, A. J., Sweeney, C., Tanhua, T., Tans, P. P., Tian, H., Tilbrook, B., Tubiello, F., van der Werf, G., Vuichard, N., Wada, C., Wanninkhof, R., Watson, A., Willis, D., Wiltshire, A. J., Yuan, W., Yue, C., Yue, X., Zaehle, S., & Zeng, J. (2021). Global Carbon Budget 2021. *Earth Syst. Sci. Data Discuss.*, *2021*, 1-191. https://doi.org/10.5194/essd-2021-386

Friggens, N. L., Hester, A. J., Mitchell, R. J., Parker, T. C., Subke, J.-A., & Wookey, P. A. (2020). Tree planting in organic soils does not result in net carbon sequestration on decadal timescales. *Global Change Biology*, *26*(9), 5178-5188. https://doi.org/https://doi.org/10.1111/gcb.15229

Fuss, S., Lamb, W., F. , Callaghan, M., W. , Hilaire, J., Creutzig, F., Amann, T., Beringer, T., Garcia, W. d. O., Hartmann, J., Khanna, T., Luderer, G., Nemet, G., F., Rogelj, J., Smith, P., Vicente, J. L., Wilcox, J., Dominguez, M. d. M. Z., & Minx, J., C. . (2018). Negative emissions—Part 2: Costs, potentials and side effects. *Environmental Research Letters*, *13*(6), 063002. http://stacks.iop.org/1748-9326/13/i=6/a=063002

Gerten, D., Heck, V., Jägermeyr, J., Bodirsky, B. L., Fetzer, I., Jalava, M., Kummu, M., Lucht, W., Rockström, J., Schaphoff, S., & Schellnhuber, H. J. (2020). Feeding ten billion people is possible within four terrestrial planetary boundaries. *Nature Sustainability*, *3*(3), 200-208. https://doi.org/10.1038/s41893-019-0465-1

Gleeson, T., Wang-Erlandsson, L., Zipper, S. C., Porkka, M., Jaramillo, F., Gerten, D., Fetzer, I., Cornell, S. E., Piemontese, L., Gordon, L. J., Rockström, J., Oki, T., Sivapalan, M., Wada, Y., Brauman, K. A., Flörke, M., Bierkens, M. F. P., Lehner, B., Keys, P., Kummu, M., Wagener, T., Dadson, S., Troy, T. J., Steffen, W., Falkenmark, M., & Famiglietti, J. S. (2020). The Water Planetary Boundary: Interrogation and Revision. *One Earth*, *2*(3), 223-234. https://doi.org/https://doi.org/10.1016/j.oneear.2020.02.009

Gómez-González, S., Ochoa-Hueso, R., & Pausas, J. G. (2020). Afforestation falls short as a biodiversity strategy. *Science*, *368*(6498), 1439-1439. https://doi.org/doi:10.1126/science.abd3064

Grantham, H. S., Duncan, A., Evans, T. D., Jones, K. R., Beyer, H. L., Schuster, R., Walston, J., Ray, J. C., Robinson, J. G., Callow, M., Clements, T., Costa, H. M., DeGemmis, A., Elsen, P. R., Ervin, J., Franco, P., Goldman, E., Goetz, S., Hansen, A., Hofsvang, E., Jantz, P., Jupiter, S., Kang, A., Langhammer, P., Laurance, W. F., Lieberman, S., Linkie, M., Malhi, Y., Maxwell, S., Mendez, M., Mittermeier, R., Murray, N. J., Possingham, H., Radachowsky, J., Saatchi, S., Samper, C., Silverman, J., Shapiro, A., Strassburg, B., Stevens, T., Stokes, E., Taylor, R., Tear, T., Tizard, R., Venter, O., Visconti, P., Wang, S., & Watson, J. E. M. (2020). Anthropogenic modification of forests means only 40% of remaining forests have high ecosystem integrity. *Nature Communications*, *11*(1), 5978. https://doi.org/10.1038/s41467-020-19493-3

Griscom, B. W., Adams, J., Ellis, P. W., Houghton, R. A., Lomax, G., Miteva, D. A., Schlesinger, W. H., Shoch, D., Siikamäki, J. V., Smith, P., Woodbury, P., Zganjar, C., Blackman, A., Campari, J., Conant, R. T., Delgado, C., Elias, P., Gopalakrishna, T., Hamsik, M. R., Herrero, M., Kiesecker, J., Landis, E., Laestadius, L., Leavitt, S. M., Minnemeyer, S., Polasky, S., Potapov, P., Putz, F. E., Sanderman, J., Silvius, M., Wollenberg, E., & Fargione, J. (2017). Natural climate solutions. *Proceedings of the National Academy of Sciences*, *114*(44), 11645-11650. https://doi.org/10.1073/pnas.1710465114

Haberl, H., Beringer, T., Bhattacharya, S. C., Erb, K.-H., & Hoogwijk, M. (2010). The global technical potential of bio-energy in 2050 considering sustainability constraints. *Current Opinion in Environmental Sustainability*, *2*(5), 394-403. https://doi.org/https://doi.org/10.1016/j.cosust.2010.10.007

Hagemann, N., Joseph, S., Schmidt, H.-P., Kammann, C. I., Harter, J., Borch, T., Young, R. B., Varga, K., Taherymoosavi, S., Elliott, K. W., McKenna, A., Albu, M., Mayrhofer, C., Obst, M., Conte, P., Dieguez-Alonso, A., Orsetti, S., Subdiaga, E., Behrens, S., & Kappler, A. (2017). Organic coating on biochar explains its nutrient retention and stimulation of soil fertility. *Nature Communications*, *8*(1), 1089. https://doi.org/10.1038/s41467-017-01123-0

Hammond, W. M., Williams, A. P., Abatzoglou, J. T., Adams, H. D., Klein, T., López, R., Sáenz-Romero, C., Hartmann, H., Breshears, D. D., & Allen, C. D. (2022). Global field observations of tree die-off reveal hotter-drought fingerprint for Earth's forests. *Nature Communications*, *13*(1), 1761. https://doi.org/10.1038/s41467-022-29289-2

Hanssen, S. V., Daioglou, V., Steinmann, Z. J. N., Frank, S., Popp, A., Brunelle, T., Lauri, P., Hasegawa, T., Huijbregts, M. A. J., & Van Vuuren, D. P. (2020). Biomass residues as twenty-first century bioenergy feedstock—a comparison of eight integrated assessment models. *Climatic Change*, *163*(3), 1569-1586. https://doi.org/10.1007/s10584-019-02539-x

Harris, I., Osborn, T. J., Jones, P., & Lister, D. (2020). Version 4 of the CRU TS monthly high-resolution gridded multivariate climate dataset. *Scientific Data*, *7*(1), 109. https://doi.org/10.1038/s41597-020-0453-3

Hastings, A., Clifton-Brown, J., Wattenbach, M., Mitchell, C. P., Stampfl, P., & Smith, P. (2009). Future energy potential of Miscanthus in Europe. *GCB Bioenergy*, *1*(2), 180-196. https://doi.org/10.1111/j.1757-1707.2009.01012.x

Hayek, M. N., Harwatt, H., Ripple, W. J., & Mueller, N. D. (2021). The carbon opportunity cost of animal-sourced food production on land. *Nature Sustainability*, *4*(1), 21-24. https://doi.org/10.1038/s41893-020-00603-4

He, Y., Zhou, X., Jiang, L., Li, M., Du, Z., Zhou, G., Shao, J., Wang, X., Xu, Z., Hosseini Bai, S., Wallace, H., & Xu, C. (2017). Effects of biochar application on soil greenhouse gas fluxes: a meta-analysis. *GCB Bioenergy*, *9*(4), 743-755. https://doi.org/https://doi.org/10.1111/gcbb.12376

Heck, V., Gerten, D., Lucht, W., & Boysen, L. R. (2016). Is extensive terrestrial carbon dioxide removal a 'green' form of geoengineering? A global modelling study. *Global and Planetary Change*, *137*, 123-130. https://doi.org/http://doi.org/10.1016/j.gloplacha.2015.12.008

Heck, V., Gerten, D., Lucht, W., & Popp, A. (2018). Biomass-based negative emissions difficult to reconcile with planetary boundaries. *Nature Climate Change*, *8*(2), 151-155. https://doi.org/10.1038/s41558-017-0064-y

Hudson, L. N., Newbold, T., Contu, S., Hill, S. L. L., Lysenko, I., De Palma, A., Phillips, H. R. P., Senior, R. A., Bennett, D. J., Booth, H., Choimes, A., Correia, D. L. P., Day, J., Echeverría-Londoño, S., Garon, M., Harrison, M. L. K., Ingram, D. J., Jung, M., Kemp, V., Kirkpatrick, L., Martin, C. D., Pan, Y., White, H. J., Aben, J., Abrahamczyk, S., Adum, G. B., Aguilar-Barquero, V., Aizen, M. A., Ancrenaz, M., Arbeláez-Cortés, E., Armbrecht, I., Azhar, B., Azpiroz, A. B., Baeten, L., Báldi, A., Banks, J. E., Barlow, J., Batáry, P., Bates, A. J., Bayne, E. M., Beja, P., Berg, Å., Berry, N. J., Bicknell, J. E., Bihn, J. H., Böhning-Gaese, K., Boekhout, T., Boutin, C., Bouyer, J., Brearley, F. Q., Brito, I., Brunet, J., Buczkowski, G., Buscardo, E., Cabra-García, J., Calviño-Cancela, M., Cameron, S. A., Cancello, E. M., Carrijo, T. F., Carvalho, A. L., Castro, H., Castro-Luna, A. A., Cerda, R., Cerezo, A., Chauvat, M., Clarke, F. M., Cleary, D. F. R., Connop, S. P., D'Aniello, B., da Silva, P. G., Darvill, B., Dauber, J., Dejean, A., Diekötter, T., Dominguez-Haydar, Y., Dormann, C. F., Dumont, B., Dures, S. G., Dynesius, M., Edenius, L., Elek, Z., Entling, M. H., Farwig, N., Fayle, T. M., Felicioli, A., Felton, A. M., Ficetola, G. F., Filgueiras, B. K. C., Fonte, S. J., Fraser, L. H., Fukuda, D., Furlani, D., Ganzhorn, J. U., Garden, J. G., Gheler-Costa, C., Giordani, P., Giordano, S., Gottschalk, M. S., Goulson, D., Gove, A. D., Grogan, J., Hanley, M. E., Hanson, T., Hashim, N. R., Hawes, J. E., Hébert, C., Helden, A. J., Henden, J.-A., Hernández, L., Herzog, F., Higuera-Diaz, D., Hilje, B., Horgan, F. G., Horváth, R., Hylander, K., Isaacs-Cubides, P., Ishitani, M., Jacobs, C. T., Jaramillo, V. J.,

Jauker, B., Jonsell, M., Jung, T. S., Kapoor, V., Kati, V., Katovai, E., Kessler, M., Knop, E., Kolb, A., Kőrösi, Á., Lachat, T., Lantschner, V., Le Féon, V., LeBuhn, G., Légaré, J.-P., Letcher, S. G., Littlewood, N. A., López-Quintero, C. A., Louhaichi, M., Lövei, G. L., Lucas-Borja, M. E., Luja, V. H., Maeto, K., Magura, T., Mallari, N. A., Marin-Spiotta, E., Marshall, E. J. P., Martínez, E., Mayfield, M. M., Mikusinski, G., Milder, J. C., Miller, J. R., Morales, C. L., Muchane, M. N., Muchane, M., Naidoo, R., Nakamura, A., Naoe, S., Nates-Parra, G., Navarrete Gutierrez, D. A., Neuschulz, E. L., Noreika, N., Norfolk, O., Noriega, J. A., Nöske, N. M., O'Dea, N., Oduro, W., Ofori-Boateng, C., Oke, C. O., Osgathorpe, L. M., Paritsis, J., Parra-H, A., Pelegrin, N., Peres, C. A., Persson, A. S., Petanidou, T., Phalan, B., Philips, T. K., Poveda, K., Power, E. F., Presley, S. J., Proença, V., Quaranta, M., Quintero, C., Redpath-Downing, N. A., Reid, J. L., Reis, Y. T., Ribeiro, D. B., Richardson, B. A., Richardson, M. J., Robles, C. A., Römbke, J., Romero-Duque, L. P., Rosselli, L., Rossiter, S. J., Roulston, T. a. H., Rousseau, L., Sadler, J. P., Sáfián, S., Saldaña-Vázquez, R. A., Samnegård, U., Schüepp, C., Schweiger, O., Sedlock, J. L., Shahabuddin, G., Sheil, D., Silva, F. A. B., Slade, E. M., Smith-Pardo, A. H., Sodhi, N. S., Somarriba, E. J., Sosa, R. A., Stout, J. C., Struebig, M. J., Sung, Y.-H., Threlfall, C. G., Tonietto, R., Tóthmérész, B., Tscharntke, T., Turner, E. C., Tylianakis, J. M., Vanbergen, A. J., Vassilev, K., Verboven, H. A. F., Vergara, C. H., Vergara, P. M., Verhulst, J., Walker, T. R., Wang, Y., Watling, J. I., Wells, K., Williams, C. D., Willig, M. R., Woinarski, J. C. Z., Wolf, J. H. D., Woodcock, B. A., Yu, D. W., Zaitsev, A. S., Collen, B., Ewers, R. M., Mace, G. M., Purves, D. W., Scharlemann, J. P. W., & Purvis, A. (2014). The PREDICTS database: a global database of how local terrestrial biodiversity responds to human impacts. *Ecology and Evolution*, *4*(24), 4701-4735. https://doi.org/https://doi.org/10.1002/ece3.1303

Humpenöder, F., Popp, A., Bodirsky, B. L., Weindl, I., Biewald, A., Lotze-Campen, H., Dietrich, J. P., Klein, D., Kreidenweis, U., Müller, C., Rolinski, S., & Stevanovic, M. (2018). Large-scale bioenergy production: how to resolve sustainability trade-offs? *Environmental Research Letters*, *13*(2), 024011. https://doi.org/10.1088/1748-9326/aa9e3b

Humpenöder, F., Popp, A., Dietrich, J. P., Klein, D., Lotze-Campen, H., Bonsch, M., Bodirsky, B. L., Weindl, I., Stevanovic, M., & Muller, C. (2014). Investigating afforestation and bioenergy CCS as climate change mitigation strategies. *Environmental Research Letters*, *9*(6). https://doi.org/10.1088/1748-9326/9/6/064029

Hurtt, G. C., Chini, L., Sahajpal, R., Frolking, S., Bodirsky, B. L., Calvin, K., Doelman, J. C., Fisk, J., Fujimori, S., Klein Goldewijk, K., Hasegawa, T., Havlik, P., Heinimann, A., Humpenöder, F., Jungclaus, J., Kaplan, J. O., Kennedy, J., Krisztin, T., Lawrence, D., Lawrence, P., Ma, L., Mertz, O., Pongratz, J., Popp, A., Poulter, B., Riahi, K., Shevliakova, E., Stehfest, E., Thornton, P., Tubiello, F. N., van Vuuren, D. P., & Zhang, X. (2020). Harmonization of global land use change and management for the period 850–2100 (LUH2) for CMIP6. *Geosci. Model Dev.*, *13*(11), 5425-5464. https://doi.org/10.5194/gmd-13-5425-2020

Ibisch, P. L., Hoffmann, M. T., Kreft, S., Pe'er, G., Kati, V., Biber-Freudenberger, L., DellaSala, D. A., Vale, M. M., Hobson, P. R., & Selva, N. (2016). A global map of roadless areas and their conservation status. *Science*, *354*(6318), 1423-1427. https://doi.org/doi:10.1126/science.aaf7166

IEA. (2019). *World Energy Outlook 2019*. https://www.iea.org/reports/world-energy-outlook-2019

IEA. (2021). *Net Zero by 2050*. https://www.iea.org/reports/net-zero-by-2050

IPCC. (2019). *Climate Change and Land: an IPCC special report on climate change, desertification, land degradation, sustainable land management, food security, and greenhouse gas fluxes in terrestrial ecosystems [P.R. Shukla, J. Skea, E. Calvo Buendia, V. Masson-Delmotte, H.-O. Pörtner, D. C. Roberts, P. Zhai, R. Slade, S. Connors, R. van Diemen, M. Ferrat, E. Haughey, S. Luz, S. Neogi, M. Pathak, J. Petzold, J. Portugal Pereira, P. Vyas, E. Huntley, K. Kissick, M. Belkacemi, J. Malley, (eds.)]*.

IPCC. (2022). *Climate Change 2022. Mitigation of Climate Change. Working Group III contribution to the Sixth Assessment Report of the Intergovernmental Panel on Climate Change*.

IUCN&UNEP-WCMC. (2015). *The World Database on Protected Areas (WDPA)*. Retrieved 20.10.2015 from http://www.protectedplanet.net/

Jägermeyr, J., Gerten, D., Heinke, J., Schaphoff, S., Kummu, M., & Lucht, W. (2015). Water savings potentials of irrigation systems: global simulation of processes and linkages. *Hydrology Earth System Sciences*, *19*(7), 3073-3091. https://doi.org/10.5194/hess-19-3073-2015

Jägermeyr, J., Pastor, A., Biemans, H., & Gerten, D. (2017). Reconciling irrigated food production with environmental flows for Sustainable Development Goals implementation. *Nature Communications*, *8*(1), 15900. https://doi.org/10.1038/ncomms15900

Jeffery, S., Abalos, D., Prodana, M., Bastos, A. C., Groenigen, J. W. v., Hungate, B., & Verheijen, F. (2017). Biochar boosts tropical but not temperate crop yields. *Environmental Research Letters*, *12*(5), 053001. http://stacks.iop.org/1748-9326/12/i=5/a=053001

Jeffery, S., Verheijen, F. G. A., Kammann, C., & Abalos, D. (2016). Biochar effects on methane emissions from soils: A meta-analysis. *Soil Biology and Biochemistry*, *101*(Supplement C), 251-258. https://doi.org/https://doi.org/10.1016/j.soilbio.2016.07.021

Jung, M., Arnell, A., de Lamo, X., García-Rangel, S., Lewis, M., Mark, J., Merow, C., Miles, L., Ondo, I., Pironon, S., Ravilious, C., Rivers, M., Schepaschenko, D., Tallowin, O., van Soesbergen, A., Govaerts, R., Boyle, B. L., Enquist, B. J., Feng, X., Gallagher, R., Maitner, B., Meiri, S., Mulligan, M., Ofer, G., Roll, U., Hanson, J. O., Jetz, W., Di Marco, M., McGowan, J., Rinnan, D. S., Sachs, J. D., Lesiv, M., Adams, V. M., Andrew, S. C., Burger, J. R., Hannah, L., Marquet, P. A., McCarthy, J. K., Morueta-Holme, N., Newman, E. A., Park, D. S., Roehrdanz, P. R., Svenning, J.-C., Violle, C., Wieringa, J. J., Wynne, G., Fritz, S., Strassburg, B. B. N., Obersteiner, M., Kapos, V., Burgess, N., Schmidt-Traub, G., & Visconti, P. (2021). Areas of global importance for conserving terrestrial biodiversity, carbon and water. *Nature Ecology & Evolution*, *5*(11), 1499-1509. https://doi.org/10.1038/s41559-021-01528-7

Kalt, G., Lauk, C., Mayer, A., Theurl, M. C., Kaltenegger, K., Winiwarter, W., Erb, K.-H., Matej, S., & Haberl, H. (2020). Greenhouse gas implications of mobilizing agricultural biomass for energy: a reassessment of global potentials in 2050 under different food-system pathways. *Environmental Research Letters*, *15*(3), 034066. https://doi.org/10.1088/1748-9326/ab6c2e

Kammann, C., Ippolito, J., Hagemann, N., Borchard, N., Cayuela, M. L., Estavillo, J. M., Fuertes-Mendizabal, T., Jeffery, S., Kern, J., Novak, J., Rasse, D., Saarnio, S., Schmidt, H.-P., Spokas, K., & Wrage-Mönnig, N. (2017). Biochar as a tool to reduce the agricultural greenhouse-gas burden – knowns, unknowns and future research needs. *Journal of Environmental Engineering and Landscape Management*, *25*(2), 114-139. https://doi.org/10.3846/16486897.2017.1319375

Koch, A., & Kaplan, J. O. (2022). Tropical forest restoration under future climate change. *Nature Climate Change*. https://doi.org/10.1038/s41558-022-01289-6

Konis, K., & Schwendinger, F. (2020). R Interface to 'lp_solve' v.5.5.2.0.17.7. In.

Kreidenweis, U., Humpenöder, F., Stevanović, M., Bodirsky, B. L., Kriegler, E., Lotze-Campen, H., & Popp, A. (2016). Afforestation to mitigate climate change: impacts on food prices under consideration of albedo effects. *Environmental Research Letters*, *11*(8), 085001.

Laird, D. A., Brown, R. C., Amonette, J. E., & Lehmann, J. (2009). Review of the pyrolysis platform for coproducing bio-oil and biochar. *Biofuels, Bioproducts and Biorefining*, *3*(5), 547-562. https://doi.org/https://doi.org/10.1002/bbb.169

Lamarque, J. F., Dentener, F., McConnell, J., Ro, C. U., Shaw, M., Vet, R., Bergmann, D., Cameron-Smith, P., Dalsoren, S., Doherty, R., Faluvegi, G., Ghan, S. J., Josse, B., Lee, Y. H., MacKenzie, I. A., Plummer, D., Shindell, D. T., Skeie, R. B., Stevenson, D. S., Strode, S., Zeng, G., Curran, M., Dahl-Jensen, D., Das, S., Fritzsche, D., & Nolan, M. (2013). Multi-model mean nitrogen and sulfur deposition from the Atmospheric Chemistry and Climate Model Intercomparison Project (ACCMIP): evaluation of historical and projected future changes. *Atmos. Chem. Phys.*, *13*(16), 7997-8018. https://doi.org/10.5194/acp-13-7997-2013

Lehmann, J., Cowie, A., Masiello, C. A., Kammann, C., Woolf, D., Amonette, J. A., Cayuela, M. L., Camps-Arbestain, M., & Whitman, T. (2021). Biochar in Climate Change Mitigation. *Nature Geoscience*. https://doi.org/https://doi.org/10.1038/s41561-021-00852-8

Lehner, B., & Döll, P. (2004). Development and validation of a global database of lakes, reservoirs and wetlands. *Journal of Hydrology*, *296*(1), 1-22. https://doi.org/https://doi.org/10.1016/j.jhydrol.2004.03.028

Lenton, T. M., Rockström, J., Gaffney, O., Rahmstorf, S., Richardson, K., Steffen, W., & Schellnhuber, H. J. (2019). Climate tipping points—too risky to bet against. *Nature*, *575*, 592–595.

Lenzi, D., Lamb, W. F., Hilaire, J., Kowarsch, M., & Minx, J. C. (2018). Don't deploy negative emissions technologies without ethical analysis. In: Nature Publishing Group.

Lewis, S. L., Wheeler, C. E., Mitchard, E. T., & Koch, A. (2019). Restoring natural forests is the best way to remove atmospheric carbon. In: Nature Publishing Group.

Li, W., Ciais, P., Makowski, D., & Peng, S. (2018). A global yield dataset for major lignocellulosic bioenergy crops based on field measurements. *Scientific Data*, *5*(1), 180169. https://doi.org/10.1038/sdata.2018.169

Littleton, E. W., Dooley, K., Webb, G., Harper, A. B., Powell, T., Nicholls, Z., Meinshausen, M., & Lenton, T. M. (2021). Dynamic modelling shows substantial contribution of ecosystem restoration to climate change mitigation. *Environmental Research Letters*, *16*(12), 124061. https://doi.org/10.1088/1748-9326/ac3c6c

Melo, L. C. A., Lehmann, J., Carneiro, J. S. d. S., & Camps-Arbestain, M. (2022). Biochar-based fertilizer effects on crop productivity: a meta-analysis. *Plant and Soil*. https://doi.org/10.1007/s11104-021-05276-2

Mueller, N. D., Gerber, J. S., Johnston, M., Ray, D. K., Ramankutty, N., & Foley, J. A. (2012). Closing yield gaps through nutrient and water management. *Nature*, *490*(7419), 254-257. https://doi.org/10.1038/nature11420

Nemet, G., F. , Callaghan, M., W., Creutzig, F., Fuss, S., Hartmann, J., Hilaire, J., Lamb, W., F., Minx, J., Rogers, S., & Smith, P. (2018). Negative emissions—Part 3: Innovation and upscaling. *Environmental Research Letters*, *13*(6), 063003. http://stacks.iop.org/1748-9326/13/i=6/a=063003

Newbold, T., Hudson, L. N., Arnell, A. P., Contu, S., De Palma, A., Ferrier, S., Hill, S. L. L., Hoskins, A. J., Lysenko, I., Phillips, H. R. P., Burton, V. J., Chng, C. W. T., Emerson, S., Gao, D., Pask-Hale, G., Hutton, J., Jung, M., Sanchez-Ortiz, K., Simmons, B. I., Whitmee, S., Zhang, H., Scharlemann, J. P. W., & Purvis, A. (2016). Has land use pushed terrestrial biodiversity beyond the planetary boundary? A global assessment. *Science*, *353*(6296), 288-291. https://doi.org/10.1126/science.aaf2201

NOAA ESRL. (2019). *Atmospheric Carbon Dioxide Fractions from quasi-continuous measurements at Mauna Loa, Hawaii* http://esrl.noaa.gov/gmd/ccgg/trends/

Noon, M. L., Goldstein, A., Ledezma, J. C., Roehrdanz, P. R., Cook-Patton, S. C., Spawn-Lee, S. A., Wright, T. M., Gonzalez-Roglich, M., Hole, D. G., Rockström, J., & Turner, W. R. (2022). Mapping the irrecoverable carbon in Earth's ecosystems. *Nature Sustainability*, *5*(1), 37-46. https://doi.org/10.1038/s41893-021-00803-6

OECD, & FAO. (2020). *OECD-FAO Agricultural Outlook 2020-2029*. https://doi.org/doi:https://doi.org/10.1787/1112c23b-en

Olson, D. M., Dinerstein, E., Wikramanayake, E. D., Burgess, N. D., Powell, G. V. N., Underwood, E. C., D'amico, J. A., Itoua, I., Strand, H. E., Morrison, J. C., Loucks, C. J., Allnutt, T. F., Ricketts, T. H., Kura, Y., Lamoreux, J. F., Wettengel, W. W., Hedao, P., & Kassem, K. R. (2001). Terrestrial Ecoregions of the World: A New Map of Life on Earth: A new global map of terrestrial ecoregions provides an innovative tool for conserving biodiversity. *BioScience*, *51*(11), 933-938. https://doi.org/10.1641/0006-3568(2001)051[0933:Teotwa]2.0.Co;2

Ostberg, S. (2022). Introducing a toolbox for creating crop- and irrigation-specific land use inputs for dynamic global vegetation models. *in preperation*.

Ostberg, S., Lucht, W., Schaphoff, S., & Gerten, D. (2013). Critical impacts of global warming on land ecosystems. *Earth System Dynamics*, *4*, 347-357. https://doi.org/10.5194/esd-4-347-2013

Ostberg, S., Schaphoff, S., Lucht, W., & Gerten, D. (2015). Three centuries of dual pressure from land use and climate change on the biosphere. *Environmental Research Letters*, *10*. https://doi.org/Artn 044011

10.1088/1748-9326/10/4/044011

Pastor, A. V., Ludwig, F., Biemans, H., Hoff, H., & Kabat, P. (2014). Accounting for environmental flow requirements in global water assessments. *Hydrol. Earth Syst. Sci.*, *18*(12), 5041-5059. https://doi.org/10.5194/hess-18-5041-2014

Phalan, B., Onial, M., Balmford, A., & Green, R. E. (2011). Reconciling Food Production and Biodiversity Conservation: Land Sharing and Land Sparing Compared. *Science*, *333*, 1289-1291. https://doi.org/10.1126/science.1208742

Phyllis2. (2022). *Phyllis2, database for (treated) biomass, algae, feedstocks for biogas production and biochar* TNO Biobased and Circular Technologies. https://phyllis.nl/

Poikane, S., Kelly, M. G., Salas Herrero, F., Pitt, J.-A., Jarvie, H. P., Claussen, U., Leujak, W., Lyche Solheim, A., Teixeira, H., & Phillips, G. (2019). Nutrient criteria for surface waters under the European Water Framework Directive: Current state-of-the-art, challenges and future outlook. *Science of The Total Environment*, *695*, 133888. https://doi.org/https://doi.org/10.1016/j.scitotenv.2019.133888

Pongratz, J., Reick, C. H., Raddatz, T., Caldeira, K., & Claussen, M. (2011). Past land use decisions have increased mitigation potential of reforestation. *Geophysical Research Letters*, *38*, n/a-n/a. https://doi.org/10.1029/2011GL047848

Potapov, P., Laestadius, L., & Minnemeyer, S. (2011). Global map of forest landscape restoration opportunities. *Word Resources Institute. Washington, DC*.

Pour, N., Webley, P. A., & Cook, P. J. (2018). Potential for using municipal solid waste as a resource for bioenergy with carbon capture and storage (BECCS). *International Journal of Greenhouse Gas Control*, *68*, 1-15. https://doi.org/https://doi.org/10.1016/j.ijggc.2017.11.007

Randolph, P., Bansode, R. R., Hassan, O. A., Rehrah, D., Ravella, R., Reddy, M. R., Watts, D. W., Novak, J. M., & Ahmedna, M. (2017). Effect of biochars produced from solid organic municipal waste on soil quality parameters. *Journal of Environmental Management*, *192*, 271-280. https://doi.org/https://doi.org/10.1016/j.jenvman.2017.01.061

Razzaghi, F., Obour, P. B., & Arthur, E. (2020). Does biochar improve soil water retention? A systematic review and meta-analysis. *Geoderma*, *361*, 114055. https://doi.org/https://doi.org/10.1016/j.geoderma.2019.114055

Realmonte, G., Drouet, L., Gambhir, A., Glynn, J., Hawkes, A., Köberle, A. C., & Tavoni, M. (2019). An inter-model assessment of the role of direct air capture in deep mitigation pathways. *Nature Communications*, *10*(1), 3277. https://doi.org/10.1038/s41467-019-10842-5

Rockström, J., Gaffney, O., Rogelj, J., Meinshausen, M., Nakicenovic, N., & Schellnhuber, H. J. (2017). A roadmap for rapid decarbonization. *Science*, *355*(6331), 1269-1271. https://doi.org/10.1126/science.aah3443

Rockström, J., Steffen, W., Noone, K., Persson, A., Chapin, F. S., Lambin, E., Lenton, T. M., Scheffer, M., Folke, C., Schellnhuber, H. J., Nykvist, B., de Wit, C. A., Hughes, T., van der Leeuw, S., Rodhe, H., Sorlin, S., Snyder, P. K., Costanza, R., Svedin, U., Falkenmark, M., Karlberg, L., Corell, R. W., Fabry, V. J., Hansen, J., Walker, B., Liverman, D., Richardson, K., Crutzen, P., & Foley, J. (2009). Planetary Boundaries: Exploring the Safe Operating Space for Humanity. *Ecology and Society*, *14*(2). http://www.ecologyandsociety.org/vol14/iss2/art32/

Rogelj, J., Luderer, G., Pietzcker, R. C., Kriegler, E., Schaeffer, M., Krey, V., & Riahi, K. (2015). Energy system transformations for limiting end-of-century warming to below 1.5 °C [Perspective]. *Nature Climate Change*, *5*, 519. https://doi.org/10.1038/nclimate2572

Rosa, L., Sanchez, D. L., & Mazzotti, M. (2021). Assessment of carbon dioxide removal potential via BECCS in a carbon-neutral Europe [10.1039/D1EE00642H]. *Energy & Environmental Science*, *14*(5), 3086-3097. https://doi.org/10.1039/D1EE00642H

Rose, S. K., Popp, A., Fujimori, S., Havlik, P., Weyant, J., Wise, M., van Vuuren, D., Brunelle, T., Cui, R. Y., Daioglou, V., Frank, S., Hasegawa, T., Humpenöder, F., Kato, E., Sands, R. D., Sano, F., Tsutsui, J., Doelman, J., Muratori, M., Prudhomme, R., Wada, K., & Yamamoto, H. (2022). Global biomass supply modeling for long-run management of the climate system. *Climatic Change*, *172*(1), 3. https://doi.org/10.1007/s10584-022-03336-9

Schaphoff, S., Forkel, M., Müller, C., Knauer, J., von Bloh, W., Gerten, D., Jägermeyr, J., Lucht, W., Rammig, A., Thonicke, K., & Waha, K. (2018). LPJmL4 – a dynamic global vegetation model with managed land –

Part 2: Model evaluation. *Geosci. Model Dev.*, *11*(4), 1377-1403. https://doi.org/10.5194/gmd-11-1377-2018

Schaphoff, S., von Bloh, W., Rammig, A., Thonicke, K., Biemans, H., Forkel, M., Gerten, D., Heinke, J., Jägermeyr, J., Knauer, J., Langerwisch, F., Lucht, W., Müller, C., Rolinski, S., & Waha, K. (2018). LPJmL4 – a dynamic global vegetation model with managed land – Part 1: Model description. *Geosci. Model Dev.*, *11*(4), 1343-1375. https://doi.org/10.5194/gmd-11-1343-2018

Schmidt, H. P., Anca-Couce, A., Hagemann, N., Werner, C., Gerten, D., Lucht, W., & Kammann, C. (2018). Pyrogenic Carbon Capture & Storage (PyCCS). *GCB Bioenergy*. https://doi.org/10.1111/gcbb.12553

Scholes, R. J., & Biggs, R. (2005). A biodiversity intactness index. *Nature*, *434*(7029), 45-49. https://doi.org/10.1038/nature03289

Schueler, V., Weddige, U., Beringer, T., Gamba, L., & Lamers, P. (2013). Global biomass potentials under sustainability restrictions defined by the European Renewable Energy Directive 2009/28/EC. *GCB Bioenergy*, *5*(6), 652-663. https://doi.org/https://doi.org/10.1111/gcbb.12036

Schwärzel, K., Zhang, L., Montanarella, L., Wang, Y., & Sun, G. (2020). How afforestation affects the water cycle in drylands: A process-based comparative analysis. *Global Change Biology*, *26*(2), 944-959. https://doi.org/https://doi.org/10.1111/gcb.14875

Searle, S., & Malins, C. (2015). A reassessment of global bioenergy potential in 2050. *GCB Bioenergy*, *7*(2), 328-336. https://doi.org/https://doi.org/10.1111/gcbb.12141

Seddon, N., Turner, B., Berry, P., Chausson, A., & Girardin, C. A. J. (2019). Grounding nature-based climate solutions in sound biodiversity science. *Nature Climate Change*, *9*(2), 84-87. https://doi.org/10.1038/s41558-019-0405-0

Sitch, S., Smith, B., Prentice, I. C., Arneth, A., Bondeau, A., Cramer, W., Kaplan, J. O., Levis, S., Lucht, W., Sykes, M. T., Thonicke, K., & Venevsky, S. (2003). Evaluation of ecosystem dynamics, plant geography and terrestrial carbon cycling in the LPJ dynamic global vegetation model. *Global Change Biology*, *9*, 161-185. https://doi.org/10.1046/j.1365-2486.2003.00569.x

Skujiņš, J. (1981). Nitrogen cycling in arid ecosystems. *Ecological Bulletins*(33), 477-491.

Smith, B., Wårlind, D., Arneth, A., Hickler, T., Leadley, P., Siltberg, J., & Zaehle, S. (2014). Implications of incorporating N cycling and N limitations on primary production in an individual-based dynamic vegetation model. *Biogeosciences*, *11*(7), 2027-2054. https://doi.org/10.5194/bg-11-2027-2014

Smith, P., Adams, J., Beerling, D. J., Beringer, T., Calvin, K. V., Fuss, S., Griscom, B., Hagemann, N., Kammann, C., Kraxner, F., Minx, J. C., Popp, A., Renforth, P., Vicente, J. L. V., & Keesstra, S. (2019). Land-Management Options for Greenhouse Gas Removal and Their Impacts on Ecosystem Services and the Sustainable Development Goals. *Annual Review of Environment and Resources*, *44*(1), 255-286. https://doi.org/10.1146/annurev-environ-101718-033129

Smith, P., Haberl, H., Popp, A., Erb, K.-h., Lauk, C., Harper, R., Tubiello, F. N., de Siqueira Pinto, A., Jafari, M., Sohi, S., Masera, O., Böttcher, H., Berndes, G., Bustamante, M., Ahammad, H., Clark, H., Dong, H., Elsiddig, E. A., Mbow, C., Ravindranath, N. H., Rice, C. W., Robledo Abad, C., Romanovskaya, A., Sperling, F., Herrero, M., House, J. I., & Rose, S. (2013). How much land-based greenhouse gas mitigation can be achieved without compromising food security and environmental goals? *Global Change Biology*, *19*(8), 2285-2302. https://doi.org/https://doi.org/10.1111/gcb.12160

Smith, P., Nkem, J., Calvin, K., Campbell, D., Cherubini, F., Grassi, G., Korotkov, V., Hoang, A. L., Lwasa, S., McElwee, P., Nkonya, E., Saigusa, N., Soussana, J.-F., & Taboada, M. A. (2019). *Interlinkages Between Desertification, Land Degradation, Food Security and Greenhouse Gas Fluxes: Synergies, Trade-offs and Integrated Response Options. In: Climate Change and Land: an IPCC special report on climate change, desertification, land degradation, sustainable land management, food security, and greenhouse gas fluxes in terrestrial ecosystem [P.R. Shukla, J. Skea, E. Calvo Buendia, V. Masson-Delmotte, H.- O. Portner, D. C. Roberts, P. Zhai, R. Slade, S. Connors, R. van Diemen, M. Ferrat, E. Haughey, S. Luz, S. Neogi, M. Pathak, J. Petzold, J. Portugal Pereira, P. Vyas, E. Huntley, K. Kissick, M. Belkacemi, J. Malley, (eds.)]*.

Sonntag, S., Pongratz, J., Reick, C. H., & Schmidt, H. (2016). Reforestation in a high-CO2 world—Higher mitigation potential than expected, lower adaptation potential than hoped for. *Geophysical Research Letters*, *43*(12), 6546-6553. https://doi.org/https://doi.org/10.1002/2016GL068824

Soto-Navarro, C., Ravilious, C., Arnell, A., de Lamo, X., Harfoot, M., Hill, S. L. L., Wearn, O. R., Santoro, M., Bouvet, A., Mermoz, S., Le Toan, T., Xia, J., Liu, S., Yuan, W., Spawn, S. A., Gibbs, H. K., Ferrier, S., Harwood, T., Alkemade, R., Schipper, A. M., Schmidt-Traub, G., Strassburg, B., Miles, L., Burgess, N. D., & Kapos, V. (2020). Mapping co-benefits for carbon storage and biodiversity to inform conservation policy and action. *Philosophical Transactions of the Royal Society B: Biological Sciences*, *375*(1794), 20190128. https://doi.org/doi:10.1098/rstb.2019.0128

Steffen, W., Richardson, K., Rockström, J., Cornell, S. E., Fetzer, I., Bennett, E. M., Biggs, R., Carpenter, S. R., de Vries, W., de Wit, C. A., Folke, C., Gerten, D., Heinke, J., Mace, G. M., Persson, L. M., Ramanathan, V., Reyers, B., & Sörlin, S. (2015). Planetary boundaries: Guiding human development on a changing planet. *Science*, *347*(6223). https://doi.org/10.1126/science.1259855

Steffen, W., Rockström, J., Richardson, K., Lenton, T. M., Folke, C., Liverman, D., Summerhayes, C. P., Barnosky, A. D., Cornell, S. E., Crucifix, M., Donges, J. F., Fetzer, I., Lade, S. J., Scheffer, M., Winkelmann, R., & Schellnhuber, H. J. (2018). Trajectories of the Earth System in the Anthropocene. *Proceedings of the National Academy of Sciences*. https://doi.org/10.1073/pnas.1810141115

Stehfest, E., Bouwman, L., van Vuuren, D. P., den Elzen, M. G. J., Eickhout, B., & Kabat, P. (2009). Climate benefits of changing diet. *Climatic Change*, *95*(1), 83-102. https://doi.org/10.1007/s10584-008-9534-6

Stehfest, E., van Zeist, W.-J., Valin, H., Havlik, P., Popp, A., Kyle, P., Tabeau, A., Mason-D'Croz, D., Hasegawa, T., Bodirsky, B. L., Calvin, K., Doelman, J. C., Fujimori, S., Humpenöder, F., Lotze-Campen, H., van Meijl, H., & Wiebe, K. (2019). Key determinants of global land-use projections. *Nature Communications*, *10*(1), 2166. https://doi.org/10.1038/s41467-019-09945-w

Stenzel, F., Gerten, D., Werner, C., & Jägermeyr, J. (2019). Freshwater requirements of large-scale bioenergy plantations for limiting global warming to 1.5 °C. *Environmental Research Letters*, *14*(8), 084001. https://doi.org/10.1088/1748-9326/ab2b4b

Strefler, J., Bauer, N., Humpenöder, F., Klein, D., Popp, A., & Kriegler, E. (2021). Carbon dioxide removal technologies are not born equal. *Environmental Research Letters*, *16*(7), 074021. https://doi.org/10.1088/1748-9326/ac0a11

Tudge, S. J., Purvis, A., & De Palma, A. (2021). The impacts of biofuel crops on local biodiversity: a global synthesis. *Biodiversity and Conservation*, *30*(11), 2863-2883. https://doi.org/10.1007/s10531-021-02232-5

UNEP-WCMC, UNEP, & IUCN. (2020). *Protected Planet Report 2020*.

UNEP. (1997). *World Atlas of Desertification* (N. Middleton & D. Thomas, Eds.). John Wiley & Sons.

UNEP. (2022). *Spreading like Wildfire – The Rising Threat of Extraordinary Landscape Fires. A United Nations Environment Programme (UNEP) Rapid Response Assessment. Nairobi.*

UNFCCC. (2015). Adoption of the Paris Agreement FCCC/CP/2015/L.9/Rev.1.

van der Esch, S., ten Brink, B., Stehfest, E., Bakkenes, M., Sewell, A., Bouwman, A., Meijer, J., Westhoek, H., van den Berg, M., & van den Born, G. J. (2017). Exploring future changes in land use and land condition and the impacts on food, water, climate change and biodiversity: scenarios for the UNCCD Global Land Outlook.

Van der Leeuw, S. E. (2008). Climate and society: Lessons from the past 10 000 years. *AMBIO: A Journal of the Human Environment*, *37*(sp14), 476-482. http://www.bioone.org/doi/pdf/10.1579/0044-7447-37.sp14.476

Van Zanten, H. H. E., Herrero, M., Van Hal, O., Röös, E., Muller, A., Garnett, T., Gerber, P. J., Schader, C., & De Boer, I. J. M. (2018). Defining a land boundary for sustainable livestock consumption. *Global Change Biology*, *24*(9), 4185-4194. https://doi.org/https://doi.org/10.1111/gcb.14321

von Bloh, W., Schaphoff, S., Müller, C., Rolinski, S., Waha, K., & Zaehle, S. (2018). Implementing the nitrogen cycle into the dynamic global vegetation, hydrology, and crop growth model LPJmL (version 5.0). *Geosci. Model Dev.*, *11*(7), 2789-2812. https://doi.org/10.5194/gmd-11-2789-2018

Wang-Erlandsson, L., Tobian, A., van der Ent, R. J., Fetzer, I., te Wierik, S., Porkka, M., Staal, A., Jaramillo, F., Dahlmann, H., Singh, C., Greve, P., Gerten, D., Keys, P. W., Gleeson, T., Cornell, S. E., Steffen, W., Bai, X., & Rockström, J. (2022). A planetary boundary for green water. *Nature Reviews Earth & Environment*. https://doi.org/10.1038/s43017-022-00287-8

Weng, Z., Van Zwieten, L., Singh, B. P., Tavakkoli, E., Joseph, S., Macdonald, L. M., Rose, T. J., Rose, M. T., Kimber, S. W. L., Morris, S., Cozzolino, D., Araujo, J. R., Archanjo, B. S., & Cowie, A. (2017). Biochar built soil carbon over a decade by stabilizing rhizodeposits [Article]. *Nature Climate Change*, *7*, 371-376. https://doi.org/10.1038/nclimate3276

Werner, C., Schmidt, H. P., Gerten, D., Lucht, W., & Kammann, C. (2018). Biogeochemical potential of biomass pyrolysis systems for limiting global warming to 1.5 °C. *Environmental Research Letters*, *13*(4), 044036. https://doi.org/https://doi.org/10.1088/1748-9326/aabb0e

Werner, C. L., W., Gerten, D., & Kammann, C. (2022). Potential of land-neutral negative emissions through biochar sequestration [in revision]. *Earth's Future*.

Willett, W., Rockström, J., Loken, B., Springmann, M., Lang, T., Vermeulen, S., Garnett, T., Tilman, D., DeClerck, F., Wood, A., Jonell, M., Clark, M., Gordon, L. J., Fanzo, J., Hawkes, C., Zurayk, R., Rivera, J. A., De Vries, W., Majele Sibanda, L., Afshin, A., Chaudhary, A., Herrero, M., Agustina, R., Branca, F., Lartey, A., Fan, S., Crona, B., Fox, E., Bignet, V., Troell, M., Lindahl, T., Singh, S., Cornell, S. E., Srinath Reddy, K., Narain, S., Nishtar, S., & Murray, C. J. L. (2019). Food in the Anthropocene: the EAT Lancet Commission on healthy diets from sustainable food systems. *The Lancet*, *393*(10170), 447-492. https://doi.org/10.1016/S0140-6736(18)31788-4

Wirsenius, S. (2000). *Human use of land and organic materials: modeling the turnover of biomass in the global food system*. Chalmers University of Technology.

Woolf, D., Amonette, J. E., Street-Perrott, F. A., Lehmann, J., & Joseph, S. (2010). Sustainable biochar to mitigate global climate change. *Nature Communications*, *1*, 56. https://doi.org/10.1038/Ncomms1053

Woolf, D., Lehmann, J., Ogle, S., Kishimoto-Mo, A. W., McConkey, B., & Baldock, J. (2021). Greenhouse Gas Inventory Model for Biochar Additions to Soil. *Environmental science & technology*, *55*(21), 14795-14805. https://doi.org/10.1021/acs.est.1c02425

Wu, W., Hasegawa, T., Ohashi, H., Hanasaki, N., Liu, J., Matsui, T., Fujimori, S., Masui, T., & Takahashi, K. (2019). Global advanced bioenergy potential under environmental protection policies and societal transformation measures. *GCB Bioenergy*, *11*(9), 1041-1055. https://doi.org/https://doi.org/10.1111/gcbb.12614

Ye, L., Camps-Arbestain, M., Shen, Q., Lehmann, J., Singh, B., & Sabir, M. (2020). Biochar effects on crop yields with and without fertilizer: A meta-analysis of field studies using separate controls. *Soil Use and Management*, *36*(1), 2-18. https://doi.org/10.1111/sum.12546

Yuan, J.-H., Xu, R.-K., Wang, N., & Li, J.-Y. (2011). Amendment of Acid Soils with Crop Residues and Biochars. *Pedosphere*, *21*(3), 302-308. https://doi.org/https://doi.org/10.1016/S1002-0160(11)60130-6

Zhang, B., Tian, H., Lu, C., Dangal, S. R. S., Yang, J., & Pan, S. (2017). Global manure nitrogen production and application in cropland during 1860–2014: a 5 arcmin gridded global dataset for Earth system modeling. *Earth Syst. Sci. Data*, *9*(2), 667-678. https://doi.org/10.5194/essd-9-667-2017

Appendix

Input data for LPJmL simulations

For the analysis in this study LPJmL is driven by climate data from the Climatic Research Unit, CRU TS version 4.03 (Harris et al., 2020) in combination with NO3 and NH4 deposition rates from Lamarque et al. (2013) and atmospheric CO_2 concentration from NOAA ESRL (2019) (Table S1). Further, scenarios of land management are based on the CFT-specific extent of cropland and pasture, including the fraction of irrigated areas, as prepared by Ostberg (2022) under consolidation of HYDE3.2 (Klein Goldewijk et al., 2017) and irrigated areas from Siebert et al. (2015) (Table S1). The availability of irrigation water is reduced by the withdrawals for households, industry and livestock (HIL) taken from the ISIMIP2b database (Frieler et al., 2017). In addition to the water management of cropland, the fertilizer input is prescribed for each CFT based on the mineral fertilizer data from the harmonization of global land use change and management (LUH2) for CMIP6 (Hurtt et al., 2020). This N input from mineral sources is supplemented by manure, for which we assume an available share of 60% from the data on manure application provided by Zhang et al. (2017) to represent the less accessible N composition according to Elliott et al. (2015).

Table S1: Input data

Input	Description	Time period	Source
Temperature	Daily mean temperatures from the Climatic Research Unit, CRU TS version 4.03	1901-2015	Harris et al. (2020)
Precipitation	Daily precipitation from the Climatic Research Unit, CRU TS version 4.03	1901-2015	Harris et al. (2020)
Cloudiness	Daily cloud cover from the Climatic Research Unit, CRU TS version 4.03	1901-2015	Harris et al. (2020)
NO3 deposition		1850-2015	Lamarque et al. (2013)
NH4 depostion		1850-2015	Lamarque et al. (2013)
CO_2 in the atmosphere			NOAA ESRL (2019)
Land use	The distribution of CFTs and the share of irrigated land per crop in each grid cell is derived from the cropland and pasture extent in HYDE 3.2 (Klein Goldewijk et al., 2017), combined with cultivation data of specific crops for each country from FAO and the extent of areas irrigated from Siebert et al. (2015). The irrigation system is determined by suitability for crops as described by Jägermeyr et al. (2015).	1500-2015	Ostberg (2022), in prep.
Fertilizer	Crop-specific mineral fertilizer rates from LUH2 (Hurtt et al., 2020) supplemented by 60% of the manure N provided in Zhang et al. (2017) representing the less accessible N composition of manure according to Elliott et al. (2015)	1860-2015	Hurtt et al. (2020), Zhang et al. (2017)
HIL water use	Water withdrawals for households, industry and livestock (HIL) provided by the ISIMIP2b database.	1901-2005 and at constant level afterwards	Frieler et al. (2017)

Details on used biome classifications

A LPJmL derived biome classification

LPJmL grid cells were classified into 16 distinct biomes based on simulated composition of plant functional types under potential natural vegetation (see Figure 1) as described in Ostberg et al. (2013) and (Ostberg et al., 2015). The classification scheme was adapted to the new model version by decreasing the tree cover threshold for boreal forests (to 10%), increasing the maximum annual mean temperature for arctic tundra (to 0°C) and introducing an additional constraint for boreal forest to exclude cells which are temperate according to the Köppen-Geiger climate classification (Beck et al., 2018). The latter is necessary as temperate and boreal plant functional types have similar characteristics resulting in an ambiguous border between these biomes when solely focusing on tree species. Further, as the competitiveness of tropical evergreen trees is underestimated in the used LPJmL version (likely due to N feedbacks), cells were assigned to tropical evergreen rainforest if tropical evergreen trees contributed at least one third to total tree cover (instead of 0.5). While the LPJmL derived biome classification has been well validated against satellite data (Ostberg et al., 2013), not yet fully understood N feedbacks lead to minor anomalies in biome distribution in LPJmL5 (e.g. too large extent of boreal deciduous forest in comparison to boreal evergreen forest, see Figure 1). The analysis and model adaption addressing these shortcomings are currently still in the process.

B Biome classification from Olson et al. (2001)

Shapefiles with the geographic extent of the 14 biomes from Olson et al. (2001) were rasterized to a LPJmL compatible grid. Grid cells with missing biome classification were assigned to the most prevalent biome within the neighbouring cells. For the land-system change PB, the biome *Mediterranean Forests, Woodlands & Shrub* was split into *Mediterranean Forests* and *Mediterranean Woodlands & Shrub* based on simulated potential tree cover in LPJmL (>50% = forest). Only cells assigned as Mediterranean Forests were then included as potential natural forest areas for the land-system change PB calculation.

Biochar-mediated yield increases

Recent studies indicate significant yield increases with biochar application to soils in small rates (ca. t ha^{-1}) as fertilizer enhancer. Applying lower rates of 1 t ha^{-1} biochar as a fertilizer enhancer (mean of 0.9 t ha^{-1} in Melo et al. (2022)), instead of 15-20 t ha^{-1} when used as soil conditioner, reduces the biochar demand and allows for long-term practice with annual applications. A recent meta-analysis by Melo et al. (2022) dedicated to biochar as fertilizer enhancer derives a mean effect of 16% yield increase (95% confidence interval 9–23%) compared to the fertilized control for biochar produced at HHT >400°C containing >30% C, matching our parametrization of 500°C HHT and >80% C content of the char. This is in line with other most recent meta-analyses on the effect of biochar application in general, i.e. 14% yield increase compared to the fertilized control reported in Bai et al. (2022) and 15% for (sub-)tropical soils, our region of focus for LCN-PyCCS, in Ye et al. (2020). To account for uncertainties regarding the effect of biochar application on crop yields, such as soil properties, biochar characteristics and management practices, we assessed a range of yield increase levels: 15% as the standard scenario representing the mean effect of the meta-analyses and a range of 10% -20% , similar to the confidence interval in Melo et al. (2022).

Biosphere integrity and land-system change PB status based on biomes from Olson et al. (2001)

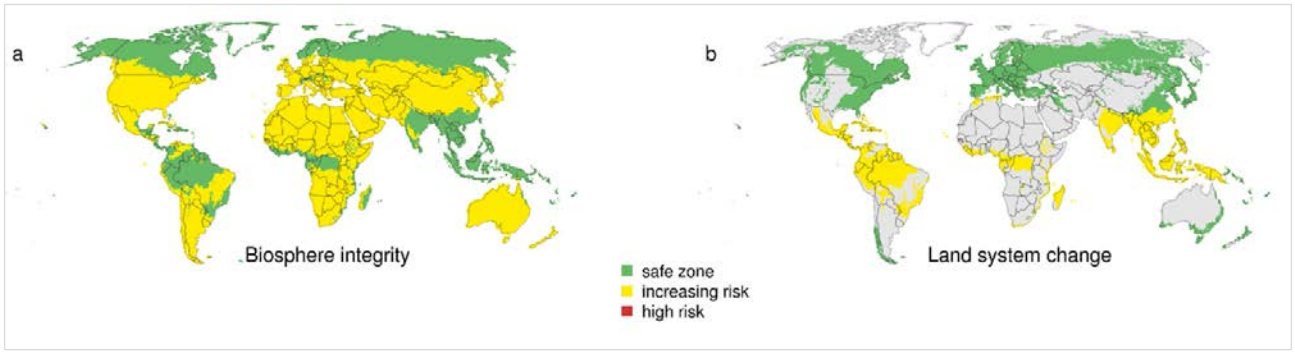

Fig. S1: Simulated status of the biosphere integrity and land-system change PBs for current agricultural land use (a: 2005 land use, b: 2015 land use). The status is based on biome extents from Olson et al. (2001). Cells where the land-system change boundary definition does not apply are displayed in grey (all non-forest biomes).

References

Bai, S. H., Omidvar, N., Gallart, M., Kämper, W., Tahmasbian, I., Farrar, M. B., Singh, K., Zhou, G., Muqadass, B., Xu, C.-Y., Koech, R., Li, Y., Nguyen, T. T. N., & van Zwieten, L. (2022). Combined effects of biochar and fertilizer applications on yield: A review and meta-analysis. *Science of The Total Environment*, *808*, 152073. https://doi.org/https://doi.org/10.1016/j.scitotenv.2021.152073

Beck, H. E., Zimmermann, N. E., McVicar, T. R., Vergopolan, N., Berg, A., & Wood, E. F. (2018). Present and future Köppen-Geiger climate classification maps at 1-km resolution. *Scientific Data*, *5*(1), 180214. https://doi.org/10.1038/sdata.2018.214

Elliott, J., Müller, C., Deryng, D., Chryssanthacopoulos, J., Boote, K. J., Büchner, M., Foster, I., Glotter, M., Heinke, J., Iizumi, T., Izaurralde, R. C., Mueller, N. D., Ray, D. K., Rosenzweig, C., Ruane, A. C., & Sheffield, J. (2015). The Global Gridded Crop Model Intercomparison: data and modeling protocols for Phase 1 (v1.0). *Geosci. Model Dev.*, *8*(2), 261-277. https://doi.org/10.5194/gmd-8-261-2015

Frieler, K., Lange, S., Piontek, F., Reyer, C. P. O., Schewe, J., Warszawski, L., Zhao, F., Chini, L., Denvil, S., Emanuel, K., Geiger, T., Halladay, K., Hurtt, G., Mengel, M., Murakami, D., Ostberg, S., Popp, A., Riva, R., Stevanovic, M., Suzuki, T., Volkholz, J., Burke, E., Ciais, P., Ebi, K., Eddy, T. D., Elliott, J., Galbraith, E., Gosling, S. N., Hattermann, F., Hickler, T., Hinkel, J., Hof, C., Huber, V., Jägermeyr, J., Krysanova, V., Marcé, R., Müller Schmied, H., Mouratiadou, I., Pierson, D., Tittensor, D. P., Vautard, R., van Vliet, M., Biber, M. F., Betts, R. A., Bodirsky, B. L., Deryng, D., Frolking, S., Jones, C. D., Lotze, H. K., Lotze-Campen, H., Sahajpal, R., Thonicke, K., Tian, H., & Yamagata, Y. (2017). Assessing the impacts of 1.5 °C global warming – simulation protocol of the Inter-Sectoral Impact Model Intercomparison Project (ISIMIP2b). *Geosci. Model Dev.*, *10*(12), 4321-4345. https://doi.org/10.5194/gmd-10-4321-2017

Harris, I., Osborn, T. J., Jones, P., & Lister, D. (2020). Version 4 of the CRU TS monthly high-resolution gridded multivariate climate dataset. *Scientific Data*, *7*(1), 109. https://doi.org/10.1038/s41597-020-0453-3

Hurtt, G. C., Chini, L., Sahajpal, R., Frolking, S., Bodirsky, B. L., Calvin, K., Doelman, J. C., Fisk, J., Fujimori, S., Klein Goldewijk, K., Hasegawa, T., Havlik, P., Heinimann, A., Humpenöder, F., Jungclaus, J., Kaplan, J. O., Kennedy, J., Krisztin, T., Lawrence, D., Lawrence, P., Ma, L., Mertz, O., Pongratz, J., Popp, A., Poulter, B., Riahi, K., Shevliakova, E., Stehfest, E., Thornton, P., Tubiello, F. N., van Vuuren, D. P., & Zhang, X. (2020). Harmonization of global land use change and management for the period 850–2100 (LUH2) for CMIP6. *Geosci. Model Dev.*, *13*(11), 5425-5464. https://doi.org/10.5194/gmd-13-5425-2020

Jägermeyr, J., Gerten, D., Heinke, J., Schaphoff, S., Kummu, M., & Lucht, W. (2015). Water savings potentials of irrigation systems: global simulation of processes and linkages. *Hydrology Earth System Sciences*, *19*(7), 3073-3091. https://doi.org/10.5194/hess-19-3073-2015

Klein Goldewijk, K., Beusen, A., Doelman, J., & Stehfest, E. (2017). Anthropogenic land use estimates for the Holocene – HYDE 3.2. *Earth Syst. Sci. Data*, *9*(2), 927-953. https://doi.org/10.5194/essd-9-927-2017

Lamarque, J. F., Dentener, F., McConnell, J., Ro, C. U., Shaw, M., Vet, R., Bergmann, D., Cameron-Smith, P., Dalsoren, S., Doherty, R., Faluvegi, G., Ghan, S. J., Josse, B., Lee, Y. H., MacKenzie, I. A., Plummer, D., Shindell, D. T., Skeie, R. B., Stevenson, D. S., Strode, S., Zeng, G., Curran, M., Dahl-Jensen, D., Das, S., Fritzsche, D., & Nolan, M. (2013). Multi-model mean nitrogen and sulfur deposition from the Atmospheric Chemistry and Climate Model Intercomparison Project (ACCMIP): evaluation of historical and projected future changes. *Atmos. Chem. Phys.*, *13*(16), 7997-8018. https://doi.org/10.5194/acp-13-7997-2013

Melo, L. C. A., Lehmann, J., Carneiro, J. S. d. S., & Camps-Arbestain, M. (2022). Biochar-based fertilizer effects on crop productivity: a meta-analysis. *Plant and Soil*. https://doi.org/10.1007/s11104-021-05276-2

NOAA ESRL. (2019). *Atmospheric Carbon Dioxide Fractions from quasi-continuous measurements at Mauna Loa, Hawaii* http://esrl.noaa.gov/gmd/ccgg/trends/

Olson, D. M., Dinerstein, E., Wikramanayake, E. D., Burgess, N. D., Powell, G. V. N., Underwood, E. C., D'amico, J. A., Itoua, I., Strand, H. E., Morrison, J. C., Loucks, C. J., Allnutt, T. F., Ricketts, T. H., Kura, Y., Lamoreux, J. F., Wettengel, W. W., Hedao, P., & Kassem, K. R. (2001). Terrestrial Ecoregions of the World: A New

Map of Life on Earth: A new global map of terrestrial ecoregions provides an innovative tool for conserving biodiversity. *BioScience*, *51*(11), 933-938. https://doi.org/10.1641/0006-3568(2001)051[0933:Teotwa]2.0.Co;2

Ostberg, S. (2022). Introducing a toolbox for creating crop- and irrigation-specific land use inputs for dynamic global vegetation models. *in preperation*.

Ostberg, S., Lucht, W., Schaphoff, S., & Gerten, D. (2013). Critical impacts of global warming on land ecosystems. *Earth System Dynamics*, *4*(2), 347-357. https://doi.org/10.5194/esd-4-347-2013

Ostberg, S., Schaphoff, S., Lucht, W., & Gerten, D. (2015). Three centuries of dual pressure from land use and climate change on the biosphere. *Environmental Research Letters*, *10*(4), 044011. https://doi.org/10.1088/1748-9326/10/4/044011

Siebert, S., Kummu, M., Porkka, M., Döll, P., Ramankutty, N., & Scanlon, B. R. (2015). A global data set of the extent of irrigated land from 1900 to 2005. *Hydrol. Earth Syst. Sci.*, *19*(3), 1521-1545. https://doi.org/10.5194/hess-19-1521-2015

Ye, L., Camps-Arbestain, M., Shen, Q., Lehmann, J., Singh, B., & Sabir, M. (2020). Biochar effects on crop yields with and without fertilizer: A meta-analysis of field studies using separate controls. *Soil Use and Management*, *36*(1), 2-18. https://doi.org/10.1111/sum.12546

Zhang, B., Tian, H., Lu, C., Dangal, S. R. S., Yang, J., & Pan, S. (2017). Global manure nitrogen production and application in cropland during 1860–2014: a 5 arcmin gridded global dataset for Earth system modeling. *Earth Syst. Sci. Data*, *9*(2), 667-678. https://doi.org/10.5194/essd-9-667-2017